Chondrocyte Regulation by IL-I and IGF-I:
Interconnection Between Anabolic and Catabolic Factors

Ryan Michael Porter

Dissertation submitted to the Faculty of the
Virginia Polytechnic Institute and State University
in partial fulfillment of the requirements
for the degree of

Doctor of Philosophy
in
Chemical Engineering

Dr. Kimberly F. Williams, Chair
Aaron S. Goldstein
Richey M. Davis
R. Michael Akers

October 14, 2005
Blacksburg, VA

Keywords: articular chondrocytes, osteoarthritis, equine, interleukin-1 (IL-1),
insulin-like growth factor-I (IGF-I), cell signaling

Chondrocyte Regulation by IL-I and IGF-I:
Interconnection Between Anabolic and Catabolic Factors

Ryan Michael Porter

(ABSTRACT)

Articular cartilage functions to reduce the mechanical stresses associated with diarthrodial joint movement, protecting these joints over a lifetime of use. Tissue function is maintained through the balance between synthesis and resorption (i.e., metabolism) of extracellular matrix (ECM) by articular chondrocytes (ACs). Two important hormonal regulators of cartilage metabolism are interleukin-1 (IL-1) and insulin-like growth factor-I (IGF-I). These factors have antagonistic effects on chondrocyte activity, and during the progression of osteoarthritis, IL-1 is thought to promote chondrocyte hyporesponsiveness to IGF-I. To better understand how the anabolic (IGF-I) and catabolic (IL-1) stimuli are linked within articular cartilage, we examined the mechanisms by which IL-1 regulates the IGF-I signaling system of ACs. Equine chondrocytes from non-arthritic stifle joints were multiplied over serial passages, re-differentiated in alginate beads, and stimulated with recombinant equine IL-1β. Chondrocytes were assayed for type I IGF receptor (IGF-IR), IGF binding proteins (IGFBPs), and endogenously-secreted IGF-I. Our experimental findings solidify the significance of IL-1 as a key regulator of IGF-I signaling within articular cartilage, demonstrating that regulation of the IGF-I system occurs through both direct (transcription) and indirect (proteolysis) mechanisms. These results have implications for molecular therapies (e.g., gene transfer) directed at reversing osteoarthritic cartilage deterioration.

The presented research concerns not only cartilage biology but also tissue engineering strategies for cartilage repair. Alginate hydrogel culture has been reported to re-establish chondrocytic phenotype following monolayer expansion, but studies have not addressed effects on the signaling systems responsible for chondrocyte metabolism. We investigated whether chondrocyte culture history influences the IGF-I system and its regulation by IL-1. ACs expanded by serial passaging were either encapsulated in alginate beads or maintained on tissue culture plastic (TCP). Bead and TCP cells were plated at high-density, stimulated with IL-1β, and assayed for expression of IGF-I signaling mediators. Intermediate alginate culture yielded disparate basal levels of IGF-IR and IGFBP-2, which were attributed to differential transcription.

The distinct mediator profiles coincided with varied effects of exogenous IL-1β and IGF-I on collagen Ia1 expression and cell growth rate. This study demonstrates that culture strategy impacts the IGF-I system of ACs, likely impacting their capability to mediate cartilage repair.

Dedication

This dissertation is dedicated to my parents, Suzanne and Michael Porter.

Thanks, mom and dad, for the unwavering guidance and support.

Author's Acknowledgements

Table of Contents

List of Figures

Appendix C: Computational Model of Extracellular IL-1 Signaling

List of Tables

Chapter 1: Introduction

1.1   Motivation for Research

Articular cartilage functions to reduce the mechanical stresses associated with diarthrodial joint movement, protecting these joints over a lifetime of use. The spatially-variable matrix that defines cartilage function is maintained by specialized cells known as chondrocytes. In response to hormonal and biomechanical stimuli, these cells secrete both the collagen and proteoglycan building blocks of cartilage as well as their respective catabolic proteases. The balance (i.e., homeostasis) between chondrocyte-mediated synthesis and resorption is responsible for tissue longevity. Though resilient to frequent strain, articular cartilage has limited capacity for endogenous repair in response to focal injury or the progression of osteoarthritis.

Osteoarthritis, also known as degenerative joint disease or osteoarthrosis, is the most common cause of physical disability among adults. The disorder, which primarily affects the diarthrodial joints, can be described as a deterioration of articular cartilage. Macroscopic effects include fibrillation and eventual erosion of the cartilage surface, schlerosis of the subchondral bone, and formation of bony outgrowths known as osteophytes. These alterations are associated with inflammation, chronic pain, and limited mobility. According to the National Institute of Arthritis and Musculoskeletal and Skin Diseases, over 20 million Americans are afflicted with osteoarthritis (OA), with clinical symptoms most prevalent in the elderly [http://www.niams.nih.gov/hi/topics/arthritis/oahandout.pdf].

The pathogenesis of OA is complex, as the disorder develops slowly from an undetermined sequence of biochemical and biomechanical cues. These signals lead to a loss of extracellular matrix (ECM) homeostasis within articular cartilage, such that protease-mediated degradation exceeds the rate of repair mechanisms. Insulin-like growth factor-I (IGF-I) and interleukin-1 (IL-1) are two of the most important hormonal regulators of chondrocytes, and both are thought to play key roles in the development of OA [1]. While they have been reported to have opposing effects on proteoglycan and collagen synthesis, the mechanisms by which these polypeptide hormones regulate chondrocyte activity have not been fully characterized.

The overall objective of this research was to better describe the signaling systems of IGF-I and IL-1 for articular chondrocytes in an effort to understand how these networks are interconnected with articular cartilage. Equine articular chondrocytes were selected for an *in*

vitro culture model. A recently characterized recombinant equine IL-1β (rEqIL-1β) [2] was used with this model to more accurately reproduce *in vivo* stimulation by elevated cytokine levels. Due to the relative homology between equine and human genotypes and similarities observed between their respective disease states [3], conclusions derived from this work have implications for the pathogenesis of OA within both species. Furthermore, insights from these studies could aid in the development of molecular and tissue engineering approaches to articular cartilage repair.

1.2   Research Aims

1.2.1 *To identify the mechanisms by which interleukin-1 (IL-1) regulates the insulin-like growth factor-I (IGF-I) signaling system of equine articular chondrocytes.*

The lack of sufficient ECM repair observed in OA has been partially attributed to a reduced responsiveness of articular chondrocytes to the anabolic growth factor IGF-I [4-6]. IL-1 suppresses IGF-I effects on chondrocyte metabolic activity [7, 8], and this cytokine is thought to contribute to the IGF-I hyporesponsive state [6]. IGF-I activity is mediated by signaling receptors (IGF-IR) as well as high-affinity binding proteins (IGFBPs). Our first study addressed how IL-1β – through interactions with its own signaling system – impacts the levels of IGF-I mediators (**Figure 1.1**). For our experimental model, articular chondrocytes were extracted from equine stifle joints, grown on tissue culture plastic to expand their numbers, and encapsulated within alginate beads to re-establish cell phenotype. Isolated bead cells were stimulated with IL-1β and assayed for IGF-IR, IGFBP, and endogenous IGF-I synthesis at both the transcript and protein levels. We hypothesized that IL-1β regulates IGF-I signaling by controlling the levels of IGF-IR and IGFBPs. The results are discussed in Chapter 3.

1.2.2 *To determine the influence of chondrocyte culture history on basal levels of IGF-I system components and their regulation by IL-1β.*

Tissue engineering strategies for cartilage repair often involve the *in vitro* expansion and of chondrocytes on tissue culture plastic (TCP), which leads to the loss of cell phenotype (i.e., dedifferentiation) after multiple passages [9-11]. Although 3-D suspension in hydrogels (e.g., alginate beads) has been shown to recover chondrocytic phenotype [12-16], the effects of these

culture strategies on hormonal signaling networks has not been considered. To investigate whether chondrocyte culture history influences the IGF-I signaling mediators and their regulation by IL-1, articular chondrocytes were either cultured as described in section 1.2.1 or grown continuously on TCP for comparison with intermediate alginate suspension (**Figure 1.2**). Bead and TCP cell monolayers were analyzed for IGF-I signaling mediators as well as for indicators of relative chondrocytic phenotype (cell growth, collagen expression). We postulated that culture pathway shapes the IGF-I signaling system of articular chondrocytes, altering their phenotypic response to exogenous IL-1β and IGF-I. Our findings are presented in Chapter 4.

1.3   Organization of Presented Work

Whereas Chapter 1 has provided a brief overview of the biomedical problems of interest and the specific research aims, a more in-depth review of the relevant scientific literature is made available in Chapter 2. Experimental results associated with the primary objectives are discussed in Chapters 3 and 4. The implications of these studies are summarized in Chapter 5, which also introduces future directions for research based on preliminary studies described in the appendices. Appendix A concerns cell-surface binding of IGF-I and attempts to identify contributing IGFBPs, Appendix B addresses the role of MAP-kinase signaling in the principal research findings, and Appendix C introduces a preliminary mathematical model of the extracellular domain of the IL-1 signaling system.
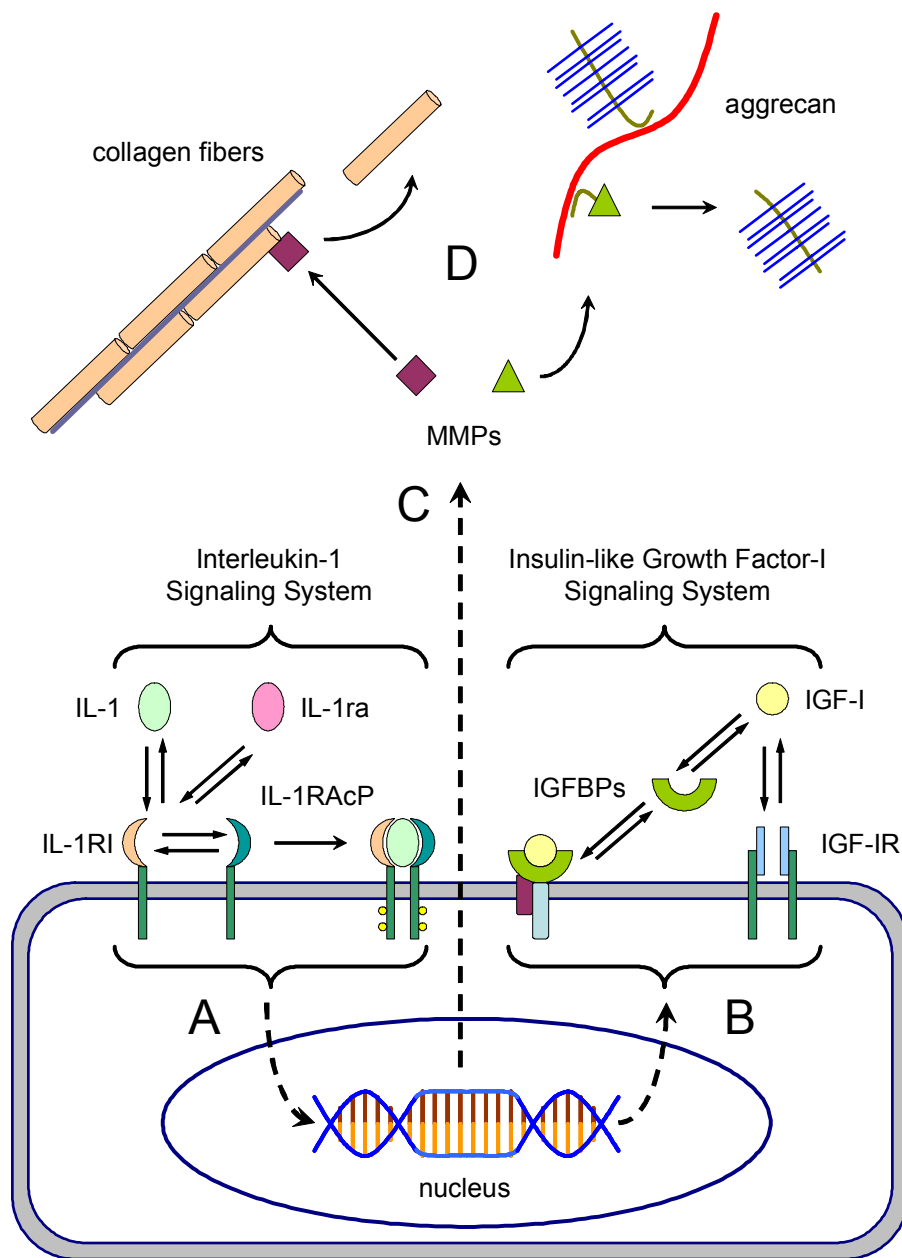
Figure 1.1. Characterizing the effects of IL-1β on the IGF-I signaling system. (**A**) IL-1 signal is transduced via a heterodimeric receptor complex. (**B**) The cytokine is thought to regulate the IGF-I signaling system, including the type I IGF receptor (IGF-IR) and both solution and cell-surface-sequestered binding proteins (IGFBPs). (**C**) IL-1 also stimulates matrix metalloproteinases (MMPs) that mediate its catabolic effects. (**D**) MMPs degrade cartilage extracellular matrix proteins such as type II collagen fibers and aggrecan.
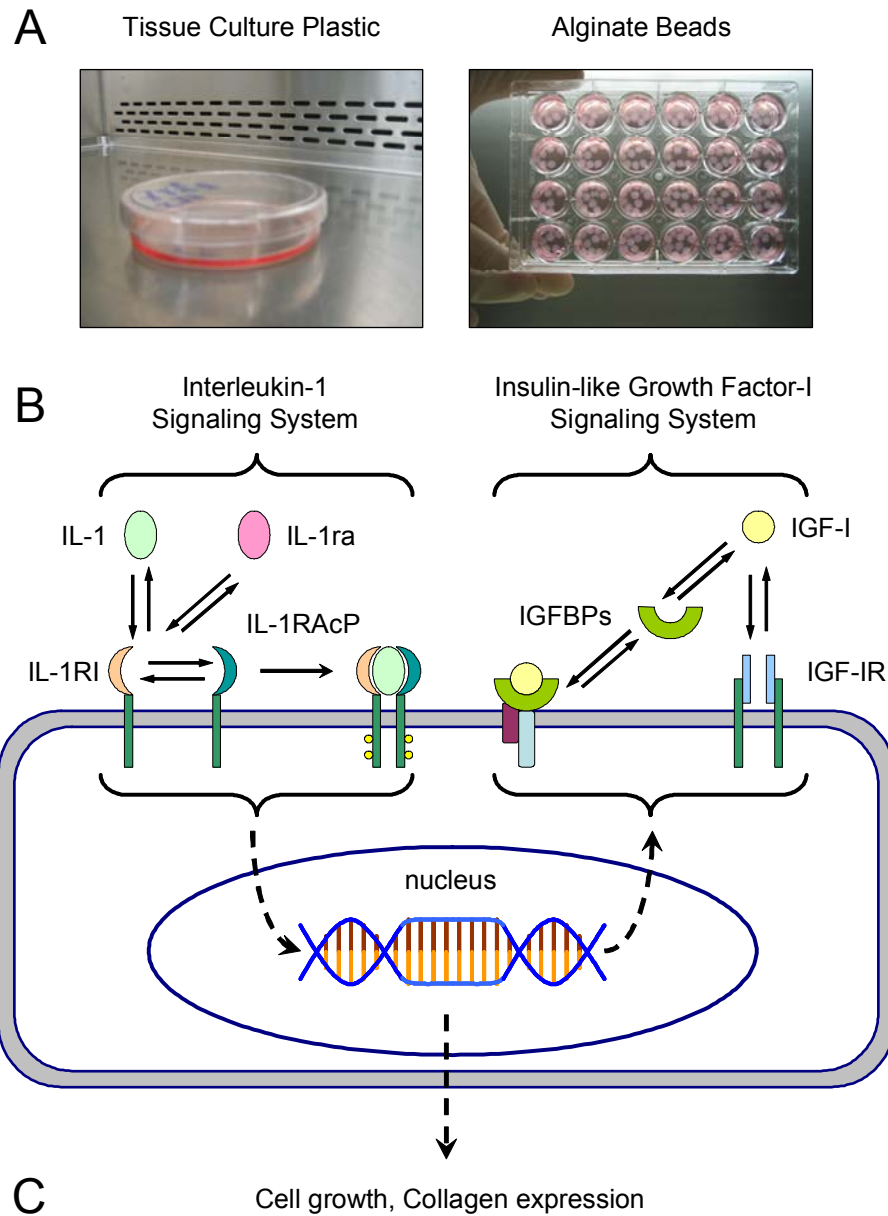
Figure 1.2. Examining the impact of culture strategy on the IGF-I system. (**A**) Articular chondrocytes isolated from equine stifle joints were expanded by serial passage as monolayers and either encapsulated in alginate beads (right) or maintained on tissue culture plastic (TCP; left). (**B**) Bead and TCP cells were plated at high-density, treated with IL-1β for 48 hr, and assayed for production of type I IGF receptor (IGF-IR), IGF binding proteins (IGFBPs), and endogenous IGF-I. (**C**) Culture pathway effects on the IGF-I system could alter phenotypic response (e.g., cell growth, collagen synthesis) of chondrocytes to exogenous IL-1 or IGF-I. Photographs courtesy of Casey MacQueen.

Chapter 2: Literature Review

2.1   Articular Cartilage

2.1.1   *Anatomy and Function*

Articular cartilage is among the most complex of connective tissues. Localized within diarthrodial (synovial) joints at the ends of long bones, this class of hyaline cartilage is completely avascular, aneural, and alymphatic. The articular surface is immersed in synovial fluid, which acts as a source of nutrients as well as hormonal signals. Tissue composition and architecture between this surface and the subchondral bone define the functional roles of articular cartilage: it provides low-friction articulation between surfaces within the synovial cavity and serves to both absorb and distribute compressive loads between bones. These functions are necessary for maintaining the musculoskeletal system over a lifetime of use.

2.1.2   *Extracellular Matrix Composition*

Articular cartilage consists of a network of collagen fibrils that contains a hydrated matrix of proteoglycans (e.g., aggrecan, decorin, biglycan), additional matrix glycoproteins (e.g., fibronectin, vitronectin), and a sparse cell population [17-19]. Fibrillar collagen constitutes >50% of the dry weight of cartilage. Heterotypic macrofibrils (**Figure 2.1**) are predominately constructed of type II collagen (about 90% of fibril weight) along with types IX and XI. Type II collagen is secreted by chondrocytes in the form of short procollagens – each consisting of three $\alpha1(II)$ polypeptide chains arranged in a helix – with carboxy- and amino-terminal extensions. Procollagens are converted to tropocollagens by extracellular cleavage of the extensions, and microfibrils form by end-to-end and lateral cross-linking of the tropocollagen monomers. Macrofibrils, ranging from 10 to 100 nm in diameter throughout cartilage, are assembled from cross-linked microfibrils. Type XI collagen is found within the core of macrofibrils, nucleating their assembly, wheras type IX collagen is found cross-linked to the surface of macrofibrils (antiparallel to their longitudinal axis) [20] and may link them to other matrix proteins. These collagen macrofibrils provide both tangential and longitudinal tensile strength to the articular cartilage.

The other principal macromolecular component of cartilage is a set of proteoglycans (approximately 20-30% of the tissue dry weight). Of these, the predominant proteoglycan found in articular cartilage is the aggrecan aggregate, which is made up of a large hyaluronan chain along which aggrecan monomers are noncovalently bound. Each aggrecan monomer (**Figure 2.2**) is composed of an individual protein backbone with branches of short keratin and chondroitin sulfate glycosaminoglycan (GAG) chains. The aggrecan core protein has three globular domains domains known as G1-G3. The amino-terminal G1 domain non-covalently binds with hyaluronan. GAG chains primarily bind to a linear region of the core protein located between the G2 and carboxy-terminal G3 domains. Attachment of the core protein to hyaluronan is stabilized by a link protein. A single aggrecan aggregate may bind as many as 100 aggrecan monomers, immobilized it within the network of collagen fibrils. The highly sulfated aggregate is extremely hydrophilic and yields a matrix that is about 70-80% water by volume [18]. Water retention produces an osmotic swelling pressure that is key to articular cartilage elasticity and compressive strength.

2.1.3 *Articular Chondrocytes*

The macromolecular composition of articular cartilage is maintained by specialized cells known as chondrocytes [17-19]. These cells are distributed throughout cartilage, but make up less than 5% of the tissue by volume [17]. Chondrocytes differentiate from mesenchymal progenitor cells during tissue development. With cartilage maturation, cell division slows so that growth is negligible within healthy adult cartilage. Chondrocytes maintain cartilage homeostasis by synthesizing new proteoglycans and collagen and by secreting proteases specific to these macromolecules. They communicate with their environment via both hormonal (e.g., cytokines, growth factors) and cell adhesion receptors. Chondrocyte adhesion receptors include integrins (fibronectin, collagens), anchorin, and CD44 (hyaluronan). The extracellular environment immediately surrounding chondrocytes, known as the pericellular matrix, is distinct from the bulk volume of cartilage. This region contains mostly decorin and aggrecan within a highly branched network of type VI collagen, which may mediate the binding of chondrocytes to matrix components. Surrounding the pericellular matrix is a region of relatively intact aggrecan called the territorial matrix. Within the deep layers of cartilage (see section 2.1.4), even further-

removed matrix, known as interterritorial regions, contains higher concentrations of partially degraded aggrecan.

2.1.4 *Zonal Organization of Cartilage*

The organization of articular cartilage components varies with depth (**Figure 2.3**), and the distinct zones each contribute to the overall tissue functions [17-19]. The layer of cartilage comprising the articular surface is known as the superficial (or tangential) zone. Within this region the collagen fibrils preferentially align parallel to the articular surface, and the proportion of proteoglycan is lower than in deeper regions. This configuration allows for increased resistance to shear forces during joint articulation and minimizes transport of water from deeper zones to the synovium in response to compression. Chondrocytes within this layer, which are elongated in the tangential direction, contribute to the lubricating properties of the articular surface by secreting the protein lubricin. Below the superficial zone is a region known as the intermediate zone (or midzone). Unlike the superficial layer, collagen fibrils in the intermediate zone are more randomly oriented and form an interlocking meshwork. Furthermore, proteoglycan content is higher within this zone. This region is primarily responsible for the absorption and transmission of compressive loads. Chondrocytes within the intermediate zone are rounded and relatively sparse. The next region of articular cartilage is referred to as the radial (or deep) zone. Aggrecan content is higher in this zone, but collagen fibrils are reduced. The fibrils that are present have a relatively large diameter and are oriented in the radial direction (or longitudinal with respect to the bone). Radial zone chondrocytes are also rounded, but unlike the other regions, these cells are found clustered in vertical columns. A layer of calcified cartilage acts as a buffer between the uncalcified layers and subchondral bone. The border between calcified and uncalcified cartilage is called the tidemark. Radially-oriented collagen fibrils extend below the tidemark, but proteoglycans do not. Chondrocytes embedded within calcified cartilage are hypertrophic and synthesize type X collagen. The convoluted interface between calcified cartilage and subchondral bone, called the cement line, helps maintain cartilage-bone adhesion.

2.2   Osteoarthritic Cartilage

2.2.1   *Anatomical and Functional Alterations*

Osteoarthritis (OA), also known as degenerative joint disease or osteoarthrosis, is a chronic disorder characterized by the deterioration of articular cartilage (**Figure 2.4**).   The osteoarthritic condition progresses slowly from a combination of hormonal and biomechanical factors [17, 21].   Regarding mechanical regulation, structural disruptions of the cartilage matrix by insufficient, excessive, or irregular loading may contribute to the development/progression of OA.   The fibrillation (i.e., roughening) of articular surfaces constitutes an early manifestation of the disorder.   Progression of fibrillation leads to abnormal loading of cartilage and the development of fissures that extend into the tissue, eventually reaching the subchondral bone.   This erosion of articular surface results in subchondral bone stiffening and osteophyte (bone spur) formation.   The release of cartilage fragments into the synovium induces an inflammatory response from synovial cells and macrophages.   Common clinical symptoms of this disorder include substantial joint pain, stiffness, and loss of mobility.

2.2.2   *Biochemical Alterations*

At the molecular level, OA has been attributed to a shift in the balance between synthesis and degradation of ECM macromolecules by articular chondrocytes.   The alterations in matrix metabolism are complex and vary with progression of the disorder.   During the early stages of OA, proteoglycan synthesis actually increases [22], resulting in cartilage thickening [23].   However, the relative composition of GAGs synthesized by osteoarthritic chondrocytes is abnormal [22].   In more advanced osteoarthritic cartilage, proteoglycan synthesis is reduced and the rate of ECM degradation exceeds anabolic repair mechanisms [24].   The changes in proteoglycan and collagen synthesis may contribute to the increase in water content observed within osteoarthritic cartilage [18].   Chondrocytes have been observed to proliferate and form cell clusters in arthritic cartilage [25].

Increased levels of matrix metalloproteinases (MMPs) [26-28] enhance degradation of collagen fibrils and proteoglycans.   The MMP family of zinc-dependent proteases includes collagenases 1, 2, and 3 (MMPs 1, 8, and 13), gelatinases (non-fibrillar collagenases) A and B (MMPs 2 and 9), and stromelysin-1 (MMP-3) [29].   The collagenases cleave the Gly^{975}-Leu^{976}

bond of the α1(II) chain in fibrillar collagens (e.g., types II, IX, X, and XI), producing three-quarter and one-quarter-length fragments [30, 31]. Stromelysin-1 (MMP-3) has a broad range of targets, cleaving aggrecan core protein as well as fibrillar collagens near cross-linking hydroxylysine sites [32]. This protease can also activate the proforms of other MMPs, including MMP-1 [33] and MMP-9 [34]. The gelatinases (MMP-2 and MMP-9) are thought to degrade collagen XI, aggrecan core protein, and link protein [35-37]. Tissue inhibitors of metalloproteinases (TIMPs), which inactivate MMPs by non-covalent binding in a 1:1 complex [38], are also synthesized by chondrocytes and synovial cells. However, MMP activity exceeds that of TIMPs within osteoarthritic cartilage [39, 40]. In addition to MMPs/TIMPs, aggrecanases 1 and 2, members of the ADAM protein family, have also been identified in arthritic cartilage [41] and cleave aggrecan core protein at multiple sites through MMP-independent mechanisms [42].

The proinflammatory cytokines interleukin-1 (IL-1) and tumor necrosis factor-α (TNF-α) are thought to be the principal regulators of cartilage degradation [43, 44]. These cytokines are secreted by synovial cells and chondrocytes. Their levels are enhanced within arthritic joints, stimulating the production of other inflammatory mediators such as prostaglandin E_2 (PGE$_2$), nitrix oxide (NO), and other pro-inflammatory cytokines (e.g., IL-6, IL-8) [45]. TNF-α plays a key role in joint inflammation, but not necessarily cartilage destruction [46], and may regulate the latter by enhancing synovial cell synthesis of IL-1 [47].

2.3   Insulin-like Growth Factor-I and Articular Cartilage

2.3.1 *The IGF Signaling System*

Insulin-like growth factor-I (IGF-I) is a member of the IGF family of proteins, otherwise known as somatomedins [48], which also includes IGF-II and insulin [49]. The two IGF isoforms, IGF-I and IGF-II, have molecular weights of 7.5 and 7.4 kDa, respectively [50, 51], and are structurally similar to one another [52] and to proinsulin [53]. Circulating levels of IGF-I are produced by the liver in response to growth hormone (GH) stimulation by the pituitary gland [54]. In addition to its endocrine activity, IGF-I is secreted by cells from a variety of tissues and acts through autocrine/paracrine mechanisms to regulate cell growth, differentiation, and various metabolic activities [55-58].

IGF biological activities are mediated by two specific transmembrane receptors, type I and type II, with substantially different structures and functions. The type I receptor (IGF-IR) is a heterotetrameric glycoprotein composed of two extracellular α subunits (~130 kDa each) and two transmembrane β subunits (~90 kDa each). The α and β subunits are linked by disulfide bridges, forming a tetramer complex with two $\alpha\beta$ dimers [59]. The α subunits – with cystein-rich domains – are responsible for ligand binding [60]. Each β subunit has a tyrosine kinase domain within the cytoplasmic portion of its chain. Upon ligand binding to the α subunits, a conformational change in β subunits leads to trans-autophoshorylation of tyrosine residues in the tyrosine kinase domains [61], and the activated receptor tyrosine kinases activate intracellular signal transduction pathways (**Figure 2.5**) [49, 62]. Specifically, the receptor tyrosine kinases phosphorylate additional tyrosines in neighboring domains of the β subunits (e.g., juxtamembrane, carboxy-terminal domains), and the resulting phosphotyrosines act as docking sites for the insulin receptor substrate (IRS) and src homology and collagen (Shc) proteins [63]. These adapter proteins in turn recruit and activate additional kinases that are associated with multiple signaling pathways [49]. IRS-1 activates the phosphatidylinositol 3-kinase (PI3-K) pathway by recruiting the p85 subunit of PI3-K [64], while Shc activates the mitogen-activated protein kinase (MAPK) pathways by association with growth factor receptor-bound protein 2 (Grb2) and subsequent activation of the G-protein Ras [65]. The type I receptor mediates most biological effects of both IGF isoforms [66].

Type II IGF receptor is composed of a single transmembrane chain (~220 kDa) with a large, cysteine-rich extracellular domain and a short cytoplasmic domain [67]. This receptor is identical to the cation-independent mannose-6-phosphate receptor [68], which mediates transport of bound proteins to lysosomes [69]. The Type II receptor does not have the signaling capabilities of IGF-IR [70], but is thought to function as a clearance mechanism for IGF-II [71]. IGF-I has less affinity for type II receptor compared to IGF-II [57], whereas IGF-II and insulin have less affinity for IGF-IR relative to IGF-I [72, 73].

In addition to transmembrane receptors, a group of extracellular IGF binding proteins (IGFBPs) have high affinity for the IGFs and regulate their biological activity [74]. Six distinct binding proteins (IGFBPs 1-6), representing separate gene products, have been purified and characterized to-date from multiple tissue sources [75]. IGFBPs 1-5 bind both IGF-I and IGF-II with similar affinity, whereas IGFBP-6 has a significantly higher affinity for IGF-II [76].

Circulating IGFBPs act as carriers for IGF-I and prolong its half-life during transport to target tissues. Within tissues, locally secreted binding proteins can be found soluble in the interstitial fluid, bound to ECM components, or bound to cell surfaces [77]. IGF sequestration by IGFBPs can either inhibit growth factor activity by reducing IGF-IR binding or potentiate activity by protecting IGF from proteolytic degradation and localizing ligand in proximity to IGF-IR. The precise regulatory roles depend on the specific binding protein and the environmental conditions (e.g., extracellular matrix composition, protease activity, pH) [78-80]. For example, IGFBP binding to cell surface proteins may act to reduce their affinity for IGFs, releasing the growth factors in close proximity to receptors. IGFBP-2 binds with cell surface proteoglycans in the brain, and its binding to chondroitin-6-sulfate *in vitro* lowered affinity for IGF-I 3-fold [81]. IGFBP-1 and IGFBP-2 both have RGD motifs near their carboxy termini [82], which are known to bind cell surface integrins [83]. Proteolytic degradation of binding proteins may also affect their regulatory actions. Both serine proteases [84] and MMPs [85, 86] have been reported to degrade IGFBPs into fragments with reduced affinity for IGF-I.

2.3.2   *Effects of IGF-I on Cartilage Homeostasis*

IGF activity was first reported nearly a half-century ago in cartilage, in which the authors described a GH-dependent serum factor that was able to stimulate radiolabeled sulfate incorporation into chondroitin sulfate [87]. Since that time, a great deal of information has been collected on the role of IGFs in cartilage metabolism. IGF-I is substantially more potent than IGF-2 in cartilage explants [88]: whereas IGF-I stimulates collagen [89] and proteoglycan [88, 90-92] synthesis in adult cartilage, IGF-II regulates glucose metabolism in mature cartilage and growth in fetal tissue [93]. Both human and bovine articular chondrocytes express IGF-IR [4, 73, 94]. IGF binding proteins 2, 3, 4, and 5 have been identified in cartilage from human and animal sources [95-98]. IGFBP-2 is strongly cell-associated in bovine cartilage [99].

In osteoarthritic cartilage, chondrocytes secrete higher levels of IGF-I [100-102]. Moreover, IGF-I receptor synthesis has been reported at normal [98] or higher [4, 103] levels for human osteoarthritic chondrocytes. However, chondrocytes are non-responsive to the growth factor in osteoarthritic cartilage explants [4] and in experimental OA models [5, 6]. It has been postulated that non-responsiveness could be attributed to increased secretion of IGFBPs by osteoarthritic chondrocytes [98, 101, 104].

2.4   Interleukin-1 and Articular Cartilage

2.4.1   *The IL-1 Signaling System*

Composition of the interleukin-1 (IL-1) signaling system resembles that of the IGF-I axis: this network includes multiple ligand isoforms, both signaling and non-signaling membrane receptors, and soluble proteins with high affinity for ligands.   IL-1 is a pro-inflammatory cytokine which plays an important regulatory role in the immune system and affects multiple tissues/organ systems, including the blood vessels, central nervous system, gastrointestinal tract, joints, and lungs [105].   IL-1 constitutes a subfamily with two isoforms, IL-1α and IL-1β, which are products of separate genes but are relatively homologous, having similar biological activity. Both forms are synthesized as (32 kDa) precursors that are cleaved into 17.5 kDa mature forms. ProIL-1α is active and cleaved by the calcium-dependent, neutral protease calpain [106]. Conversely, proIL-1β is inactive until processed into the mature form by a cysteine-dependent protease known as IL-β converting enzyme (ICE) or caspase-1 [107].   In addition to the two agonists, the IL-1 family also includes a naturally occurring IL-1 receptor antagonist (IL-1ra), which competes with IL-1α/β for receptor binding but does not transduce signal [108, 109].

The compliment of IL-1 receptors is complex and their interactions are still being characterized (**Figure 2.6**).   Two transmembrane IL-1 receptors with ligand binding capability have been identified to-date: the 80 kDa type I receptor (IL-1RI) [110] and the 68 kDa type II receptor (IL-1RII) [111].   The IL-1 receptor subfamily also includes a transmembrane co-receptor known as the IL-1 receptor accessory protein (IL-1RAcP) [112].   These proteins all have extracellular regions that contain three immunoglobulin(Ig)-like domains.   The IL-1 subfamily has been classified within the Toll/IL-1 receptor (TIR) superfamily, since these proteins – with the exception of IL-1RII – share a conserved 200 amino acid cytoplasmic domain, the TIR domain, with the Toll-like receptor (TLR) subfamily [113].   IL-1α and β exert their biological actions through interaction with IL-1RI [114].   Ligand-bound IL-1RI associates with IL-1RAcP to form a heterodimeric receptor complex [115], which is required for transduction of IL-1 signal [116-119].   The accessory protein is thought to stabilize the IL-1/IL-1RI complex, slowing dissociation of IL-1 from the complex [120].   Type II receptor binds IL-1α/β, but lacks the cytoplasmic TIR domain and does not transduce signal [111], despite

association with IL-1RAcP after ligand binding [121, 122]. IL-1RII is believed to function as a decoy receptor, inhibiting IL-1 activity by sequestering both ligand and accessory protein from IL-1RI [123]. IL-1ra also inhibits IL-1 activity by binding with IL-1RI to form a complex that cannot associate with IL-1RAcP to transduce signal [112].

In addition to their transmembrane forms, IL-1RI, IL-1RII, and IL-1RAcP also have soluble forms (sIL-IRI, sIL-1RII, and sIL-1RAcP) that are produced either by proteolytic cleavage of the extracellular domains from transmembrane receptors [124] or by translation of alternative mRNA slice variants [112, 125, 126]. The functions of these soluble receptors have not been fully characterized, but initial studies have suggested inhibitory actions on ligand activity [125, 127-130]. For example, soluble type II receptor has similar binding affinity for IL-1α/β as its membrane-bound counterpart, but reduced affinity for IL-1ra, so that its inhibitory effects are additive to that of the receptor antagonist [127, 130]: whereas sIL-1RII acts at the ligand level, IL-1ra acts at the receptor level. Conversely, the combined inhibition of sIL-1RI and IL-1ra is less than that of either agent alone [127]. IL-1 and IL-1ra have similar affinities for sIL-1RI, and thus IL-1ra may compete with IL-1 for sIL-1RI, producing IL-1ra/sIL-1RI complexes and reducing the number of both inhibitor pools. The soluble accessory protein (sIL-1RAcP) also suppresses IL-1 signaling [125, 128], possibly by enhancing sIL-1RII affinity for IL-1 [129].

2.4.2 *IL-1 Signal Transduction*

As described above, association of bound IL-1/IL-1RI with IL-1RAcP initiates signal transduction (**Figure 2.7**) [113]. Heterodimeric complex formation likely leads to conformation change in the two cytoplasmic TIR domains. These changes allow for myeloid differentiation (MyD) marker 88 (MyD88) [119, 131] and Toll-interacting protein (Tollip) [132] adapter proteins to be recruited to specific locations along the TIR domains [133]. MyD88 may associate with both receptor and co-receptor TIR domains as a dimer [134]. IL-1 receptor associated kinase (IRAK) then rapidly translocates to the receptor complex and interacts with the 'death' domain (DD) of MyD88 [135, 136]. Two forms of this serine/threonine kinase have been identified, IRAK-1 and IRAK-2, with the latter associating preferentially with the IL-1RI cytoplasmic domain [131]. Tollip is complexed with IRAK-1 prior to receptor association, likely interacting with the N-terminal DD of IRAK, and may inhibit IRAK dimerization [132].

14

Tollip translocates to the receptor complex along with IRAK, allowing for association of IRAK and MyD88 DDs. Two Tollip/IRAK complexes may be recruited to interact with MyD88 adapters along both TIR domains. Once bound to the receptor complex, the kinase domain of IRAK-1 is autophosphorylated [137]. The activated kinase then catalyzes multiple autophosphorylations along the proline-, serine-, threonine-rich (ProST) region, which lies between the kinase and N-terminal DD regions. Hyperphosphorylation of IRAK-1 introduces several negative charges along ProST region, leading to dissociation from Tollip and the receptor complex [132, 137]. Dissociated IRAK-1 interacts with tumor necrosis factor (TNF) receptor associated factor 6 (TRAF6) within the cytosol [135]. IRAK also recruits the membrane-associated TAB2, which stands for transforming growth factor β (TGFβ)-activated kinase 1 (TAK1) binding protein 2 [138]. TAB2 allows for association of TAK1 and its activator protein TAB1 to form a complex with IRAK and TRAF6 [139]. Complex formation leads to the addition of polyubiquitin chains onto TRAF6 [140], which in turn induces autophosphorylation of TAK-1 [141]. TAK-1, a mitogen-activated protein kinase (MAPK) kinase kinase (MAPKKK) [142], phosphorylates IκB-kinase β (IKKβ) and MKK6 [143]. These kinases activate multiple pathways, including nuclear factor-kappa B (NF-κB) and the MAPK family. IL-1 may also stimulate the PI3-K pathway [144-146].

2.4.3 *IL-1 Activation of MAPKs*

Interleukin-1 has been reported to activate members of the MAPK family in both rabbit and human articular chondrocytes and a human chondrosarcoma cell line [147-149]. This family includes extracellular signal-regulated kinases (ERK-1 and-2), p38 MAPK, and c-Jun NH_2-terminal kinases (JNKs; also known as stress-activated protein kinases, SAPKs) [150]. Recent studies have utilized specific MAPK inhibitors to demonstrate the role of these kinases in IL-1 regulation of chondrocyte gene expression. For example, IL-1 induction of collagenase-3 (MMP-13) gene expression in human articular chondrocytes and a chondrosarcoma cell line (SW-1353) required activation of both the p38 and JNK MAPKs as well as AP-1 and NF-κB transcription factors [149, 151]. Liacini *et al.* [152] confirmed these conclusions using both human and bovine articular chondrocytes, adding that stromelysin-1 (MMP-3) expression was mediated by the same set of MAPKs and transcription factors. Mendes *et al.* [153] demonstrated that p38 MAPK and NF-κB are independent mediators required for the IL-1-induced expression

of inducible nitric oxide synthase (iNOS), an enzyme that produces the inflammatory mediator nitric oxide (NO). However, ERK-1/2 and AP-1 are not involved in this mechanism.

Of the available MAPK inhibitors, the suppressing actions of SB203580, PD98059, and U0126 have been demonstrated most frequently in chondrocyte cultures [149 2001, 152, 154, 155]. SB203580 has been shown to inhibit p38 MAPK at lower concentrations (1 μM) and JNK at higher levels (25 μM) [156, 157]. PD98059 suppresses inactive forms of MAPK/ERK kinase-1 (MEK-1), the activator for ERKs-1 and -2 [158]. U0126 inhibits both active and inactive forms of MEK-1 and MEK-2 [159].

2.4.4 *Effects of IL-1 on Cartilage Homeostasis*

Interleukin-1 is produced within diarthrodial joints by synovial cells [160] and healthy articular chondrocytes [161, 162]. The type I receptor is also expressed by chondrocytes [161]. IL-1α and IL-1β are present in a molar ratio of about 1:4 in adult human cartilage [163], and both IL-1β and its activator ICE are preferentially localized within the superficial layer [164]. Exogenous IL-1 is a potent catabolic regulator of articular chondrocytes, inhibiting proteoglycan synthesis [165, 166] and enhancing proteoglycan degradation [165, 167]. IL-1 inhibits aggrecan synthesis by down-regulating core protein expression [168]. The cytokine also regulates collagen synthesis in human chondrocyte cultures, down-regulating type II expression and up-regulating types I and III [169, 170]. IL-1 enhances cartilage degradation by stimulating the secretion of MMPs [171-174] and the inflammatory mediators PGE$_2$ [175, 176] and NO [177, 178].

Interleukin-1 has been implicated as a major factor in the cartilage deterioration associated with OA [179, 180]. In arthritic joints, increased concentrations have been observed within both cartilage [181-183] and surrounding synovial fluid [184, 185]. Moreover, IL-1RI density is higher on both chondrocytes [186] and synovial fibroblasts [187] from osteoarthritic joints. Enhanced secretion of IL-1 may be attributed more to synovial fibroblasts and synovium-associated macrophages [160] than articular chondrocytes [103]. Increased IL-1 secretion may be regulated by fibronectin fragments [188] and TNF-α activity [47]. In experimental OA models, blocking of IL-1 activity with receptor antagonist by intraarticular injection [43] or by gene transfer of IL-1ra [189, 190] prevented cartilage degradation, indicating the importance of IL-1 in OA etiology.

As described above, IGF-I and IL-1 have opposite effects on cartilage homeostasis. In addition, each factor counteracts the activity of the other when co-incubated. IGF-I reverses the catabolic effects of cartilage explants exposed to IL-1 [7, 191] by inhibiting degradative activities [192]. IGF-I also blocked IL-1-induced collagen degradation in bovine cartilage and inhibited IL-1-induced expression of MMP-1, MMP-3 and MMP-13 mRNAs in bovine and human articular chondrocytes [193]. Similarly, IL-1 blocks IGF-I-stimulated proteoglycan synthesis in porcine [7] and rat [8] cartilage explants. The cytokine enhances synthesis of binding protein IGFBP-3 in human and rat articular chondrocyte cultures [194, 195] and IGFBP-5 [196] in ovine cultures. IL-1 may also decrease IGF-IR tyrosine phosphorylation, an initial step in IGF signal transduction, by inducing nitric oxide synthesis, though the underlying mechanism has not been identified [197]. Using an experimental OA model, IL-1 has been identified as a cofactor in the hyporesponsiveness of osteoarthritic chondrocytes to IGF-I [6].

2.5   *In vitro* Culture Models for Articular Chondrocytes

2.5.1   *Tissue Culture Plastic*

The classical model for mammalian cell culture *in vitro* involves adherence of cells to treated plastics such as polystyrene. This system simplifies analysis of cellular activity in terms of treatment administration and homogeneity of cell populations. Furthermore, tissue culture plastic (TCP) has been utilized for the expansion of donor cells – isolated from small biopsies – whose numbers are insufficient for defect repair strategies [13, 198, 199]. These cells can be reintroduced to defect sites by direct injection or embedded within engineered scaffolds. For example, articular chondrocytes cultured with this methodology have been re-injected into human [200, 201] and equine [202] diarthrodial joints, a procedure known as autologous chondrocyte transplantation (ACT), with promising effects on cartilage reconstruction. Expanded articular and nasal septal chondrocytes have also been used for engineered neocartilage [203-205].

One problem with this culture strategy is that primary chondrocytes lose their characteristic phenotype, or dedifferentiate, after serial passaging on TCP [9-11]. Cells become elongated, and synthesis of type II collagen decreases in favor of types I and III, such that dedifferentiated chondrocytes resemble fibroblasts. Furthermore, proteoglycan synthesis is

altered [206, 207], as synthesis of aggrecan decreases and smaller proteoglycans increases. Chondrocyte dedifferentiation may be mediated by changes in intracellular actin organization during TCP culture, as the shift in collagen synthesis coincides with the development of well-defined actin cables [207]. The specific changes in phenotype are dependent on cell seeding density [199, 208], passage number [205], and soluble factors within the culture medium [169, 170, 209]. Therefore, culture methods that maintain or restore chondrocyte phenotype have been developed for both tissue engineering and cell biology applications [10, 12].

2.5.2 *Alginate Bead Culture*

Within the past decade, alginate gels have been established as an attractive alternative for chondrocyte culture *in vitro* [210-212]. Alginate, a linear polysaccharide of *L*-guluronic and *D*-mannuronic acids (two uronic acids), is derived from marine brown algae. Though unsulfated, this polysaccharide is negatively charged and polymerizes to form a gel in the presence of calcium or other divalent cations [213]. This gel can be readily dissociated with the addition of a chelating agent (e.g., sodium citrate, ethylenediamine tetra-acetic acid (EDTA)), allowing for rapid recovery of cells and synthesized ECM molecules for analysis. Articular chondrocytes encapsulated in calcium alginate remain phenotypically stable for up to 8 months in culture, synthesizing a cartilage-like matrix within the gel [212, 214, 215]. These chondrocytes synthesized both aggrecan and a cross-linked collagen network made up of types II, IX and XI [215]. Two distinct matrix compartments were characterized within these cultures: a cell-associated matrix (CM) with aggrecan anchored to cell-bound hyaluronan, and a further-removed matrix (FRM) that separates from the cells and CM following gel dissociation. Aggrecan within the CM was turned over at a faster rate than aggrecan that had migrated to the FRM [214]. Chondrocyte characteristics also varied throughout the beads: cells near the bead surface were flattened, whereas those found deeper within the bead were more round and surrounded by a denser matrix [212].

The bead culture system described above has been used to study chondrocyte metabolic activity *in vitro*, including their responses to growth factors and cytokines [15, 16, 216-221]. Furthermore, chondrocytes that were dedifferentiated following monolayer expansion have been shown to redifferentiate after a short period in alginate beads [12-16]. Therefore, the alginate system has been explored as a scaffold for reestablishing chondrocyte phenotype prior to

implantation [13, 198, 199]. However, little work has been done to determine how alginate bead culture affects chondrocyte signaling. Thomas *et al.* [218] cultured a temperature-sensitive articular chondrocyte cell line (tsT/ACAC62) in alginate, subcultured the cells in high-density monolayer, and demonstrated that IL-1 increases cyclooxygenase-2 (COX-2) expression through a p38 MAPK-dependent mechanism. They also noted that alginate culture enhanced IL-1 stimulation of p38 activity. Robbins *et al.* [222] used the same cell line to show that IL-1 down-regulation of type II collagen (α1(II)) expression was also dependent on p38 MAPK and that overall levels of α1(II) mRNA were higher in alginate culture compared to cells maintained on TCP.

2.6 Equine Models for Cartilage Metabolism and Joint Disease

2.6.1 *Equine Osteoarthritis*

The equine osteoarthritic disease state is similar to that described in section 2.2 [21]. Elevated concentrations of IL-1 [223] and released GAG [224] have been detected in synovial fluid from horses with OA. The activity of various MMPs, including the gelatinases (MMP-2 and MMP-9) [35], are also elevated. As with human OA, progression of equine joint destruction has been attributed to an imbalance between cartilage matrix degradation and repair mechanisms.

2.6.2 *Equine models for articular cartilage metabolism*

Multiple studies on equine cartilage explant cultures have demonstrated the catabolic effects of exogenous IL-1 on proteoglycan metabolism [223, 225-228]. However, these studies used recombinant IL-1 from other species to examine cytokine effects. It has been suggested that the species source of IL-1 significantly influences biological response [229, 230], which may be attributed to differences in amino acid sequence among species. The sequence homology between human and equine IL-1 has been reported to be 66.4% [231] and 71.6% [232] for IL-1α and 66.7% [232] and 72.7% [231] for IL-1β. Recently characterized recombinant equine IL-1α and IL-1β have been used to examine cytokine effects on proteoglycan turnover and prostaglandin E_2 secretion in equine cartilage explants [2] as well as MMP/TIMP gene expression in high-density equine chondrocyte monolayers [233].

Equine articular chondrocytes have been successfully isolated and cultured on TCP [234]. These cells dedifferentiated with multiple passages and took on a fibroblast-like morphology after the fifth passage. Equine chondrocytes have also been cultured on TCP coated with poly(2-hydroxy)ethyl methacrylate, a surface that maintains the spherical morphology of chondrocytes, to show that IL-1 up-regulates collagenase-1 expression to a greater extent than TIMP-1 [235]. Synthesis of MMP-2 and MMP-3, but not MMP-9, were also enhanced in response to IL-1 treatment. When equine chondrocytes are grown in alginate, the ECM formed after 30 days resembles that described for other species [212, 214, 215], with distinct compartmentalization of multiple proteoglycans [236]. This culture model has been used to demonstrate that equine chondrocyte secretion of gelatinases (MMP-2 and MMP-9) was regulated by treatment with TGFβ [237].
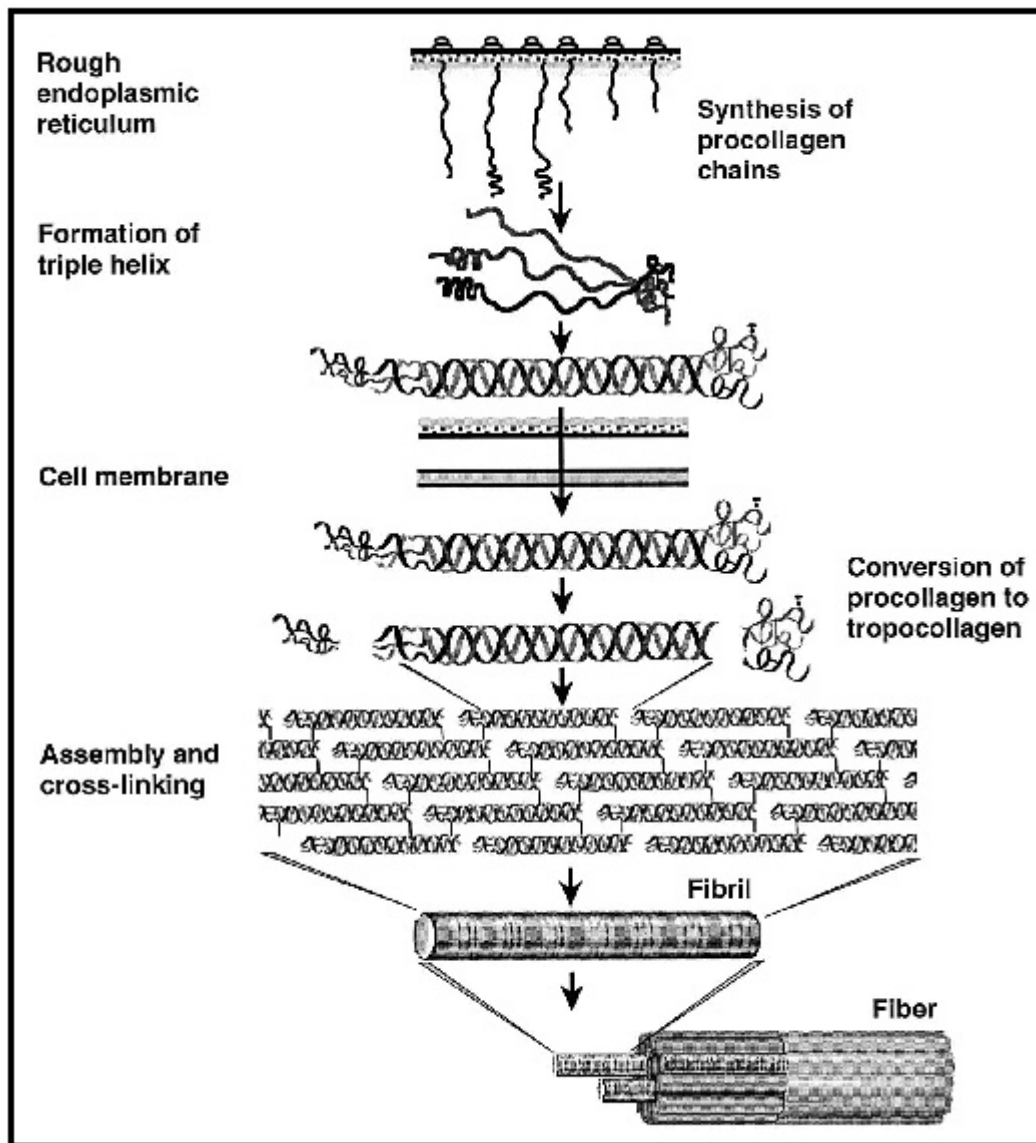
Figure 2.1. Synthesis of type II collagen macrofibrils. Collagen is synthesized within the endoplasmic reticulum as individual a1(II) chains with amino- and carboxy-terminal extensions. These individual a1(II) chains are arranged in a triple helix to form procollagen. After secretion from the cell, the procollagens are converted to tropocollagens by proteolytic cleavage of the extensions. Microfibrils form by end-to-end and lateral cross-linking of tropocollagen monomers. Macrofibrils (fibers) are assembled from cross-linked microfibrils. Reprinted with permission from Kielty CM, Hopkinson I, Grant ME. Collagen: the collagen family, structure, assembly, and organization in the extracellular matrix. In: Royce PM, Steinmann BS, eds. Connective Tissue and Its Inheritable Disorders: Molecular, Genetic, and Medical Aspects. New York, NY: Wiley-Liss; 1993: 113.
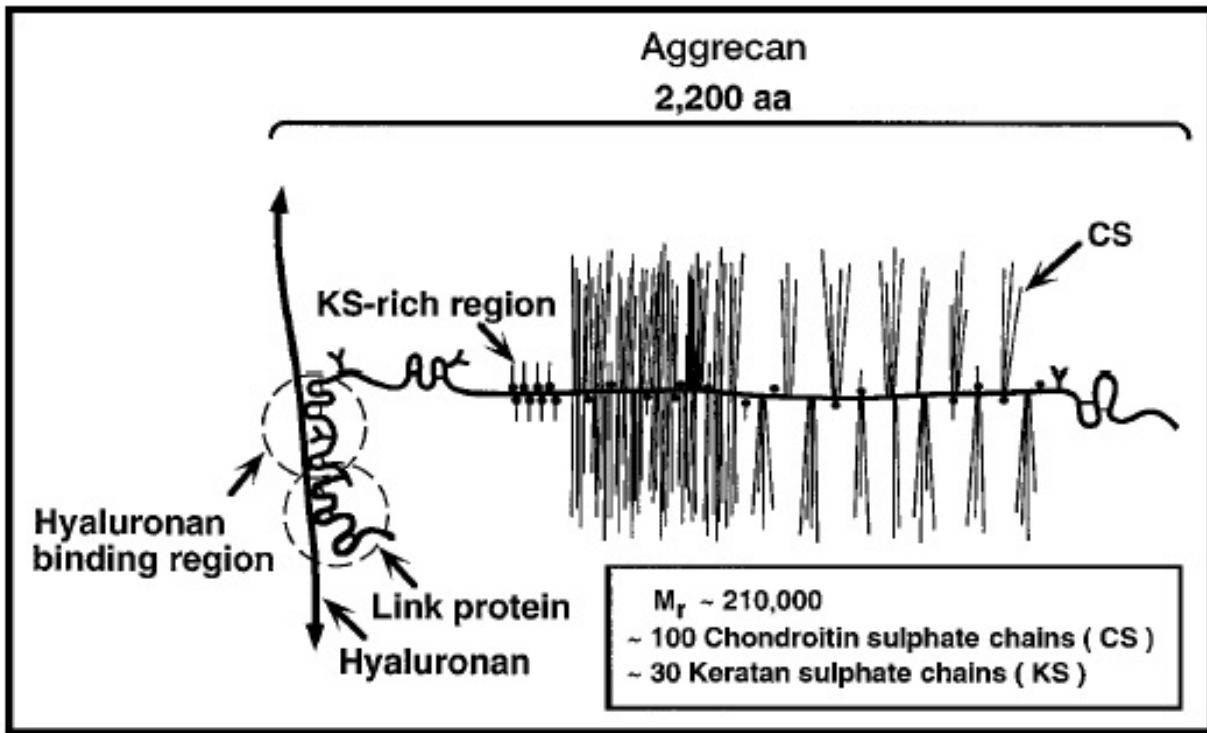
Figure 2.2. Structure of the aggrecan monomer. Aggrecan monomers (~210,000 kDa) consist of a core protein and attached keratin and chondroitin sulfate glycosaminoglycan (GAG) chains. The aggrecan core protein has three globular domains named (G1, G2 amd G3). Aggrecan monomers non-covalently bind to long hyaluronan chains to form large aggrecates. Monomer binding occurs at the amino-terminal G1 domain and is stabilized by a link protein. GAG chains attach primarily to a region between the G2 and carboxy-terminal G3 domains. Reprinted with permission from Heinegard D, Oldberg, A. Glycosylated matrix proteins. In: Royce PM, Steinmann BS, eds. Connective Tissue and Its Inheritable Disorders: Molecular, Genetic, and Medical Aspects. New York, NY: Wiley-Liss; 1993: 193.
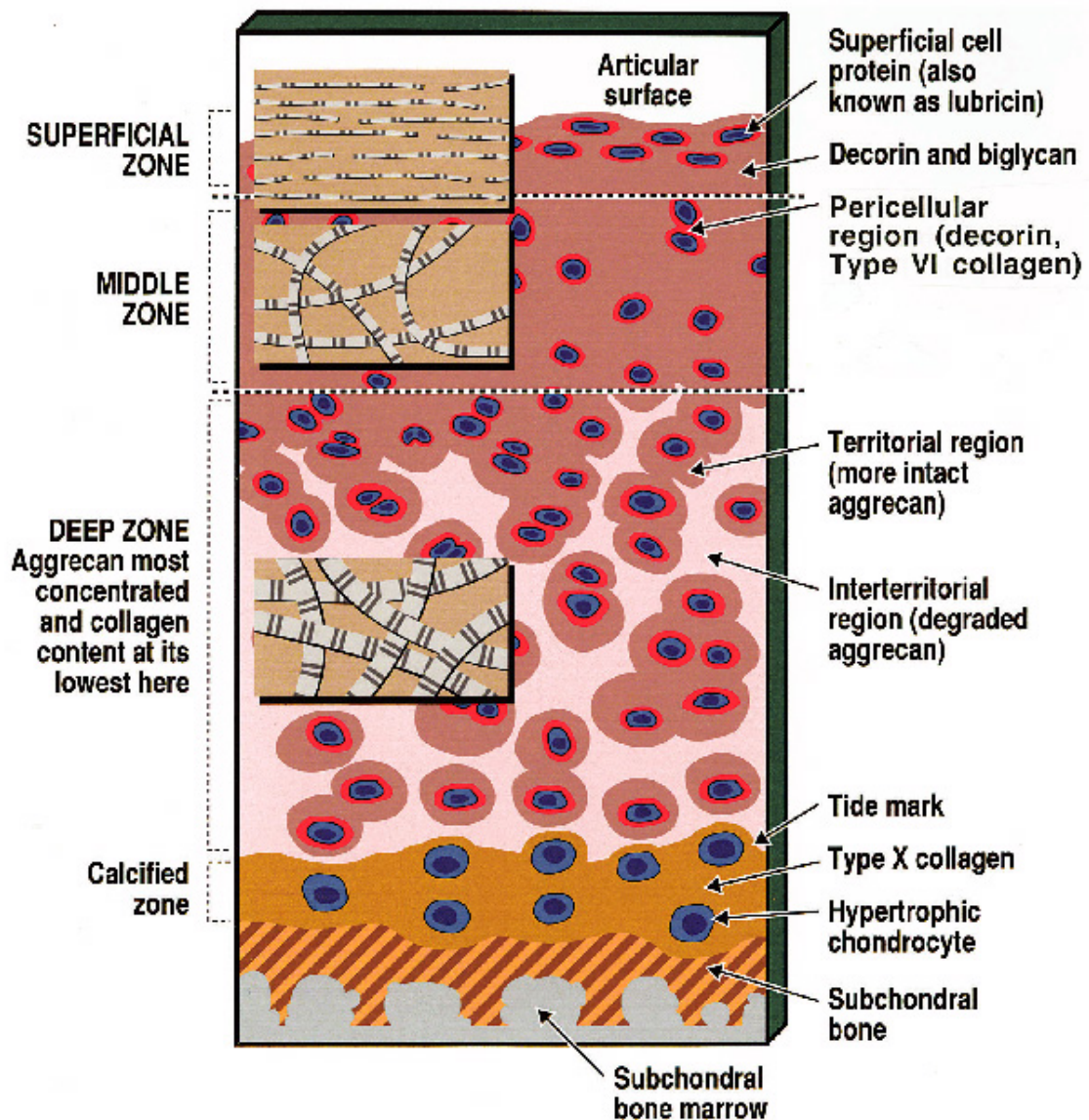
Figure 2.3. Zonal organization of articular cartilage. Four distinct cartilage layers are represented from the articular surface to the subchondral bone: superficial, middle, deep, and calcified zones. Chondrocytes are blue. Insets show relative thickness and orientation of collagen macrofibrils within the various zones. Furthermore, color schemes indicate distinct regions of matrix composition that are related to cell proximity: pericellular (red), territorial (dark brown), and interterritorial (pink). Reprinted from *Clinical Orthopaedics and Related Research*, v391S, Poole AR, Kojima T, Yasuda T, Mwale F, Kobayashi M, and S Laverty, Composition and Structure of Articular Cartilage: a Template for Tissue Repair, p. S28, Copyright 2001, with permission from Lippincott Williams & Wilkins.

A Healthy Joint

In a healthy joint, the ends of bones are encased in smooth cartilage. Together, they are protected by a joint capsule lined with a synovial membrane that produces synovial fluid. The capsule and fluid protect the cartilage, muscles, and connective tissues.

A Joint With Osteoarthritis

With osteoarthritis, the cartilage becomes worn away. Spurs grow out from the edge of the bone, and synovial fluid increases. Altogether, the joint feels stiff and sore.

Figure 2.4. Progression of osteoarthritis in the diarthrodial joint. Early on there is a fibrillation, or roughening, of the articular surface that eventually progresses into the development of fissures that extend towards the subchondral bone. The erosion of cartilage leads to subchondral bone stiffening and osteophyte (bone spur) formation. Cartilage fragments are released into the synovium, inducing an inflammatory response from synovial cells. Common clinical symptoms of advanced OA include substantial joint pain, stiffness, and loss of mobility. Figure from the NIAMS website:

http://www.niams.nih.gov/hi/topics/arthritis/oahandout.htm
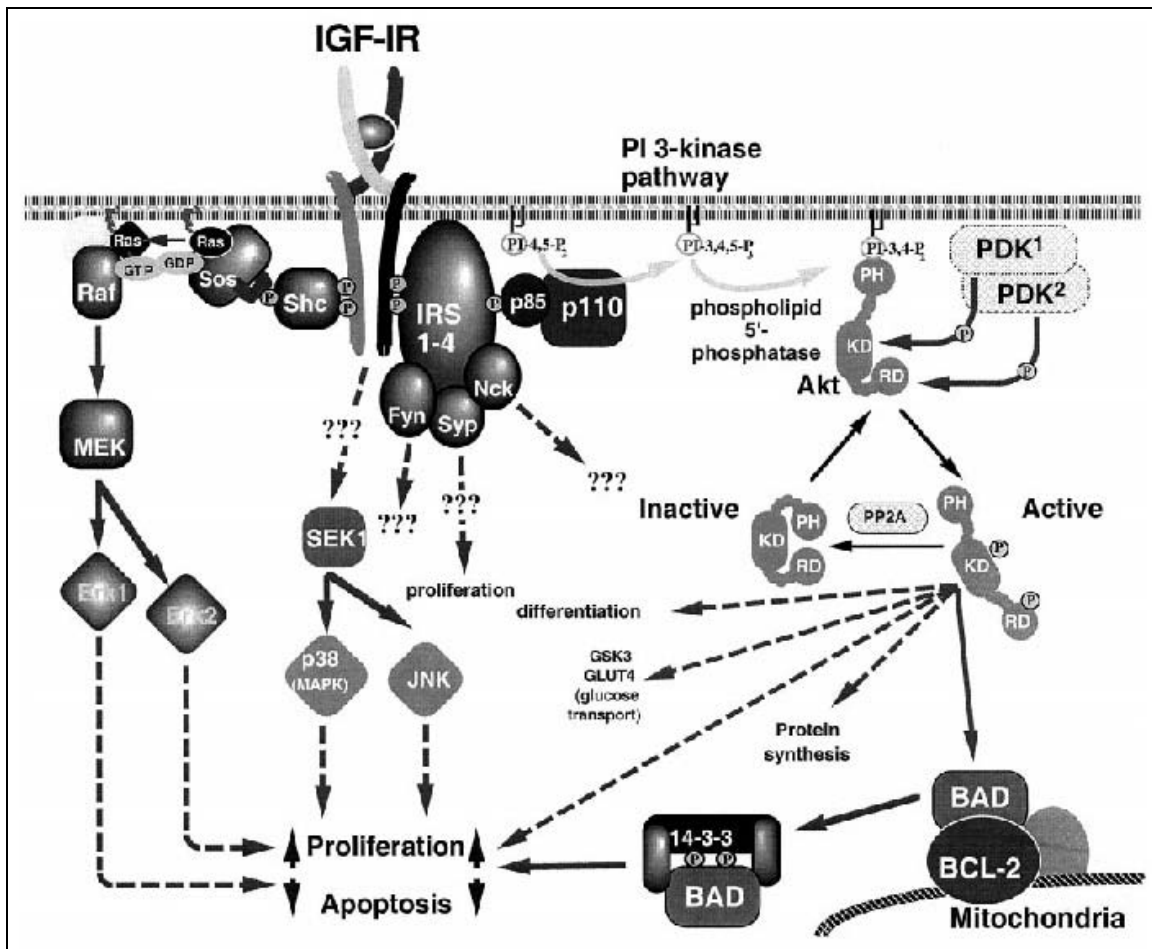
Figure 2.5. IGF-I signal transduction pathways. Ligand binding to type I receptor (IGF-IR) leads to autophosphorylation of tyrosines on its cytoplasmic β subunits. Shc and insulin receptor substate (IRS) adapter proteins are recruited to phosphotyrosine residues on the β subunits and are activated by receptor tyrosine kinases. These adapter proteins then recruit other adapter proteins and kinases to the receptor complex, initiating multiple signal transduction pathways. The mitogen-activated protein kinases (MAPKs) ERK-1/2 are activated by way of the G-protein Ras following Shc interactions with Grb2/SOS adapter proteins. The phosphatidylinositol 3-kinase (PI3-K) pathway is activated through IRS interaction with the p85 subunit of PI3-K. Reprinted from *Endocrine Reviews*, v22, Le Roith D, Bondy C, Yakar S, Liu J, and Butler A, The Somatomedin Hypothesis: 2001, p. 62, Copyright 2001, The Endocrine Society.
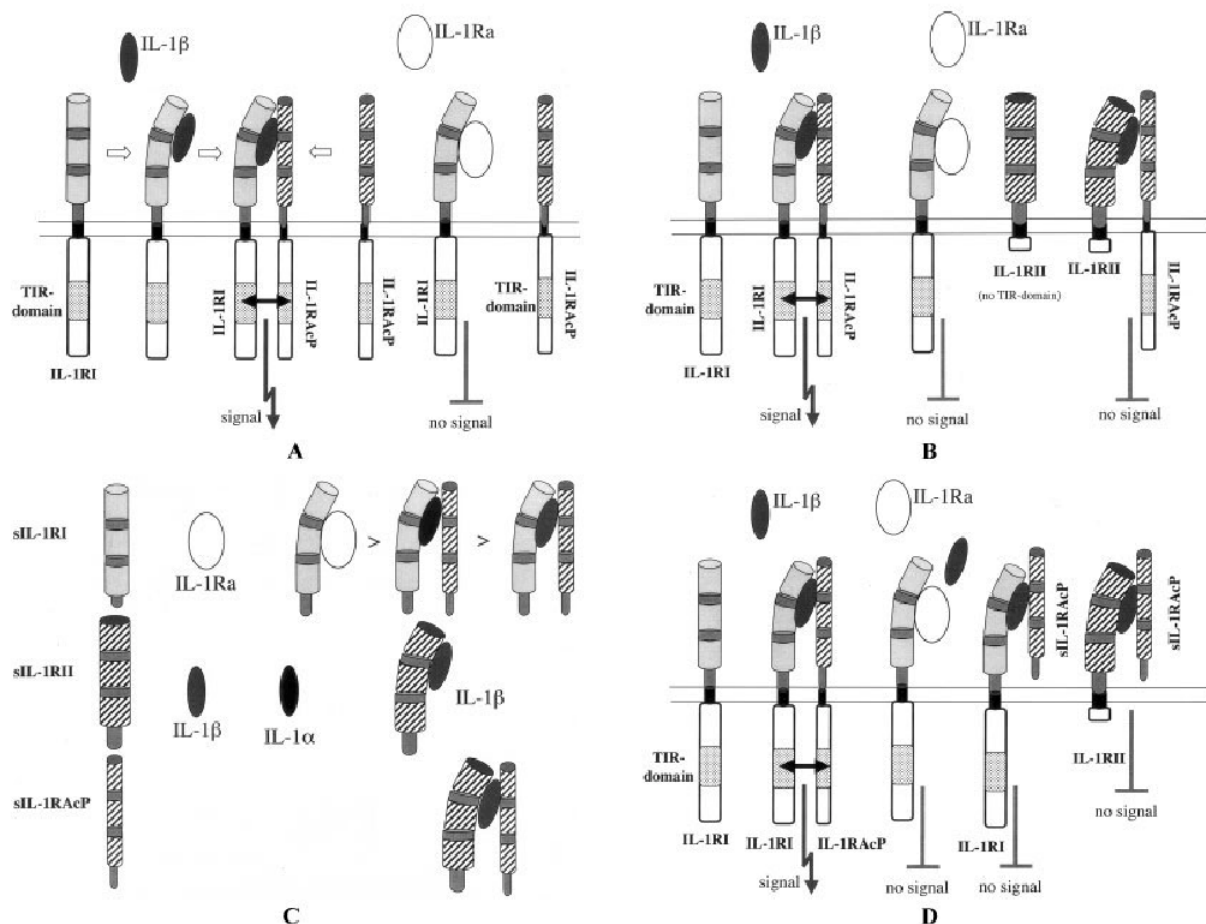
Figure 2.6. The extracellular IL-1 signaling system. (**A**) IL-1 receptor type I (IL-1RI) binding to IL-1β recruits IL-1 receptor accessory protein (IL-1RAcP) to form a high-affinity heterodimeric signaling complex, and proximity of the intracellular Toll–IL-1 receptor (TIR) domains initiates a signal. However, when IL-1 receptor antagonist (IL-1ra) occupies the ligand binding site of IL-1RI, IL-1RAcP cannot be recruited and thus no signal is transduced. The affinity of IL-1ra for IL-1RI is greater than that of IL-1β. (**B**) Some cell types, including chondrocytes, express IL-1 receptor type II (IL-1RII). Also referred to as a "decoy" receptor, IL-1RII has a greater binding affinity for IL-1β than IL-1RI but lacks the intracellular TIR domains and thus cannot transduce signal. IL-1β bound to IL-1RII can also form a high-affinity complex with IL-1RAcP. Cells expressing this receptor benefit from both IL-1ra blockade of IL-1RI as well as the decoy effect of IL-1RII. (**C**) The extracellular domains of each receptor chain occur naturally *in vivo*, produced by either proteolytic release of cell-bound receptor or constitutive secretion of mRNA splice variants. Soluble IL-1RI (sIL-1RI) binds IL-1ra with greater affinity than for IL-1β, and therefore may act as a sink for IL-1ra. Soluble IL-1RII (sIL-1RII) binds IL-1β and neutralizes its activities. Soluble IL-1RAcP (sIL-1RAcP) does not bind IL-1β but rather forms a high-affinity complex with the sIL-1RII, enhancing inhibition of IL-1β activity. (**D**) Soluble IL-1RAcP may form a complex with either IL-1RI or IL-1RII and IL-1β without initiating a signal. The formation of the inactive complex of sIL-1RAcP with the cell-bound type II receptor provides for enhanced inhibition of IL-1 activity. Reprinted from *Arthritis and Rheumatism*, v52, Dinarello CA, The Many Worlds of Reducing Interleukin-1, p. 1963, Copyright 2005, with permission of Wiley-Liss Inc., a subsidiary of John Wiley & Sons, Inc.
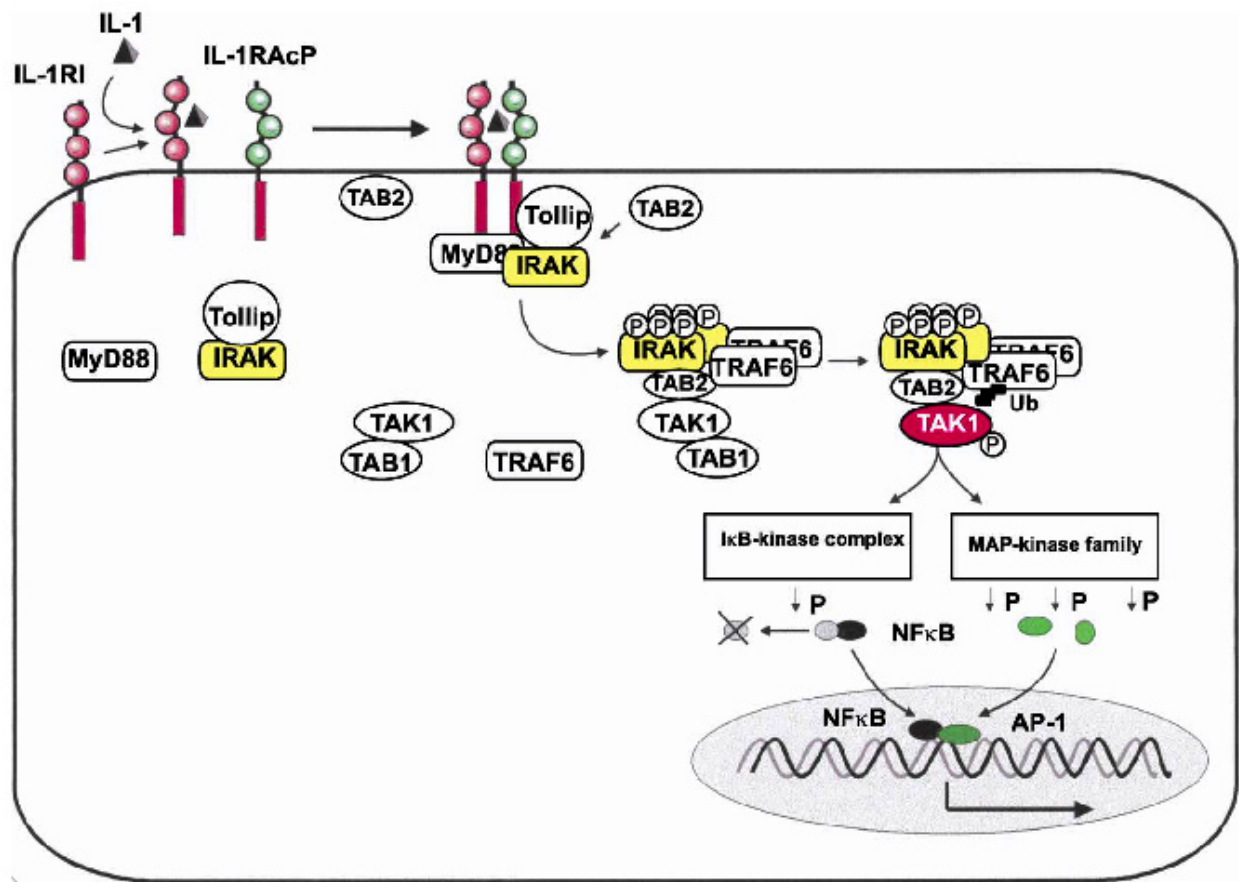
Figure 2.7. IL-1 signal transduction pathways. IL-1(α or β) first binds with type I receptor (IL-1RI), and the bound receptor associates with the co-receptor IL-1RAcP. Formation of the receptor complex leads to a conformation changes in the cytoplasmic TIR domains of IL-1RI and IL-1RAcP, and the adapter proteins MyD88 and Tollip are recruited to the complex. Tollip is bound to IRAK, and recruitment of Tollip allows for interaction between MyD88 and IRAK. IRAK becomes hyperphosphorylated, dissociates from Tollip and the receptor complex, and may form a dimer. TRAF6 then associates with IRAK through the TAB2 adapter protein, which is recruited from the membrane. TAK-1 (with its activator protein TAB1) is also recruited to this complex. Complex formation leads to the addition of polyubiquitin (polyUb) chains onto TRAF6 [140], and activated TRAF6 induces autophosphorylation of TAK-1. Activated TAK-1 may then phosphorylate other regulatory kinases within multiple signaling pathways, including mitogen-activated protein kinases (MAPKs) and IκB-kinase (IKK). Reprinted from *Biochimica et Biophysica Acta*, v1592, Martin MU and H Wesche, Summary and Comparison of the Signaling Mechanisms of the Toll/Interleukin-1 Receptor Family, p. 272, Copyright 2002, with permission from Elsevier.

Chapter 3: Regulation of the Insulin-like Growth Factor-I System by Interleukin-1

3.1   Introduction

The functional properties of articular cartilage are defined by the micro-architecture of its extracellular matrix (ECM), which includes proteoglycans (PGs) and type II collagen fibrils [18]. Cartilage homeostasis is maintained through a balance between the synthesis and resorption of these ECM components by articular chondrocytes (ACs). During the progression of osteoarthritis (OA), an imbalance develops in favor of ECM degradation, resulting in diarthrodial joint deterioration, pain, and disability [238]. ECM breakdown is mediated in part by the enhanced activity of matrix metalloproteinases (MMPs) [183], a family of zinc-dependent proteases which includes collagenases 1, 2, and 3 (MMPs 1, 8, and 13), gelatinases A and B (MMPs 2 and 9), and stromelysin 1 (MMP-3). The induction of aberrant chondrocyte activity is not completely understood, but involves a combination of biomechanical and hormonal factors.

Two of the most important hormonal regulators of cartilage metabolism are interleukin-1 (IL-1) and insulin-like growth factor-I (IGF-I) [1]. The inflammatory cytokine IL-1 has catabolic effects on articular cartilage, inhibiting PG synthesis [2, 165, 166, 223, 239] and facilitating degradation [2, 165, 239, 240]. IL-1 enhances cartilage catabolism by increasing synthesis of MMPs [172, 174, 230, 235]. Moreover, it has been shown to down-regulate type II collagen expression and up-regulate types I and III in human chondrocyte culture [169]. Elevated levels of the cytokine have been found in osteoarthritic cartilage [182, 183, 241]. In experimental OA models, blocking IL-1 signal has been shown to prevent cartilage deterioration, implicating it as a key mediator of OA progression [189, 190].

In contrast to IL-1, IGF-I is a potent anabolic regulator of chondrocyte activity. The mitogen has been shown to augment both collagen and PG synthesis *in vitro* [88, 90, 91]. IGF-I signal is transduced through its type I receptor (IGF-IR) and modulated by a set of high-affinity binding proteins, insulin-like growth factor binding proteins (IGFBPs) 1–6 [49]. These binding proteins can either inhibit or potentiate IGF-I activity, depending on the particular species and extracellular environment [75]. ACs express both IGF-I and IGF-IR [4, 73], and IGFBPs 2, 3, 4, and 5 have been identified in cartilage from multiple species [96-98]. Higher levels of IGF-I have been observed in osteoarthritic cartilage [100-102], but these chondrocytes are relatively non-responsive to the factor [4-6]. Receptor synthesis has been reported at normal [98] or higher

[103] levels for human osteoarthritic chondrocytes. It has been proposed that hyporesponsiveness to IGF-I is due to increased secretion of IGFBPs, particularly IGFBP-3 [98, 101, 104, 242].

IL-1 and IGF-I have antagonistic effects on cartilage metabolism: IGF-I has reversed the catabolic effects of IL-1 on cartilage in equine, porcine, and bovine explant models [7, 191, 192, 226], whereas IL-1 inhibited IGF-I-stimulated PG synthesis in porcine [7] and rat [8] explants and rabbit AC culture [197]. In osteoarthritic joints, IL-1 is thought to be one of multiple cofactors that induce chondrocyte hyporesponsiveness to IGF-I [6]. The cytokine has been shown to increase production of IGFBP-3 [194, 195] and IGFBP-5 [196] in AC cultures of varied species origin. However, the precise mechanisms by which IL-1 regulates the IGF-I signaling system remain unclear. Such knowledge could help direct molecular therapies, such as gene transfer [243], for osteoarthritic cartilage repair.

In this paper we characterize the IGF-I signaling system of normal equine ACs and the response of this network to IL-1. Our central hypothesis was that IL-1 regulates this signaling system at multiple levels – through both transcriptional and post-translational mechanisms. For an experimental model, cultured equine ACs were stimulated with recombinant equine IL-1β [2] at concentrations relevant to arthritic joints, since equine osteoarthritis resembles the corresponding human condition [244]. Cultures were analyzed for IGF-IR, IGFBP, and endogenous IGF-I levels and associated transcription rates. The data reveal a combination of transcriptional and proteolytic mechanisms for IGF-I system regulation by IL-1β that could alter IGF-I signaling dynamics *in vivo*.

3.2   Materials and Methods

3.2.1   *Materials*

Recombinant equine IL-1β was expressed and purified as described elsewhere [2]. Recombinant human IGF-I was purchased from PeproTech (Rocky Hill, NJ). Rabbit antisera for bovine IGFBP-2 and IGFBP-5 were acquired from Upstate (Charlottesville, VA), as was the IGF-I structural analog Y60L-IGF-I. Mouse anti-human IGF-I was a gift from Dr. Bernard Laarveld (University of Saskatchewan). Cellgro RPMI-1640 media, phosphate-buffered saline (PBS), 1X trypsin-EDTA (0.05% trypsin, 0.53 mM EDTA in HBSS w/o Ca, Mg), and penicillin-

streptomycin (P/S) stock (5,000 I.U./ml penicillin, 5,000 mg/ml streptomycin) were purchased from MediaTech (Herndon, VA). Fetal Bovine Serum was obtained from Hyclone (Logan, UT). Collagenase-D was purchased from Roche Diagnostics Corp. (Indianapolis, IN). Sodium alginate (65-75% L-guluronic acid, 25-35% D-mannuronic acid) was provided by FMC BioPolymer (Philadelphia, PA). MMP inhibitors specific for MMP-3 (N-isobutyl-N-(4-methoxyphenylsulfonyl)-glycylhydroxamic acid), MMP-2/9 ((2R)-2-[(4-biphenylylsulfonyl)amino]-3-phenylpropionic acid), and MMP-8 ((3R)-(+)-[2-(4-Methoxybenzenesulfonyl)-1,2,3,4-tetrahydroisoquinoline-3-hydroxamate]) were all acquired from CalBiochem (La Jolla, CA).

3.2.2 *Chondrocyte isolation and culture*

ACs were isolated by enzymatic digestion of cartilage from the stifle joints of 3 and 4 year-old mares euthanatized for reasons unassociated with joint disease at the Virginia-Maryland Regional College of Veterinary Medicine, based on a previous protocol [234]. Near full-thickness cartilage slivers were rinsed, minced, and digested overnight at 37°C in sterile 1% (w/v) collagenase buffer. ACs were collected by centrifugation and viable cells (>90% by trypan blue exclusion) were grown to near-confluence on 75-cm^2 culture flasks with 'complete' medium (RPMI-1640 with 10% FBS and 1% P/S). Chondrocytes were subcultured on 100-mm culture dishes and cryopreserved in complete medium with 10% dimethyl sulfoxide (DMSO). For each study, AC stocks (passage 2) were expanded to adequate numbers on culture dishes and re-differentiated by encapsulation in alginate beads, as previously described [211]. Briefly, cells were suspended in a 1.2% sodium alginate, 150 mM NaCl solution (filter-sterilized) and dispersed drop-wise into a well-mixed bath of sterile 102 mM CaCl$_2$. The resulting beads were crosslinked for an additional 10 min without mixing. Beads were rinsed twice with 150 mM NaCl and once with complete medium and transferred to 24-well plates (10 beads per one ml medium). After culturing alginate beads for 10 days, changing media every two or three days, beads were dissociated in 3 volumes of 55 mM sodium citrate, 150 mM NaCl (pH 6.8) for 15 min at 37°C. Chondrocytes were collected by centrifugation (280×g for 10 min) and seeded at ~1.3×10^5 cells/cm^2 in well plates. Forty-eight-to-72 hr post-plating, monolayers were rinsed with PBS and treated with 0, 1, or 10 ng/ml IL-1β or 50 ng/ml IGF-I in 'low-serum' media (RPMI-1640 with 0.2% FBS and 1% P/S). Plates were cultured for an additional 48 hr and

assayed as described below. For MMP inhibition studies, cells were pre-incubated in low-serum media with various MMP inhibitors (all at 40 μM) or 0.6% DMSO (vehicle) 30 min prior to addition of treatment factors. After 24 hr, an additional bolus of each inhibitor (equivalent to 40 μM) was added to a portion of the cultures.

3.2.3 *Radiolabeled ligand binding*

IGF-I was radioiodinated using a chloramine-T method [245] and used in ligand binding experiments as described previously [79]. Briefly, cells in 24-well plates were rinsed once with PBS prior to addition of 0.5 ml of sterile binding buffer (0.5% bovine serum albumin (BSA), 10 mM dextrose, 25 mM 4-(2-hydroxyethyl)-1-piperazineethanesulfonic acid (HEPES), 15 mM sodium acetate, 1.2 mM $NaSO_4 \times 7H_2O$, 5 mM KCl, 120mM NaCl, pH 7.4). Blocking factors (IGF-I or Y60L-IGF-I; 1 μg/well) were added to appropriate wells at 4°C for 15 min, followed by addition of $[^{125}I]$-IGF-I (2 ng/ml). After overnight incubation at 4°C, wells were rinsed thrice with ice-cold binding buffer, monolayers lysed in 1N NaOH for 1 hr, and samples analyzed using a COBRA II Auto-Gamma counter (Packard, Downers Grove, IL). Readings were corrected for background, converted to pg bound ligand based on counts from radiolabeled stock, and normalized by cell numbers from adjacent wells.

3.2.4 *Western blot*

Cell monolayers were rinsed with PBS and lysed in 1X Laemmli buffer (Bio-Rad, Hercules, CA). Protein concentrations were determined using a RC/DC assay kit (Bio-Rad). Sample protein (20 μg/lane) was resolved by SDS-PAGE and transferred to PVDF membranes. Non-specific binding was blocked by pre-incubating membranes with 5% nonfat milk in TBS-T (10 mM Tris-HCl, 150 mM NaCl, 0.5 mg/ml sodium azide, pH 7.4 with 0.1% Tween-20) for 30 min, followed by incubation with a rabbit antibody (Ab) specific for the IGF-IR β-subunit (Santa Cruz Biotechnology, Santa Cruz, CA) in blocking buffer (1:10000 dilution) overnight at 4°C. Membranes were rinsed three times with TBS-T and incubated with a goat anti-rabbit IgG conjugated to horseradish peroxidase (Zymed, San Francisco, CA) (1:15000 dilution in blocking buffer) for 1 hr at room temperature. After rinsing thrice with TBS-T, bound antibodies were detected on BioMax film (Kodak, Rochester, NY) using SuperSignal chemiluminescent substrate (Pierce, Rockford, IL).

To examine IGF-IR phosphorylation, treated cultures were rinsed with PBS and stimulated with a "pulse" of IGF-I (200 ng/ml in low-serum media for 10 min) prior to cell lysate collection. Controls were incubated simultaneously in low-serum media. Protein quantification, SDS-PAGE, and membrane blocking were conducted as described above. Membranes were incubated with a rabbit Ab against phosphorylated IGF-IR (Cell Signaling Techology, Beverly, MA) (1:2000 dilution in TBS-T with 5% BSA) overnight at 4°C. Secondary Ab incubation and chemiluminescent detection were performed as described above. Blots were then stripped in TBS-T with 10% SDS and β-mercaptoethanol at 50°C for 30 min, rinsed five times with TBS-T, and probed for total IGF-IR as described above.

3.2.5 *Ligand blot*

Detection of IGFBPs by western ligand blot analysis was performed according as described previously [246]. Conditioned media (CM) aliquots were concentrated 10-fold under vacuum and diluted 1:2 in loading buffer (125 mM Tris, 4% SDS, 20% glycerol, bromophenol blue, pH 6.8). Samples and protein standards were resolved on a 10% polyacrylamide gel (10 mA/gel overnight at 4°C) and transferred to nitrocellulose membranes (50 V for 6-7 hr at 4°C). Membranes were rinsed sequentially in TBS + 3% Nonidet P-40 for 30 min, TBS + 1% BSA for 2 hr, and TBS-T for 10 min. Blots were incubated overnight at 4°C in a bath of [^{125}I]-IGF-I (~$9{\times}10^4$ cpm/ml in TBS-T with 5% BSA). The following day, blots were rinsed twice with TBS-T, rinsed thrice in TBS, and exposed to BioMax film at –70°C for 3-7 days. Band sizes were identified according to protein standards.

To confirm IGFBP-2 and IGFBP-5 identities in conditioned media, CM samples were resolved by SDS-PAGE and transferred to nitrocellulose membranes as described above. Membranes were blocked for 30 min with 5% dry milk in TBS-T and incubated with rabbit anti-bovine IGFBP-2 (1:5000 in blocking buffer) or IGFBP-5 (1:2000) overnight at 4°C. Secondary Ab incubation and band detection were conducted as described under section 3.2.4.

3.2.6 *Northern blot*

RNA was isolated from cell layers using a SV Total RNA Isolation kit (Promega, Madison, WI), including DNase-I treatment to remove genomic DNA. RNA yields were determined by absorbance at 260 nm. Messenger RNA (mRNA) expression was detected as

previously described [247] using ovine IGF-I and IGFBP-2, rat IGFBP-3, and equine IGF-IR cDNA probes, which were randomly labeled with [α-^{32}P]-dATP using a Prime-a-Gene kit (Promega). Samples were diluted in formaldehyde loading buffer (Ambion, Austin, TX) with ethidium bromide and resolved on agarose-formaldehyde gels (20 μg/lane) at 115 V for 150 min. Gels were photographed over UV light with a Polaroid GelCam (Cambridge, MA). RNA was transferred to Hybond N$^+$ membranes (Amersham, Piscataway, NJ) by capillary transport and crosslinked using a Stratalinker 1800 UV Crosslinker (Stratagene, La Jolla, CA). After rinsing in 2X saline-sodium citrate (SSC) buffer (0.3 M NaCl, 0.03 M sodium citrate), membranes were pre-incubated in QuickHyb hydridization buffer (Stratagene) for 30 min at 68°C in a roller oven. Labeled probe (25 ng) and 1 μg sheared salmon sperm DNA (Ambion) were added and incubated with the membranes for an additional hour. Blots were rinsed twice with 2X SSC, 0.1% SDS (room temperature for 15 min) and once with 0.1X SSC, 0.1% SDS (60°C for 30 min), wrapped in plastic film, and exposed to BioMax film at –80°C. Band intensities were quantified by densitometry and normalized by corresponding 18S rRNA bands from gel images. For detection of additional mRNAs, blots were stripped using two rinses in pre-boiled 0.1X SSC, 0.1% SDS and re-hybridized as described above.

3.2.7 *Radioimmunoassay*

IGF-I concentrations in conditioned media were measured by radioimmunoassay, as described elsewhere [247]. CM samples (0.5 ml) were concentrated to pellets under vacuum, resuspended in extraction buffer (87.5% ethanol, 12.5% 2N HCl), and centrifuged at 13,200×g to remove IGFBPs. Supernatant was neutralized with 0.855M tris buffer, chilled at –20°C for 1hr, and centrifuged at 1800×g for 30 min at 4°C. The resulting supernatant was concentrated under vacuum and reconstituted in IGF-I assay buffer (30 mM sodium phosphate, 10 mM EDTA, 0.02% protamine sulfate, 0.05% Tween-20, pH 8.0). Sample aliquots and standards (0.05–6.5 ng IGF-I; GrowPrep, Adelaide, Australia) were diluted to a total volume of 0.5 ml in IGF-I assay buffer. After adding 100 μL mouse anti-human IGF-I (1:70,000 dilution), 100 μL [^{125}I]-IGF-I stock (~30,000 cpm) was added and the tubes were incubated at 4°C for 24 hr. Goat anti-mouse secondary Ab (Sigma, St. Louis, MO) was then added (1:20) and the tubes incubated for an additional 72 hr at 4°C. Samples and standards were diluted in 1 ml doubled-distilled PBS and

the tubes spun at 1500×*g* for 30 min at 4°C. Supernatant was removed and the remaining pellets analyzed using a COBRA II Auto-Gamma counter (Packard, Downers Grove, IL).

3.2.8 *Gelatin and casein zymography*

CM samples were diluted 1:3 in zymogram loading buffer (Bio-Rad). Samples and protein standards were loaded onto either gelatin (10%) or casein (12.5%) zymogram Ready-Gels (Bio-Rad) and resolved at 125 V for ~90 min. After cutting off the molecular weight marker lanes, gels were washed in sequential baths of zymogram renaturation and development buffers (Bio-Rad) for 30 min each with gentle agitation. The development buffer was changed and gels were incubated overnight at 37°C. The following day, gels were stained for 45-60 min in a bath of Coomassie Blue R-250 solution (Bio-Rad) and de-stained in 40% methanol, 7% acetic acid solution for 5 hr, changing the de-stain solution every 30 min. Gels were digitally photographed and band sizes estimated based on protein standards.

MMP-2 and MMP-3 identities were confirmed by western blot analysis. Briefly, CM samples were concentrated and resolved as described above, and pre-blocked membranes were probed overnight for MMP-2 and MMP-3 using 1:500 and 1:1000 dilutions, respectively, of rabbit anti-human Abs (Chemicon, Temecula, CA) in blocking buffer. Secondary Ab incubation and band detection were performed as described under section 3.2.4.

3.2.9 *Statistics*

Figure bars represent the mean ± standard error of the mean (SEM) of three replicates from a single study. All studies were repeated at least three times to confirm experimental trends, and representative data sets are shown. Unless otherwise specified, statistical significance between treatment means was determined by two-tailed Student's *t*-test (α=0.05).

3.3   Results

3.3.1 *IL-1β augments IGF-I receptor levels*

Previous work using explant [7, 8] and AC culture [197] models have shown that IL-1 treatment inhibits IGF-I-induced PG synthesis. Given that IGF-I signal transduction is directly mediated by its type I receptor, IGF-IR [49], IL-1 may act to reduce chondrocyte IGF-IR levels.

To test this hypothesis, we quantified steady-state binding of $[^{125}I]$-IGF-I as an indicator of IGF-IR surface levels. Because IGF-I can also bind to cell surface-sequestered IGFBPs, chondrocyte monolayers were pre-incubated with an excess Y60L-IGF-I, an IGF-I analog with substantially reduced affinity for IGF-IR but similar affinity for IGFBPs [248], thereby selectively inhibiting radiolabeled IGF-I association to surface IGFBPs but not to IGF-IR. As shown in **Figure 3.1.A**, 48-hr treatment with IL-1β increased subsequent $[^{125}I]$-IGF-I binding by ~60% at 1 ng/ml (p<0.05) and ~90% at 10 ng/ml (p<0.001), indicating an increase in IGF-IR in contradiction to our hypothesis. Western blot analysis of cell lysate for the IGF-IR β-subunit supported this conclusion, showing a two-fold increase in subunit intensity in response to 10 ng/ml IL-1β (**Figure 3.1.B**). Exogenous IGF-I (50 ng/ml) reduced receptor levels (~60%), in agreement with a previous study using rat chondrocytes [249]. To determine if altered IGF-IR phosphorylation coincided with enhanced receptor levels, treated cultures were stimulated with an IGF-I pulse (200 ng/ml for 10 min). Phosphorylated IGF-IR levels mirrored trends for total receptor (**Figure 3.1.C**). These studies show that normal chondrocytes exposed to IL-1 exhibit increased IGF-IR levels, implying augmented cell sensitivity to IGF-I.

3.3.2   *IL-1β reduces IGFBP-2 in conditioned media*

IGF-I signaling is regulated not only by IGF-IR but also by IGFBPs, which compete with receptor for unbound IGF-I [49]. We next examined how IL-1β impacted IGFBP levels in conditioned media by ligand blot analysis. As found in previous studies of cartilage from other species [99, 242], equine chondrocytes predominately secreted an IGFBP in the 32-34 kDa range (**Figure 3.2.A**), consistent with reported molecular weight for IGFBP-2 and confirmed by western blot analysis (**Figure 3.2.B**). Bands in the 38-40 region were also observed in longer film exposures, most likely corresponding to IGFBP-3. Bands in the 28-30 kDa range, which were confirmed to be IGFBP-5 by western blot analysis (**Figure 3.2.B**), were found in IGF-I treated samples. Averaging the optical densities of triplicate CM samples from independent wells of the same experiment, IL-1β reduced IGFBP-2 to 53 ± 18% (1 ng/ml) and 40 ± 9% (10 ng/ml) of basal levels. The 38-40 kDa band was up-regulated by IL-1β, though levels were still low relative to IGFBP-2 at the 48-hr mark (**Figure 3.2.A**). IL-1β had no consistent effects on IGFBP-5 levels. Exogenous IGF-I intensified both band doublets, particularly that of IGFBP-5.

These blots suggest that IL-1β impacts the relative composition of IGFBPs in the extracellular environment, potentially altering IGF-I localization and receptor binding.

3.3.3   *IGF-I and IGFBP-3, but not IGFBP-2 or IGF-IR, are transcriptionally regulated*

To identify potential transcriptional contributions for the IL-1β effects described above, IGF-IR, IGFBP-2, and IGFBP-3 mRNAs were probed by northern blot (**Figure 3.3**). The cytokine had no marked effect on IGF-IR message, though exogenous IGF-I down-regulated expression by ~60%. Similarly, IL-1β did not alter IGFBP-2 message, but IGF-I stimulated transcription by ~40%, in agreement with protein increases seen by ligand blot. The most pronounced response was that of IGFBP-3 mRNA, which was amplified by an order of magnitude in the presence of IL-1β.

In addition to endocrine stimulation of chondrocytes, endogenously expressed IGF-I can act through autocrine/paracrine mechanisms [250], and changes in IGF-I expression could impact IGF-IR levels. In order to assess endogenous IGF-I synthesis, this transcript was included in Northern analysis. IL-1β markedly suppressed IGF-I expression to ~40% (1 ng/ml) and ~30% (10 ng/ml) of control levels. Stimulation with exogenous IGF-I slightly decreased expression (~80% of control).

3.3.4   *IGF-I concentrations in conditioned media are diminished by IL-1β*

Northern analysis indicated a decrease in IGF-I message. To determine whether expression effects translated to extracellular protein levels, we measured IGF-I concentrations in CM by radioimmunoassay. As shown in **Table 3.1**, IL-1β decreased IGF-I levels dose-dependently, from 3.5 ± 0.4 ng/ml at basal conditions to 2.3 ± 0.5 (p=0.056) and 1.9 ± 0.3 ng/ml (p=0.013) following stimulation with 1 and 10 ng/ml, respectively. We note that this measurement includes both unbound and IGFBP-sequestered IGF-I and that the effects mirrored corresponding changes in transcript expression (**Figure 3.3**).

3.3.5   *IL-1-enhanced MMP activity mediates IGFBP-2 suppression*

Contrary to IGF-I, IGFBP-2 trends did not correlate with transcript expression. An alternative possibility is that IL-1β attenuation of IGFBP-2 involves proteolysis. IGFBP levels are known to be regulated by various protease families, including the MMPs [86]. Despite the

36

fact that MMP levels are increased in OA [183], to the best of our knowledge, their ability to catabolize IGFBPs in cartilage has not been examined. IGFBP-degrading MMPs known to be up-regulated by IL-1 in equine cartilage include gelatinase A (MMP-2) and stromelysin 1 (MMP-3) [233, 235]. Therefore, we assessed their potential role in IGFBP-2 suppression by IL-1β. First, MMP-2 and MMP-3 activities were measured by gelatin and casein zymography. Two primary regions of activity were observed in gelatin: a band at ~70 kDa and a band at ~90 kDa (**Figure 3.4.A**). The upper band was consistent with the proform of MMP-9 (pMMP-9), and the lower was confirmed as pMMP-2 by immunoblot. Regulation of pMMP-9 by either IL-1β or IGF-I was not observed. However, IL-1β increased pMMP-2 approximately two-fold at both treatment levels, and IGF-I stimulated levels by ~40%. In casein gels (**Figure 3.4.A**), sets of bands from 48-60 kDa were observed only from cultures given exogenous IL-1β. Immunoblotting identified these bands to be various proteolytic forms of MMP-3.

To test for IL-1-enhanced MMP proteolysis of IGFBP-2, cultures were pre-incubated with inhibitors specific for the gelatinases (MMP-2/9), for stromelysin 1 (MMP-3), or for collagenase-2 (MMP-8), which has also been shown to be stimulated by IL-1 and up-regulated in human osteoarthritic cartilage [183]. Relative to vehicle control (0.6% DMSO), inhibitors for MMP-2/9 and MMP-3, but not MMP-8, reversed IGFBP-2 suppression by 10 ng/ml IL-1β (**Figure 3.4.B**). Boluses of inhibitor were added to a portion of the cultures at 24 hrs, enhancing their effects relative to single-dosed cultures. Normalizing band intensities (**Figure 3.4.C**) from IL-1-treated cultures by corresponding no-treatment controls, MMP-2/9 and MMP-3 inhibitors were found to increase band ratios from 0.60 to 0.90 and 0.82, respectively, whereas MMP-8 inhibition yielded a similar ratio (0.64) to vehicle control (**Figure 3.4.C**). These results indicate that increased synthesis of MMPs, particularly gelatinase A (MMP-2) and stromelysin 1 (MMP-3), facilitates IL-1β suppression of IGFBP-2 levels.

3.4   Discussion

This paper presents the first extensive characterization of the equine chondrocyte IGF-I signaling system and demonstrates the complexity of its regulation by IL-1 (**Figure 3.5**). In the absence of hormonal stimulation, chondrocytes secrete some basal level of IGF-I, which binds with its type I surface receptor expressed on chondrocyte surfaces, resulting in receptor down-regulation and possible endogenous signal. Binding proteins, principally IGFBP-2, are also

37

secreted and mediate IGF-I activity by sequestering the growth factor and defining its proximity to chondrocyte receptors. Initial exposure to exogenous IL-1β results in suppressed expression of IGF-I, reducing autocrine/paracrine IGF-I concentrations. IGF-IR expression is not directly affected, but surface concentrations increase, most likely due to less receptor turnover resulting from less IGF-I mediated endocytosis. IGFBP-2 concentrations also diminish, though not by down-regulation of message. Rather, enhanced synthesis of catabolic MMPs, including MMP-2 and MMP-3, facilitates IGFBP-2 degradation. The increased ratio of surface receptors to binding proteins implies an initial augmentation of chondrocyte sensitivity to exogenous IGF-I. However, the strong up-regulation of IGFBP-3 transcription suggests this binding protein will have a more prominent impact on IGF-I signaling at later timepoints, possibly suppressing IGF-I signal response by sequestration of ligand. Increased IGFBP-3 levels in osteoarthritic cartilage are thought to contribute to the pathogenesis of the disorder [242], namely chondrocyte hyporesponsiveness to IGF-I anabolism [98, 104, 195]. The present study suggests normal cells may also exhibit this type of responsiveness if IL-1 exposure continues.

IL-1β was shown to augment IGF-IR levels (**Figure 3.1**), suggesting normal equine chondrocytes respond to the cytokine by becoming more sensitive to IGF-I stimulation. Such a response could serve to maintain the balance between anabolic and catabolic activities in healthy cartilage. However, the increase was not attributed to up-regulation of receptor expression. Rather, the cytokine attenuated endogenous IGF-I concentrations by down-regulating message transcription, suggesting a suppression of the autocrine/paracrine IGF-I system. Thus the increase in receptors likely represents a reduction in receptor turnover, the rate of which is mediated by ligand-receptor binding and internalization [249]. Matsumoto *et al.* [194] previously reported that IL-1β increased radiolabeled IGF-I binding in primary rat AC cultures, but they observed no effect on IGF-I expression. It should be noted, however, the authors did not distinguish IGF-I binding between IGF-IR and surface-sequestered IGFBPs. They also found IGFBP-3 secretion to be stimulated by IL-1β, suggesting increased IGF-I binding could have been attributed to elevated surface binding protein numbers.

IGF-IR synthesis has been reported at normal [98] or higher [103] levels on human osteoarthritic chondrocytes. Therefore other factors than receptor presentation must be considered to explain chondrocyte hyporesponsiveness to IGF-I observed in OA [4]. For example, reactive oxygen species such as nitric oxide (NO) may inhibit autophosphorylation of

IGF-IR tyrosine kinase domains following ligand binding, an initial step in signal transduction. Such an effect has been shown in rabbit AC culture in response to various stimulators of NO synthesis, including IL-1β [197]. We addressed this potential mechanism by stimulating cytokine-treated cultures with a pulse of IGF-I. The resulting phosphorylated IGF-IR levels mirrored the trend for total receptor (**Figure 3.1.C**). However, NO levels were not measured, and production of the reactive oxygen species may not have been sufficient to affect receptor functionality.

Perhaps the most significant findings concern IL-1β regulation of IGFBP-2. Consistent with profiles in normal human cartilage [242], IGFBP-2 was the principal binding protein secreted by equine articular chondrocytes. The suppression of IGFBP-2 levels by IL-1β was partially reversed by inhibition of MMP-2 or MMP-3 activity (**Figure 3.4**); however, this effect was not general to the MMP family, as MMP-8 inhibition did not produce a similar result. Of the MMPs not tested, collagenase 1 (MMP-1) has been reported to cleave IGFBP-2 in airway smooth muscle cells [251, 252] and might also contribute to diminished IGFBP-2. To our knowledge, this study provides the first direct evidence for chondrocyte-mediated IGFBP proteolysis by MMPs and is the first to link IGFBP-2 breakdown with MMPs 2 and 3 for any cell type. Given that MMP up-regulation has been associated with increased IL-1 levels in osteoarthritic cartilage [183], this protease family may play an unexpected role in modifying IGF-I signaling dynamics during the progression of OA. Though IGFBP-2 levels are not substantially altered in osteoarthritic cartilage [242], MMPs may modify binding protein localization relative to chondrocytes in the tissue.

The net decrease in binding protein secretion in response to IL-1β (**Figure 3.2**) was somewhat surprising in light of previous research. Both Olney *et al.* [195] and Matsumoto *et al.* [194] demonstrated increased production of IGFBP-3 following IL-1 treatment for human and rat AC cultures, respectively, and Sunic *et al.* [196] reported enhanced IGFBP-5 secretion in ovine AC culture. In the present study, IGFBP-3 and IGFBP-5 levels were relatively low during the test period. However, IL-1 had substantially amplified IGFBP-3 transcription at 48 hr, indicating this species might eventually dominate the binding protein composition of cultures with prolonged exposure to cytokine. Ligand blot analysis of conditioned media supported this hypothesis, as IL-1-enhanced IGFBP-3 levels were detected in longer film exposures. Studies of osteoarthritic cartilage have reported increased production of IGFBP-3 but not IGFBP-2 [104,

39

242], suggesting changes in the binding protein makeup of cartilage – not simply the total concentration – may prove important to the induction of IGF-I hyporesponsiveness. IGFBP sequestration of IGF-I can either inhibit or potentiate ligand activity, depending on the particular binding protein and the extracellular environment [75]. On the one hand, binding proteins can inhibit IGF-IR activation by competing for unbound ligand and facilitating clearance of autocrine/paracrine IGF-I. Alternatively, IGFBP interaction with pericellular or territorial ECM components may maintain IGF-I proximity to chondrocytes while blocking ligand proteolysis, sustaining a local reservoir for surface receptors. Russo *et al.* [81] demonstrated that IGFBP-2 binds with various glycosaminoglycans (GAGs) found in cartilage (chondroitin-6-sulfate, keratan sulfate) as well as the key functional proteoglycan aggrecan. In a recent study, this group found that IGFBP-2 binding to proteoglycans on the surface of neuroblastoma cells was mediated by its heparin-binding domain [253]. Association of IGFBP-2 with pericellular proteoglycans could potentiate IGF-I anabolic effects by localizing the growth factor in close proximity to IGF-IR. If IGFBP-2 augments IGF-I activity relative to IGFBP-3 within cartilage, a shift in composition towards the latter species may impede IGF-I anabolism in arthritic joints.

In addition to modulating IGF-I activity, IGFBPs have been reported to have IGF-independent actions on multiple cell types [75], though not specifically for articular chondrocytes. Morales [96] has shown that transforming growth factor-β (TGF-β) enhancement of IGFBP-2 in bovine cartilage culture coincided with increased PG synthesis, postulating that the binding protein mediates TGF-β activity. More recently, the author observed IGFBP-2 to be strongly cell-associated in bovine cartilage, though the associated membrane anchor(s) has yet to be identified [99]. Since IGFBP-2 contains the Arg-Gly-Asp (RGD) motif, one potential candidate is the $\alpha_5\beta_1$ integrin (fibronectin receptor), which is presented on the surface of both normal and osteoarthritic ACs [254]. Schütt and coworkers [255] recently demonstrated that IGFBP-2 surface binding inhibited tumor cell adhesion and proliferation independently of IGF-IR, identifying $\alpha_5\beta_1$ as the specific surface receptor. Notably, IGFBP-2 surface binding was strongly diminished by equimolar quantities of IGF-I or IGF-II, suggesting IGFBP-2 interaction with $\alpha_5\beta_1$ may represent a completely IGF-I-independent signaling function. These studies warrant further investigation into the role of IGFBP-2 surface association in cartilage.

3.5   Conclusions

This work further delineates the role of IL-1 as a key regulator of the IGF-I system within articular cartilage. The inflammatory cytokine enhanced signaling receptor (IGF-IR) levels, which was most likely attributed due to suppressed production of endogenous IGF-I. IL-1β also reduced IGFBP-2 levels but elevated low levels of IGFBP-3, encouraging the hypothesis that alterations in cartilage IGFBP composition promote chondrocyte hyporesponsiveness to IGF-I observed in osteoarthritic joints. IL-1β regulation of IGF-I and IGFBP-3, but not IGF-IR and IGFBP-2, were mediated by mRNA expression. IGFBP-2 suppression was partially reversed by inhibitors of MMPs-2/9 (gelatinases) and MMP-3 (stromelysin-1), implicating these MMPs as co-factors in IL-1 regulation. Promising molecular therapies for OA intervention aim to reverse cartilage degeneration by manipulating both IL-1 and IGF-I signaling with their respective chondrocyte receptors [243]. These strategies may need to address secondary mediators (MMPs, IGFBPs) for optimal restoration of metabolic homeostasis, particularly when applied during advanced stages of this chronic disorder.

3.6   Acknowledgements
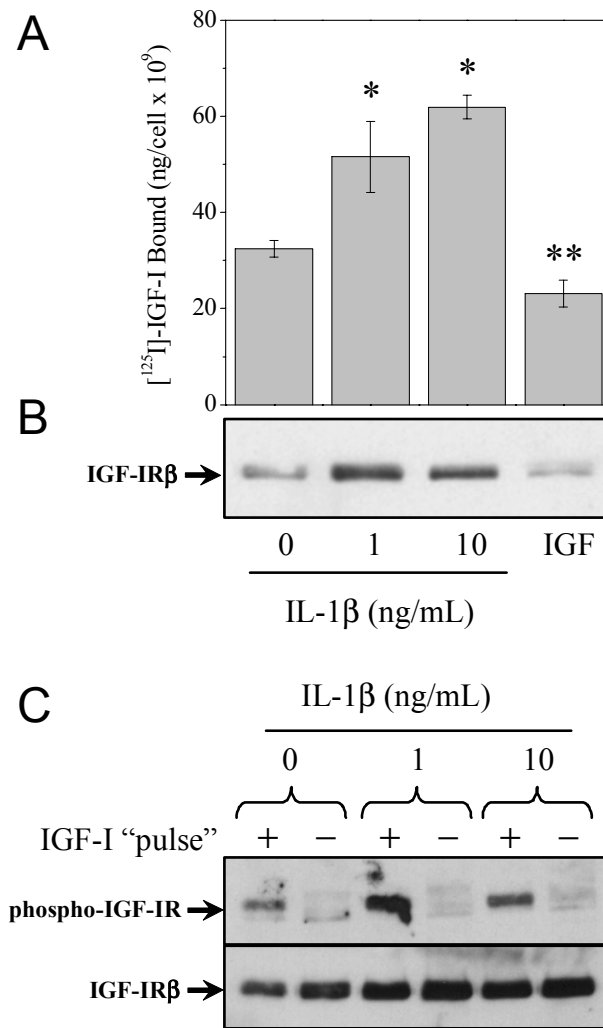
Figure 3.1. Increased IGF-I receptor levels in response to exogenous IL-1β. Chondrocytes were cultured and treated with IL-1β (0-10 ng/ml) or IGF-I (50 ng/ml) for 48 hr prior to radiolabeled binding studies (**A**) or western blot analysis (**B**). (**A**) [^{125}I]-IGF-I bound in the presence of Y60L-IGF-I (2 μg/ml), normalized by cell number presented as a function of treatment. "IGF" denotes cells treated with 50 ng/ml IGF-I in both figures. Bars indicate mean ± SEM (3 wells per treatment). ∗ and ∗∗ denote a statistically significant increase and decrease, respectively, compared to no-treatment control (p<0.05). (**B**) Cell lysate samples (20 μg) were resolved by SDS-PAGE, transferred to a membrane, and probed for the IGF-IRβ subunit (90 kDa). Results are representative of three independent experiments. (**C**) Western analysis of IGF-IR phosphorylation levels. Cell lysate samples (40 μg) from bead and TCP cell cultures were probed for the either phosphorylated (top) or total (bottom) IGF-IR subunit (bottom). Numbers indicate concentration of IL-1 treatment. "+" indicates sample was treated with 200 ng/ml IGF-I for 10 min prior to sample collection (post IL-1 treatment), while "−" indicates no administration of IGF-I.
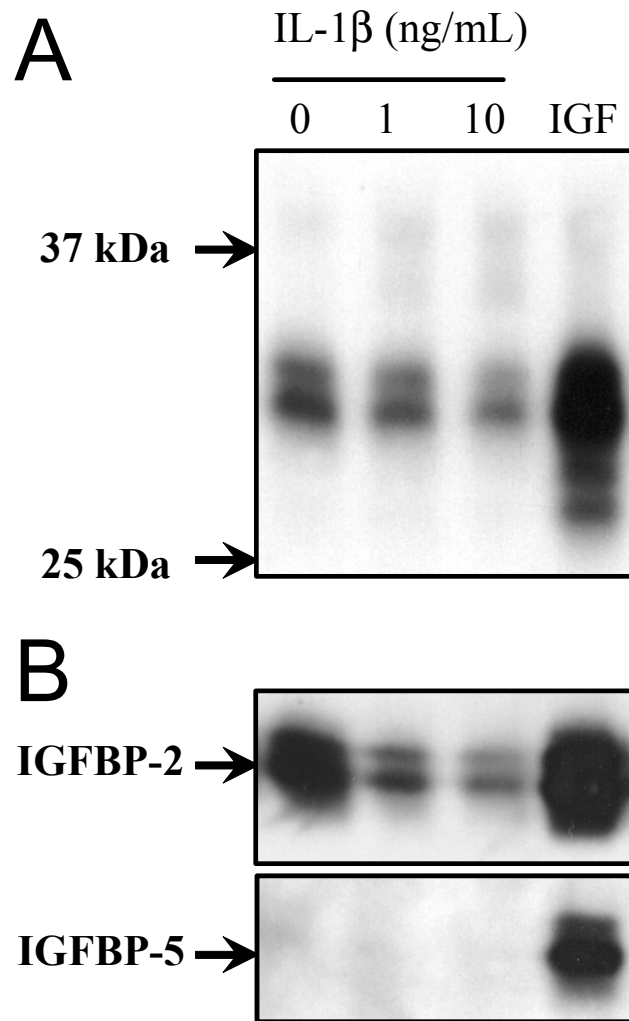
Figure 3.2. IGFBP levels in conditioned media are diminished by IL-1β. (**A**) Pooled media samples were concentrated, resolved by SDS-PAGE, and probed for the binding proteins using [^{125}I]-IGF-I. Bands doublets in the 32-34 kDa and 28-30 kDa regions were consistent with IGFBP-2 and IGFBP-5, respectively. Faint bands found in the 38-40 kDa region were more apparent in longer exposures, likely corresponding to IGFBP-3. "IGF" denotes treatment with 50 ng/ml IGF-I for all blots. (**B**) Western blot analysis using Abs specific for IGFBP-2 (top panel) and IGFBP-5 (bottom panel) confirmed the doublet identities. Blots are representative of three independent studies.
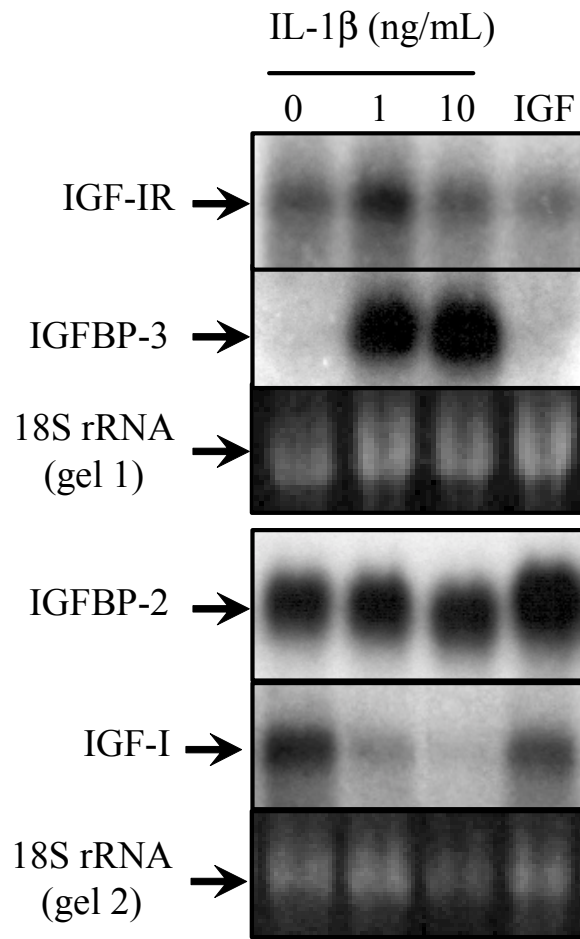
Figure 3.3. Varied transcription regulation of IGF-I system by IL-1β. Total RNA isolates were resolved on a formaldehyde-agarose gel, transferred and crosslinked onto a membrane, and probed for various messenger RNAs. Bands for IGF-I, IGFBP-2, IGF-IR, and IGFBP-3 messages were detected by autoradiography and are presented alongside corresponding 18S rRNA gel bands. "IGF" denotes cells treated with 50 ng/ml IGF-I. Northern blots are representative of three independent experiments.

Table 3.1. IGF-I concentration in conditioned media is reduced by IL-1β

IL-1 (ng/ml)	IGF-I [*] (ng/ml)	p-value [†]
0	3.5 ± 0.4	---
1	2.3 ± 0.5	0.056
10	1.9 ± 0.3	0.013

* mean ± SEM

† one-tailed Student's *t*-test vs. 0 ng/ml
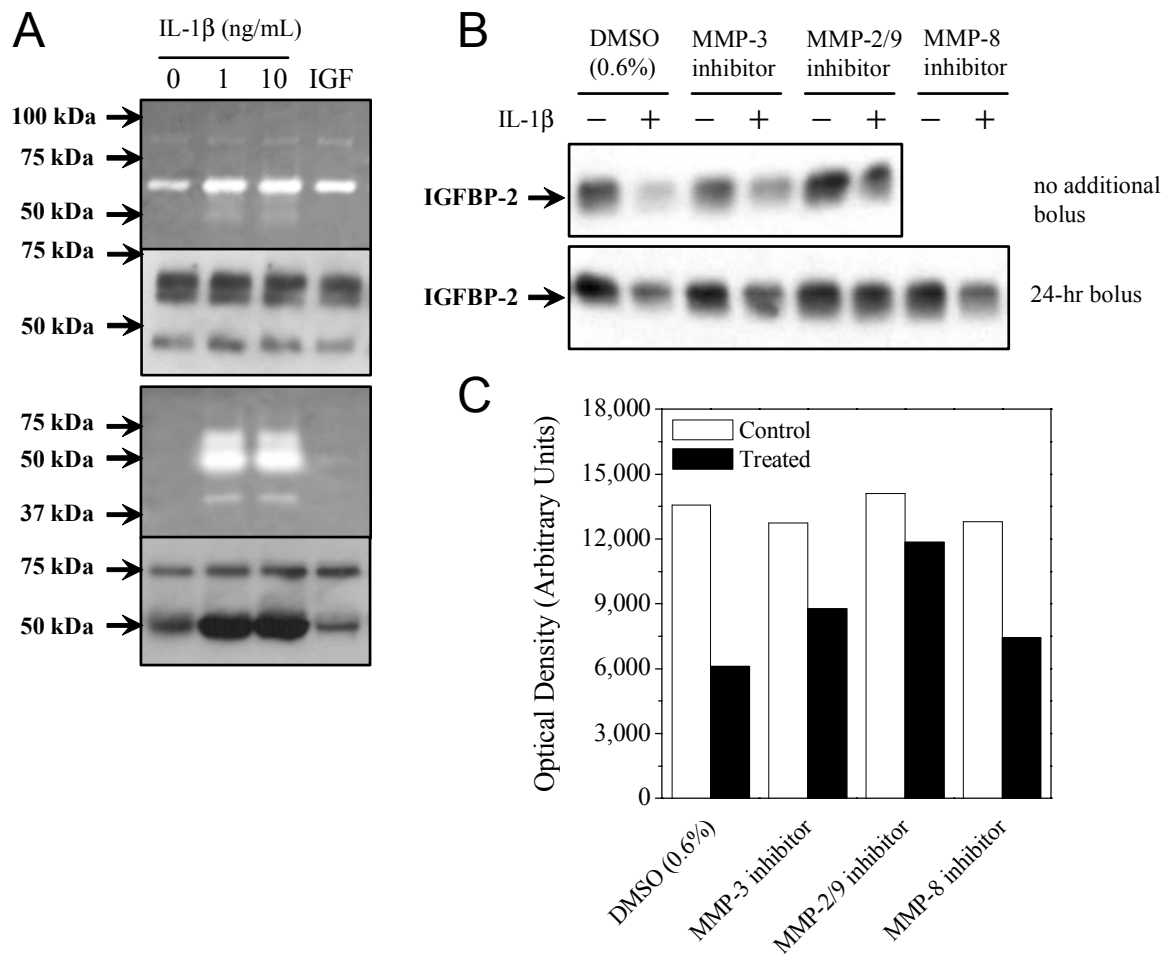
Figure 3.4. MMP inhibitors block suppression of IGFBP-2 by IL-1β. (**A**) Activity of MMPs in conditioned media. Media samples were resolved by SDS-PAGE on zymogram ready-gels of either gelatin (first panel) or casein (third panel). Two bands consistent with pMMP-9 (~90 kDa) and pMMP-2 (~70 kDa) were observed in the gelatin gel, while a set of bands consistent with MMP-3 (48-60 kDa) were found in the casein gel. "IGF" denotes cells treated with 50 ng/ml IGF-I. The identities of MMP-2 (second panel) and MMP-3 (fourth panel) were confirmed by Western blot. (**B**) Western blot analysis for IGFBP-2 from concentrated media incubated with specific inhibitors for MMP-3, MMP-2/9, or MMP-8 (all at 40 µM in DMSO) or vehicle (0.6% DMSO) in the presence (+) or absence (−) of IL-1β (10 ng/ml). A portion of the samples were given an additional bolus of inhibitor after 24 hr (bottom panel) (**C**) Densitometry of IGFBP-2 bands, in arbitrary units, of conditioned media samples from the bottom panel of (**B**). With the exception of MMP-2 and MMP-3 Western blots, all figures and blots are representative of three independent studies.
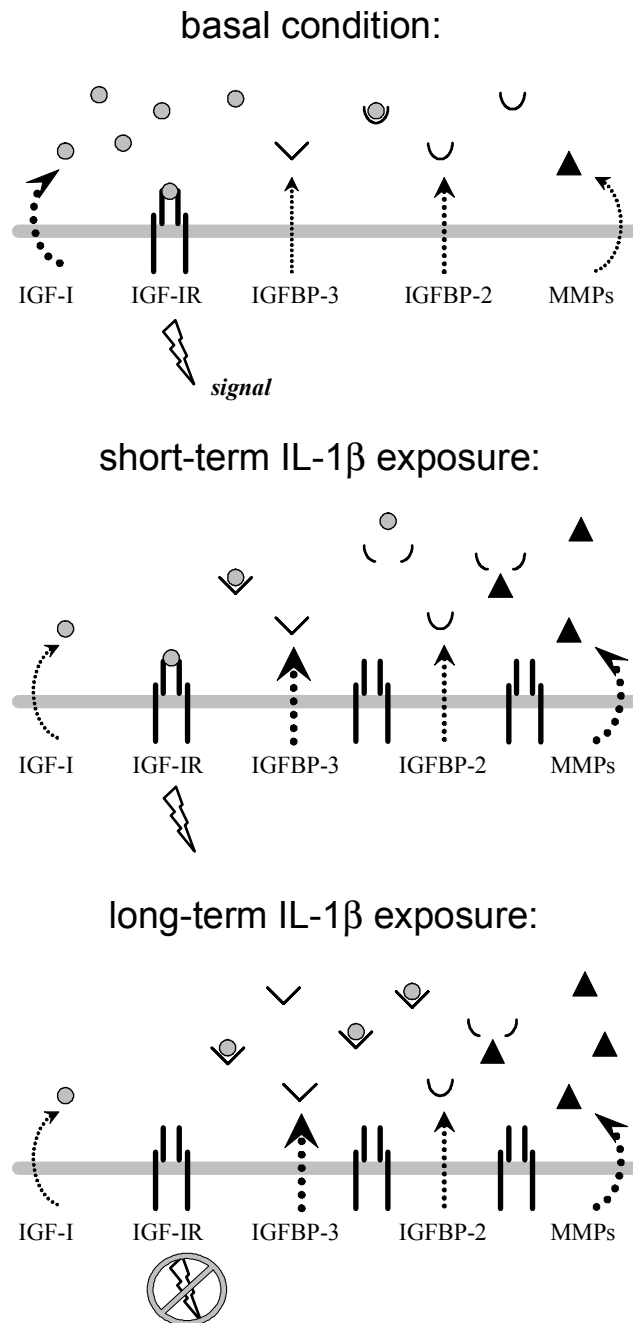
Figure 3.5. Schematic of proposed mechanisms for IGF-I system regulation by IL-1β. Under basal conditions, IGF-I receptor levels are regulated by endogenous IGF-I production. Cells respond to exogenous IL-1β insult with decreased IGF-I expression and, in turn, reduced receptor turnover. Moreover, the cytokine suppresses extracellular IGFBP-2 levels by MMP-mediated degradation. The combined effect of increased receptor availability and reduced IGFBP-2 sequestration could initially enhance chondrocyte responsiveness to exogenous IGF-I stimulation. However, the strong up-regulation of IGFBP-3 transcription suggests a more prominent role for this binding protein with continued insult, ultimately leading to diminished IGF-I responsiveness.

Chapter 4: Culture Strategy Impact on the Insulin-like Growth Factor-I System

4.1   Introduction

Articular cartilage, a specialized connective tissue, functions to reduce friction between joint surfaces and distribute compressive loads between long bones. Because the tissue lacks a direct blood supply, defects attributed to focal injury or arthritis are not readily repaired by endogenous mechanisms, constituting a need for biomedical intervention. Current strategies for cell-based cartilage repair generally involve the isolation and *in vitro* multiplication of autologous chondrocytes [200-202]. However, these methods have been limited by the need to expand chondrocyte numbers in 2-D culture, which leads to a loss of chondrocytic phenotype (i.e., dedifferentiation) after multiple passages [9-11]. Specifically, the cells take on a fibroblast-like morphology and their synthesis of type II collagen decreases in favor of types I and III. The formation of a hyaline-like cartilagenous matrix, as opposed to mechanically-inferior fibrocartilage, is critical for the long-term outcome of repair protocols [201]. *In vitro* culture strategies must therefore balance the establishment of sufficient chondrocyte numbers with the maintenance of cell functionality.

Encapsulation of chondrocytes in alginate beads has proven to be an attractive alternative to 2-D culture [210-212]. Alginate, a linear polysaccharide of L-guluronic and D-mannuronic acids, polymerizes to form a hydrogel in the presence of calcium or other divalent cations. Chondrocytes cultured in calcium alginate beads synthesize a cartilage-like matrix over an extended culture period [212, 214, 215], and cells dedifferentiated following monolayer expansion have been found to re-differentiate following introduction to alginate [12-16]. Viable cells can be easily harvested by depolymerizing the gel in the presence of a chelating agent. These properties have made alginate beads a common scaffold for studying chondrocyte physiology *in vitro* [15, 16, 216-221] and a promising substrate for maintaining or restoring chondrocytic phenotype prior to reimplantation [13, 16, 198, 199, 256].

While investigations of potential chondrocyte culture substrates have focused on phenotypic marker synthesis (e.g., type II collagen, aggrecan), cell signaling systems have not received much attention. Of these systems, the two most prominent with regard to chondrocyte homeostasis are the interleukin-1 (IL-1) and insulin-like growth factor-I (IGF-I) networks [1]. IGF-I enhances production of cartilage extracellular matrix (ECM) components [88, 90, 91],

whereas IL-1, an inflammatory cytokine, inhibits matrix synthesis and stimulates secretion of destructive proteases [172, 174, 230]. Elevated IL-1 levels induce matrix degradation in osteoarthritic cartilage [181-183], but arthritic chondrocytes demonstrate reduced responsiveness to IGF-I [4-6]. The mechanisms that lead to IGF-I hyporesponsiveness have not been characterized, though IL-1 is thought to be one of multiple cofactors [6]. Potential mediators include the type I IGF-I membrane receptor (IGF-IR) and a set of high-affinity IGF binding proteins (IGFBPs 1-6) [257]. IGF-I dysfunction within osteoarthritic cartilage advocates closer examination of this signaling system when culturing chondrocytes *in vitro* for cartilage repair, particularly when targeting arthritic joints.

We postulated that culture history influences the IGF-I signaling system of articular chondrocytes and system response to IL-1. To test this hypothesis, equine articular chondrocytes (ACs) were expanded by serial passage as monolayers and subcultured either in alginate beads (3-D) or on tissue culture plastic (2-D) (**Figure 4.1**). The two cell populations were then plated at high density, stimulated with varied concentrations of recombinant equine IL-1β or human IGF-I, and assayed for IGF-I signaling mediators. Intermediate suspension in alginate produced distinct mediator profiles at basal conditions and disparate responses to exogenous IL-1β relative to continuous monolayer culture. The results suggest culture strategy can alter the IGF-I signaling dynamics of ACs and, consequentially, their effectiveness in mediating cartilage repair.

4.2   Materials and Methods

4.2.1   *Materials*

Sodium alginate (PRONATAL LF10/60; 65-75% L-guluronic acid, 25-35% D-mannuronic acid) was provided by FMC BioPolymer (Philadelphia, PA). Cell culture dishes and well plates were purchased from Corning (Corning, NY): the polystyrene surfaces are made more hydrophilic by corona discharge, adding various ionic groups (hydroxyl, ketone, aldehyde, carboxyl) to the hydrophobic polymer chain and giving the surface a net negative charge [http://www.corning.com/lifesciences/products__services/surfaces/cellculture/stc_treated_polyst yrene.asp]. Collagenase-D was obtained from Roche Diagnostics Corp. (Indianapolis, IN). Cellgro RPMI-1640 media, phosphate-buffered saline (PBS), 1X trypsin-EDTA (0.05% trypsin, 0.53 mM EDTA in HBSS w/o Ca, Mg), and penicillin-streptomycin (P/S) stock (5,000 I.U./ml

penicillin, 5,000 mg/ml streptomycin) solutions were acquired from MediaTech (Herndon, VA). Fetal Bovine Serum was obtained from Hyclone (Logan, UT). Recombinant human IGF-I was purchased from PeproTech (Rocky Hill, NJ), whereas the structural analog Y60L-IGF-I was obtained from Upstate (Charlottesville, VA). Recombinant equine IL-1β was expressed and purified as previously described [2]. Mouse anti-human IGF-I was a gift from Dr. Bernard Laarveld (University of Saskatchewan).

4.2.2   *Chondrocyte isolation and parallel culture*

Equine ACs were isolated by enzymatic digestion of full-thickness cartilage from the stifle joints of 3 and 4 year-old mares, based on an established protocol [234]. Rinsed and diced slivers were digested with 10 ml/g of 1% collagenase buffer overnight at 37°C. After removing undigested cartilage fragments by filtration, ACs were collected by centrifugation and viable cells (>90% by Trypan Blue exclusion) were grown on 75-cm^2 culture flasks with in 'complete medium' (RPMI-1640 supplemented with 10% FBS and 1% P/S). Chondrocytes were subcultured on 100-mm dishes and cryopreserved in complete medium with 10% dimethyl sulfoxide.

For parallel culture studies, chondrocytes stocks (passage 2) were expanded to sufficient numbers by two passages on 100-mm dishes and either (i) encapsulated in alginate beads or (ii) subcultured on tissue culture plastic (TCP) (**Figure 4.1**). Alginate bead culture was conducted as previously described [211], with some modification. Briefly, cells were suspended in a solution of 1.2% sodium alginate in 150 mM NaCl and dispersed drop-wise through a 21-guage needle into a well-mixed 102 mM CaCl$_2$ bath. Suspension drops gelled instantly upon contact with the calcium solution, and resulting beads were crosslinked for an additional 10 min without mixing. After rinsing twice with 150 mM NaCl solution and once with complete medium, beads were transferred to 24-well plates (10 beads per one ml medium). For TCP culture, chondrocytes were seeded into 100-mm dishes at 2×10^5 cells/dish. After keeping bead and TCP cultures in complete media for 10 days, changing media every two or three days, cells were transferred to well plates for comparable treatment and analysis. To isolate embedded cells, beads were dissociated in 55 mM sodium citrate, 150 mM NaCl solution (pH 6.8) for 15 min at 37°C. Cell pellets were collected by centrifuged (280×*g* for 10 min) and isolated bead cells were seeded at ~1.3×10^5 viable cells/cm^2 in well plates. Forty-eight-to-72 hr post-plating, cells were rinsed with

PBS and treated with 0, 1, or 10 ng/ml IL-1β or 50 ng/ml IGF-I in 'low-serum' media (RPMI-1640 with 0.2% FBS and 1% P/S). Plates were cultured for an additional 48 hr and assayed as described below.

4.2.3 *Radiolabeled ligand binding*

IGF-I was radioiodinated using a chloramine-T method [245], and ligand binding experiments were performed as previously described [79]. Briefly, cells in 24-well plates were rinsed once with PBS, and 0.5 ml of sterile binding buffer (0.5% BSA, 10 mM dextrose, 25 mM 4-(2-hydroxyethyl)-1-piperazineethanesulfonic acid (HEPES), 15 mM sodium acetate, 1.2 mM $NaSO_4 \times 7H_2O$, 5 mM KCl, 120mM NaCl, pH 7.4) was added to each well. Blocking factors (IGF-I or Y60L-IGF-I; 1 μg/well) were added to appropriate wells at 4°C for 15 min prior to addition of $[^{125}I]$-IGF-I (2 ng/ml). After overnight incubation at 4°C, cells were rinsed thrice with ice-cold binding buffer, lysed in 1N NaOH for 1 hr, and analyzed for $[^{125}I]$ emissions using a COBRA II Auto-Gamma counter (Packard, Downers Grove, IL). Readings were corrected for background, converted to pg bound ligand based on counts from radiolabeled stock, and normalized by cell number.

4.2.4 *Western blot*

Cell layers were rinsed with PBS and lysed in 1X Laemmli buffer (Bio-Rad, Hercules, CA). Protein concentrations were determined using a RC/DC assay kit (Bio-Rad). Sample protein (30 μg/lane) was resolved by SDS-PAGE (10% gels; 150 V for ~1 hr) and transferred to PVDF membranes (100 V for 90 min). Non-specific binding was blocked by pre-incubating membranes with 5% nonfat milk in TBS-T for 30 min, followed by incubation with a rabbit antibody specific for the β subunit of IGF-IR (Santa Cruz Biotechnology, Santa Cruz, CA) in blocking buffer (1:10,000 dilution) overnight at 4°C. The membranes were then rinsed three times with TBS-T and incubated with a goat anti-rabbit IgG conjugated to horseradish peroxidase (Zymed, San Francisco, CA) (1:15,000 dilution in blocking buffer) for 1 hr at room temperature. After rinsing thrice with TBS-T, bound antibodies were detected on BioMax film using SuperSignal chemiluminescent substrate (Pierce, Rockford, IL).

4.2.5 *Ligand blot*

Detection of IGFBPs by western ligand blot analysis was performed as described previously [246]. Conditioned media (CM) samples were collected and stored at −70°C until analysis. For analysis, aliquots were concentrated 10-fold under vacuum and diluted 1:2 in loading buffer (125 mM Tris, 4% SDS, 20% glycerol, a few grains of bromophenol blue solid, pH 6.8). Samples and protein standards were resolved on a 10% polyacrylamide gel (10 mA/gel for 14 hr at 4°C) and transferred to nitrocellulose membranes (50 V for 6-7 hr at 4°C). Membranes were rinsed sequentially in TBS (10 mM Tris-HCl, 150 mM NaCl, 0.5 mg/ml sodium azide, pH 7.4) + 3% Nonidet P-40 for 30 min, TBS + 1% BSA for 2 hr, and TBS + 0.1% Tween-20 (TBS-T) for 10 min. Blots were incubated overnight at 4°C in a bath of [^{125}I]-IGF-I (~9×10^4 cpm/ml in TBS-T with 5% BSA). The following day, blots were rinsed twice with TBS-T, rinsed thrice in TBS, and exposed to BioMax XAR film (Kodak, Rochester, NY) at −70°C for 3-7 days. Band sizes were identified according to protein standards.

For detection of IGFBP-2 and IGFBP-5 in conditioned media, CM samples were resolved by SDS-PAGE and transferred to nitrocellulose membranes as described above. Membranes were blocked for 30 min with 5% dry milk in TBS-T and incubated with rabbit anti-bovine IGFBP-2 (1:10000 in blocking buffer) or IGFBP-5 (1:5000) (Upstate, Charlottesville, VA) overnight at 4°C. Secondary Ab incubation (1:15000 dilution) and band detection were conducted as described under section 4.2.4.

4.2.6 *Radioimmunoassay*

IGF-I concentrations in conditioned media (CM) were measured by radioimmunoassay, as previously described [247]. CM samples (0.5 ml) were concentrated to pellets under vacuum, resuspended in extraction buffer (87.5% ethanol, 12.5% 2N HCl), and centrifuged at 13,200×*g* to remove IGFBPs. The supernatant was pH-neutralized with 0.855M tris, chilled at −20°C for 1hr, and centrifuged at 1800×*g* for 30 min at 4°C. The resulting supernatant was concentrated under vacuum and reconstituted in IGF-I assay buffer (30 mM sodium phosphate, 10 mM EDTA, 0.02% protamine sulfate, 0.05% Tween-20, pH 8.0). Sample aliquots and standards (0.05–6.5 ng IGF-I) were diluted to a total volume of 0.5 ml in IGF-I assay buffer. After adding 100 µL mouse anti-human IGF-I (1:70,000 dilution), 100 µL [^{125}I]-IGF-I stock (~30,000 cpm) was added and the tubes were incubated at 4°C for 24 hr. Goat anti-mouse secondary Ab (Sigma, St.

Louis, MO) was then added (1:20) and the tubes incubated for an additional 72 hr at 4°C. Samples and standards were then diluted in PBS and the tubes were spun at 1500×*g* for 30 min at 4°C. The supernatant was removed and the resulting pellets analyzed using a COBRA II Auto-Gamma counter (Packard, Downers Grove, IL).

4.2.7 *Northern blot*

RNA was isolated from cell layers using a SV Total RNA Isolation kit (Promega, Madison, WI), including incubation with DNase-I to remove genomic DNA. RNA yields were determined by absorbance at 260 nm. Samples were concentrated under vacuum, re-suspended to 4 µg/µL in nuclease-free water, and stored at –70°C until analysis. Messenger RNA (mRNA) expression was analyzed as previously described [247] using ovine IGF-I, ovine IGFBP-2, rat IGFBP-3, and equine IGF-IR cDNA probes, which were randomly labeled with [α-^{32}P]-dATP using a Prime-a-Gene kit (Promega). Samples were diluted in formaldehyde loading buffer (Ambion, Austin, TX) with ethidium bromide and resolved on agarose-formaldehyde gels (20 µg/lane) at 115 V for ~150 min. The gels were photographed over UV light with a Polaroid GelCam (Cambridge, MA). RNA was transferred to Hybond N^{+} membranes (Amersham, Buckinghamshire, England) by capillary transport and crosslinked using a Stratalinker 1800 UV Crosslinker (Stratagene, La Jolla, CA). After rinsing in 2X saline-sodium citrate (SSC) buffer (0.3 M NaCl, 0.03 M sodium citrate), membranes were pre-incubated in QuickHyb hydridization buffer (Stratagene) for 30 min at 68°C in a roller oven. Labeled probe (25 ng) and 1 µg sheared salmon sperm DNA (Ambion) were added and incubated with the membranes for an additional hour. Blots were rinsed twice with 2X SSC, 0.1% SDS (room temperature for 15 min) and once with 0.1X SSC, 0.1% SDS (60°C for 30 min), wrapped in plastic film, and exposed to BioMax film at –80°C. Band intensities were quantified by densitometry and normalized by corresponding 18S rRNA bands from gel images. For detection of additional mRNAs, blots were stripped using two rinses in pre-boiled 0.1X SSC, 0.1% SDS and re-hybridized as described above.

4.2.8 *Reverse Transcription-Polymerase Chain Reaction (RT-PCR)*

One-µg aliquots of RNA were reverse transcribed using a Superscript II First-Strand Synthesis kit (Invitrogen, Carlsbad, CA), following instructions for oligo(dT)-primed synthesis.

The resulting cDNA volumes were used for polymerase chain reaction with reagents from a *Taq* PCR Master Mix kit from (Qiagen, Valencia, CA). Primer pairs specific for equine type II collagen, type I collagen (alpha 1 chain), type II collagen (alpha 2 chain), and glyceraldehyde-3-phosphate dehydrogenase (GADPH) cDNAs (**Table 4.1**) were formulated using Lasergene software (DNASTAR, Madison, WI). Templates were amplified over 30 thermal cycles using the following protocol: cycle 1 = 94°C for 2 min, T_{ann} for 1 min, 72°C for 2 min; cycles 2-29 = 94°C for 1 min, T_{ann} for 1 min, 72°C for 1 min; cycle 30 = 94°C for 1 min, T_{ann} for 1 min, 72°C for 10 min. The annealing temperature, T_{ann}, was 55°C for collagen Ia1, 50.4°C for collagen Ia2, 58.7°C for collagen II, and 61.5°C for GAPDH. PCR products were resolved on 2% agarose gels, stained in 1 μM ethidium bromide, and photographed. Band intensities were quantified by densitometry and normalized to GADPH signal.

4.2.9 *Statistics*

Figure bars present the mean ± standard error of the mean (SEM) for triplicate samples from a single experiment. Experiments were repeated at least three times, and representative data sets are shown. Differences between treatment means were identified by two-tailed Student's *t*-test, with p-values less than 0.05 considered significant.

4.3   Results

4.3.1 *Disparate basal levels and IL-1β regulation of IGF-IR*

Chondrocytes respond to IGF-I in the extracellular environment via binding of the growth factor to its type I membrane receptor, IGF-IR, which in turn initiates a signaling cascade [49]. Binding experiments with radioiodinated IGF-I were utilized to measure differences in surface receptor levels between the two culture pathways (**Figure 4.2.A**). In order to distinguish receptor binding from that associated with surface-sequestered IGFBPs, cells were pre-incubated with an excess of the structural analog Y60L-IGF-I. Relative to native IGF-I, this analog has diminished affinity for IGF-IR but similar affinity for IGFBPs [248], thereby selectively inhibiting radiolabeled ligand binding to the latter surface pool. In the presence of Y60L-IGF-I, basal [^{125}I]-IGF-I binding levels were approximately two-fold higher on TCP cells (i.e. cells maintained continuously on TCP) than their bead-derived counterparts (i.e., cells cultured in

alginate beads prior to plating and assaying on TCP) (p<0.001). Exogenous IL-1β was found to regulate receptor binding levels, but the response varied between bead and TCP cells. Specifically, the cytokine decreased Y60L-blocked binding on TCP cells (p<0.01) but increased binding on bead cell monolayers (p<0.01). Western blot analysis for the IGF-IR β-subunit supported binding study results (**Figure 4.2.B**). Basal levels of the subunit in TCP cell lysate approximately doubled that of bead cells, and IL-1β treatment reduced TCP cell levels while enhancing bead cell levels. As expected, addition of exogenous IGF-I (50 ng/ml) down-regulated IGF-IR in both cultures, likely due to increased internalization and degradation of ligand-receptor complexes [249].

4.3.2 *Elevated IGFBP-2 secretion in TCP cell-conditioned media*

In addition to IGF-IR, IGF-I signal transduction is regulated by local production of IGF binding proteins that can sequester unbound growth factor and mediate its availability for receptor binding [49]. IGFBP levels were detected by western ligand blot analysis of conditioned media (**Figure 4.3**). Both bead and TCP cell media principally contained doublet bands in the range of 32-34 kDa, which were confirmed to be alternative glycosylation forms of IGFBP-2 by western blot analysis. IGFBP-2 levels were substantially higher in the TCP cell cultures (nearly seven-fold at basal conditions). IL-1β treatment suppressed IGFBP-2 levels by approximately 50 and 60% for bead and TCP cells, respectively, whereas exogenous IGF-I enhancement was more pronounced in bead cell culture (nearly five-fold relative to control). IGF-I treatment also intensified a 28-30 kDa band doublet identified as IGFBP-5 by western blot (refer to **Figure 3.2**). Faint bands around 38-40 kDa were observed in longer film exposures, likely corresponding to IGFBP-3. Although bead and TCP cells expressed the same predominant IGFBP that displayed similar responses to exogenous factors, the marked difference in basal IGFBP-2 levels could translate to dissimilar IGF-I signaling dynamics between the two cell populations.

4.3.3 *IGF-I levels parallel trends for IGFBP-2*

IGF-I concentrations in cartilage represent the sum of endocrine contributions (via synovial fluid) and autocrine/paracrine production by chondrocytes. IGFBPs can extend IGF-I half-life in the cartilage matrix by blocking its proteolysis and inhibiting cell uptake via IGF-IR.

Consequently, elevated binding protein concentrations in TCP cell culture could result in higher IGF-I levels relative to bead cells. To assess whether endogenous IGF-I concentrations mirror IGFBP trends, conditioned media was probed for IGF-I (both unbound and IGFBP-bound fractions) by radioimmunoassay (**Figure 4.4**). At basal conditions, TCP cell media contained 12.1 ± 0.9 ng/ml IGF-I compared to 3.2 ± 0.1 ng/ml in bead cell cultures, a nearly 4-fold difference ($p<0.001$). Exogenous IL-1β decreased IGF-I levels in TCP cell culture to 7.2 ± 0.4 and 8.0 ± 0.2 ng/ml following stimulation with 1 and 10 ng/ml, respectively. IGF-I reduction in bead cell culture was only significant with 10 ng/ml IL-1β (2.3 ± 0.1, $p<0.01$). Growth factor concentrations remained substantially higher in TCP cell culture at both treatment levels ($p<0.001$). As postulated, IGF-I concentration trends paralleled those for IGFBP-2, suggesting the binding protein may extend IGF-I half-life in these cultures. Moreover, the sequestration of IGF-I by IGFBP-2 and subsequent inhibition of ligand binding to IGF-IR may account for the disparity in basal receptor levels between bead and TCP cells.

4.3.4 *Transcription rates reflect differential IGF-I mediator levels*

Clear differences in basal levels of both IGF-IR and IGFBP protein (**Figures 4.2, 4.3**) and varied cell response to IL-1β (**Figure 4.2**) indicate significant modification of these signaling systems during alginate bead culture. These effects could be mediated by transcriptional and/or post-trancriptional (e.g., proteolytic) mechanisms. In order to examine the contribution of the former, IGF-IR, IGFBP-2, and IGF-I mRNAs were detected by northern blot analysis (**Figure 4.5.A**). As observed at the protein level, TCP cultures displayed twice as much IGF-IR transcript than bead cells. Whereas IL-1β had no marked effect on IGF-IR message for bead cells, it dose-dependently suppressed mRNA levels in TCP culture (**Figure 4.5.B**). IGF-I down-regulated IGF-IR message for both culture pathways. Collectively, these results suggest that both receptor turnover and message synthesis mediate IGF-IR protein levels. With regard to IGFBP-2, basal levels of transcript were significantly higher for TCP cells compared to bead counterparts (a nearly nine-fold increase), mirroring the disparate secretion levels observed in conditioned media. A decrease in IGFBP-2 expression (~70% of control) was observed with 10, but not 1, ng/ml IL-1β for bead cells, though the cytokine did not affect IGFBP-2 transcription in TCP cells. Exogenous IGF-I enhanced IGFBP-2 transcript for bead cell cultures (~60%) but, again, had negligible effects on TCP cell message. The two cell populations also differed with

respect to IGF-I expression. Bead cells displayed measurable expression at basal conditions that was decreased in response to IL-1β. Conversely, IGF-I message was only readily detectable following IL-1β stimulation in TCP cell culture. These blots indicate that culture substrate effects on the IGF-I system are primarily attributed to transcriptional regulation, though additional mechanisms must be considered to account for system response to IL-1β.

4.3.5 *Bead and TCP cells vary in phenotypic response to IGF-I and IL-1*

Alginate bead culture has been shown to restore the chondrocytic phenotype of ACs grown for multiple passages *in vitro* [12-16], though not specifically for equine cells. To confirm a phenotypic difference between chondrocytes subcultured in alginate and those grown continuously on TCP, we compared collagen expression and cell growth rates in response to exogenous factors. RT-PCR analysis revealed that bead and TCP cells expressed measurable levels of types I and II collagen mRNAs (**Figure 4.6.A**), molecular markers of fibroblastic and chondrocytic phenotypes, respectively [11]. Bead cells demonstrated similar basal levels for collagen Iα1 but higher levels of collagen II (about three-fold over TCP cell levels). Exogenous IL-1β suppressed collagen II dose-dependently for both cell populations, as shown previously with human [169] and equine ACs [235]. However, the impact of exogenous factors on type I collagen expression varied markedly between the culture pathways. Whereas 10 ng/ml IL-1β suppressed collagen Iα1 mRNA to nearly undetectable levels in bead cell culture, the same concentration approximately tripled band intensity for TCP cells. Similarly, IGF-I treatment strongly diminished collagen I expression for bead cells and nearly tripled levels in TCP cell culture.

In addition to transcriptional differences, we investigated whether cell proliferation in response to IL-1β, which has been demonstrated for subcultured human ACs [209, 258], would be altered by alginate culture. As shown in **Figure 4.6.B**, TCP cell densities increased by approximately 30% following treatment with IL-1β or IGF-I (p<0.01), whereas bead cell densities were not altered significantly by either factor. Taken together, these experiments indicate that alginate culture altered phenotypic responses of ACs to both IL-1β and IGF-I, which may be partially associated with changes in the profile of IGF-I signaling mediators (**Figures 4.2-4**).

4.4   Discussion

The primary objective of this work was to determine whether chondrocyte culture history impacts the IGF-I signaling system. This system is known to play a key role in maintaining cartilage homeostasis [257], and its dysfunction is thought to contribute to cartilage deterioration during the progression of osteoarthritis [259]. Changes in network component synthesis following chondrocyte culture *in vitro* may determine the ability of these cells to adequately repair cartilage defects *in vivo*. However, previous evaluations of chondrocyte culture strategies have not addressed this system, which includes the type I surface receptor (IGF-IR), high-affinity binding proteins (IGFBPs), and endogenous IGF-I. In this study, we found that intermediate alginate suspension altered basal synthesis of IGF-I mediators relative to continuous culture on TCP, suppressing both IGF-IR levels (**Figure 4.2**) and IGFBP-2 secretion (**Figure 4.3**). These effects were attributed to disparate mRNA expression between bead and TCP cells (**Figure 4.5**). Higher TCP cell receptor expression could indicate a feedback response to reduced IGF-I signal transduction. However, endogenous IGF-I concentration was also higher in TCP cell culture (**Figure 4.4**), despite the fact that bead cells transcribed more IGF-I message at basal conditions. Radioimmunoassay measurements did not distinguish between free and IGFBP-bound ligand; therefore, elevated IGFBP-2 levels may sequester local IGF-I and inhibit its binding to IGF-IR, stimulating expression of more receptors in a negative feedback loop.

The degree of receptor suppression by alginate culture was less than that for IGFBP-2, so that the overall proportion of surface receptors to extracellular IGFBPs was increased. This proportionality may reflect chondrocyte responsiveness to IGF-I, as IGFBPs can attenuate IGF-I signal transduction by competing with IGF-IR for unbound ligand. In osteoarthritic cartilage, elevated IGFBP levels are thought to contribute to the IGF-I hyporesponsiveness of the tissue [98, 99, 101, 104]. Given this inhibitory function, alginate culture may augment chondrocyte responsiveness to IGF-I following extended culture on TCP, enhancing its anabolic activity. However, IGFBPs can also potentiate IGF-I signaling, depending on the particular species and the extracellular environment [49]. Follow-up studies using cartilage explant or animal models may better characterize the precise role of diminished IGFBP-2 on IGF-I signaling dynamics.

In addition to basal component levels, we examined IGF-I system regulation by IL-1β. This cytokine, which has been reported to control IGF-IR, IGFBP, and autocrine/paracrine IGF-I

synthesis in AC cultures from a number of species [194-196], is thought to be an important co-factor in the development of osteoarthritic chondrocyte hyporesponsiveness to IGF-I [6]. IGF-IR regulation by the cytokine was clearly influenced by culture pathway, as IL-1 increased receptor levels on bead cells but decreased receptors on TCP cells. The reduction in TCP cell levels was mediated by down-regulation of mRNA expression, though bead cell levels did not correlate with transcription. Endogenous IGF-I levels in bead cell culture decreased dose-dependently in response to IL-1β, as did growth factor message, implying enhanced receptor levels were likely attributable to reduced turnover in response to ligand binding.

IGF-I concentrations were also decreased by IL-1β in TCP cell culture (**Figure 4.3**), despite cytokine stimulation of transcript levels (**Figure 4.5**). Ligand concentrations were observed to parallel IGFBP-2 levels, which were reduced by IL-1β, emphasizing the role of IGFBPs in IGF-I signaling dynamics. Unlike culture system effects, IGFBP-2 regulation by IL-1β was not directly mediated by transcription for either cell population. As described in Chapter 3 (section 3.3.5), the suppression of IGFBP-2 was blunted by inhibitors of the matrix metalloproteinase (MMP) family, whose members are upregulated in cartilage and AC cultures by IL-1 [172, 174, 230, 235]. Although IGFBP-2 was proteolyzed in both culture systems, levels in IL-1-treated TCP cell cultures exceeded untreated alginate counterparts due to the marked disparity in basal expression. Given the patterns of receptor and binding protein regulation, alginate culture may enhance AC sensitivity to exogenous IGF-I in the presence of IL-1β. Such a function would prove advantageous when cultivating autologous chondrocytes for the repair of osteoarthritic cartilage. However, dedifferentiation associated with OA may not be comparable to the effects of monolayer expansion.

Two well-characterized substrates were selected as model culture systems for this study: one reported to bring about chondrocyte dedifferentiation (extended 2-D culture on TCP) [9-11], and another shown to re-establish chondrocytic phenotype (3-D suspension in alginate beads) [12-16]. In agreement with earlier work [12, 14-16], equine chondrocytes encapsulated for 10 days in alginate transcribed more type II collagen, a key matrix component of hyaline cartilage, than those grown continuously on TCP (**Figure 4.6.A**). Unexpectedly, bead and TCP cells expressed similar levels of type I collagen, a marker of the fibroblastic phenotype [11]. Although collagen I has been suppressed in short-term alginate culture following as many as three passages on TCP [12, 14-16], recent investigations of extended monolayer culture reported

limited reduction [13, 260]. It should be noted these studies examined bead and TCP cells directly from high-serum cultures. Conversely, our comparisons were made under low-serum (0.2% FBS) conditions in order to test chondrocyte response to exogenous hormonal factors yet still prevent cell apoptosis following serum starvation. We found that both IL-1β and IGF-I enhanced collagen I expression in TCP cells but suppressed transcript levels following intermediate alginate suspension. Coupled with reports of enhanced chondrocytic response to IL-1β [14] and bone morphogenetic protein-2 [15] after redifferentiation in alginate, our results suggest that the chondrogenic action of this substrate may be associated with restoration of hormonal signaling. The attenuation of cell growth response to IL-1β (**Figure 4.6.B**) further supports this interpretation. In a comparison of primary human chondrocytes with TCP-passaged chondrocytes and synovial fibroblasts, Guerne *et al.* [209] demonstrated that while IL-1 did not stimulate thymidine incorporation (i.e., DNA synthesis) of primary chondrocytes, the cytokine did increase proliferation of TCP-passaged cells. In fact, they found passaged chondrocytes behaved more like fibroblasts than primary cells, suggesting chondrocyte proliferation in response to IL-1 marks a shift toward the fibroblastic phenotype. In turn, diminished growth response implies a partial recovery of chondrocytic behavior. The shift in chondrocyte phenotypic activity following alginate suspension may be attributed the alteration of hormonal signaling networks.

4.5   Conclusions

Alginate suspension not only recovers AC synthesis of cartilage ECM components following extensive monolayer culture [12-16], but also alters basal levels of IGF-I signaling mediators and their response to interleukin-1β. Intermediate bead culture yielded relatively low IGF-IR levels that increased in response to IL-1β, whereas higher receptor levels on TCP cells were suppressed by the cytokine. TCP cells also secreted markedly higher levels of IGFBP-2, though IL-1β reduced levels for both cell populations. Concentrations of endogenous IGF-I paralleled IGFBP-2 secretion, suggesting local IGF-I levels are influenced by IGFBP-2. Disparate basal levels of IGF-IR and IGFBP-2, but not IGF-I, were attributed to relative transcript expression. The distinct IGF-I mediator profiles coincided with varied effects of exogenous IL-1β and IGF-I on collagen Ia1 expression and cell growth rate. These findings suggest a link between the IGF-I signaling system and chondrocyte redifferentiation. More

generally, however, they demonstrate the impact of culture strategy on hormonal signaling networks. Phenotypic markers alone cannot consistently predict the ability of culture-expanded chondrocytes to synthesize functionally viable cartilage *in vivo* [261]. Additional consideration of hormonal mediators may improve the evaluation of chondrocyte culture protocols for clinical cartilage repair.

4.6   Acknowledgements

Table 4.1. Primer sequences for RT-PCR

Target	Sense primer (5'-3')	Antisense primer (5'-3')	Product size (bp)	GenBank No.
Collagen Ia1	CCCCACCCCAGCCGCAAAGA	GGGGGCCAGGGAGACCACGAG	617	AF034691
Collagen II	GAAGAGCGGAGACTACTGGATTGA	AGGCGCGAGGTCTTCTGTGA	501	U62528
GAPDH	AGGGTGGAGCCAAAAGGGTCATCA	GCTTTCTCCAGGCGGCAGGTCAG	418	AF157626
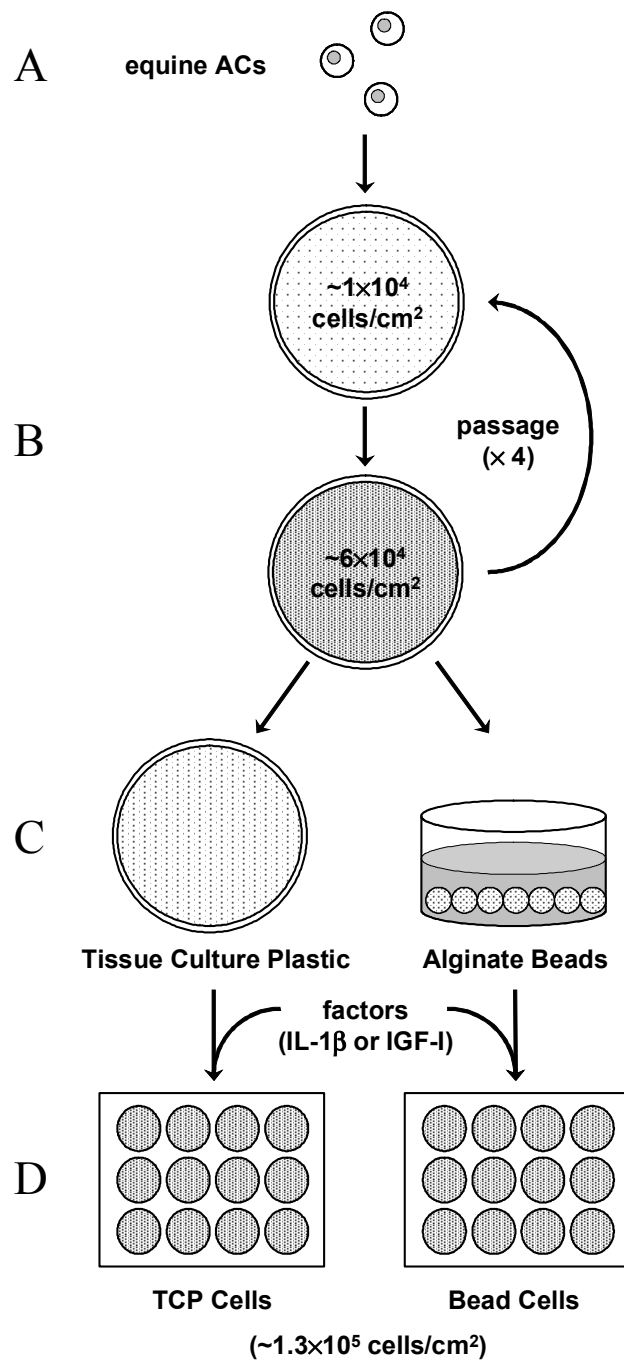
Figure 4.1. Schematic of parallel culture strategy. (**A**) Equine articular chondrocytes were isolated from articular cartilage explants, expanded in 75 cm^2 culture flasks, and cryopreserved as described in Materials and Methods. (**B**) Chondrocyte numbers were expanded (~20-fold) with two subcultures on 100-mm dishes. (**C**) Cells were then either subcultured on tissue culture plastic (TCP) (left) or encapsulated in alginate beads (right). (**D**) After 10 days of culture, cells from TCP were lifted by trypsin digestion while alginate beads were dissociated, and both chondrocyte populations were seeded as high-density monolayers for experimental studies.
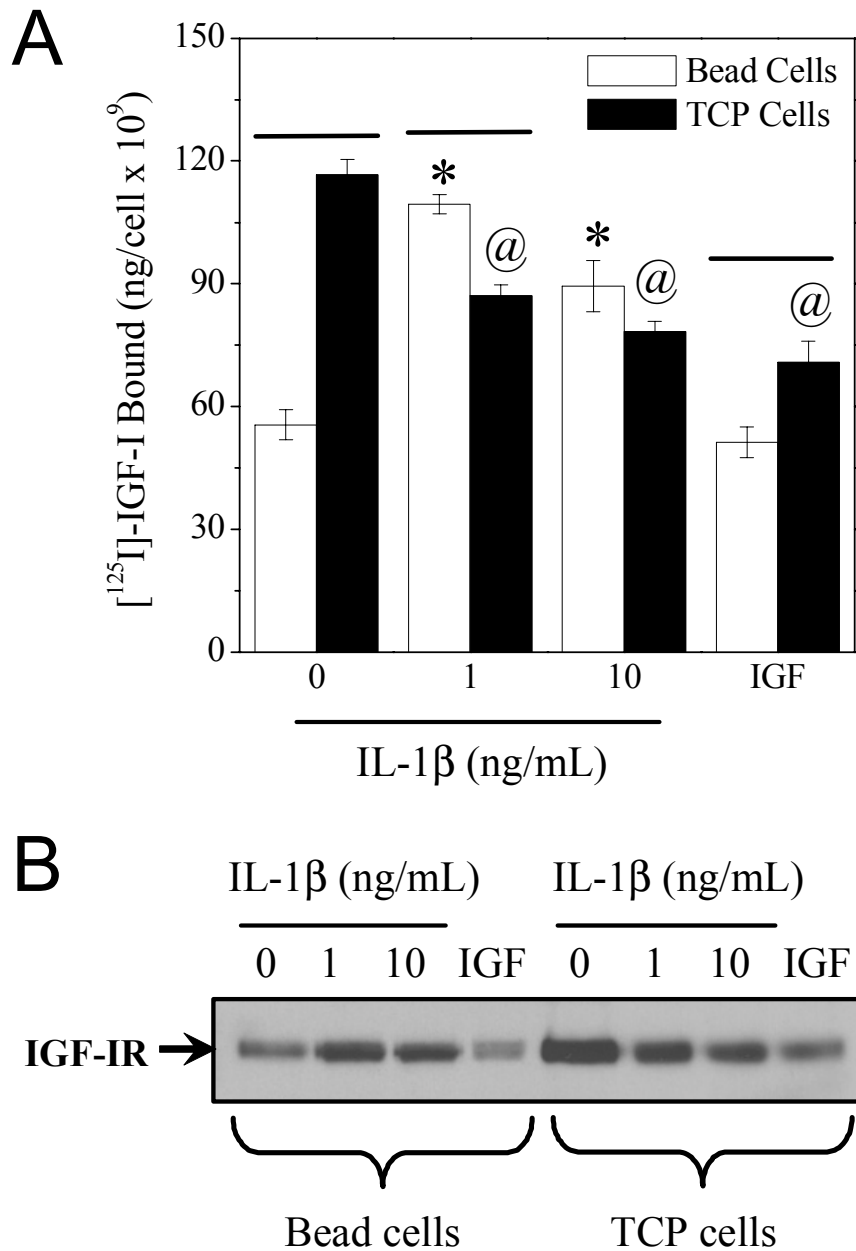
Figure 4.2. IGF-I receptor levels on bead and TCP cells. (**A**) [^{125}I]-IGF-I bound to bead (open) and TCP (filled) cell monolayers in the presence of excess Y60L-IGF-I (2 μg/ml) was measured as described in Materials and Methods. Binding levels were normalized by cell densities. Bars represent the mean ± SEM for 3 wells per treatment. ∗ (beads) or @ (TCP) denotes statistically significant differences compared to no-treatment control (p<0.05 by unpaired Students *t*-test), and horizontal bars represent significant differences between bead and TCP cell cultures at a particular treatment. (**B**) Western blot analysis of IGF-IR. Cell lysate samples (20 μg) were resolved by SDS-PAGE and probed for the IGF-IRβ subunit (90 kDa). "IGF" denotes cells treated with 50 ng/ml IGF-I. Results for both **A** and **B** are representative of three independent studies.
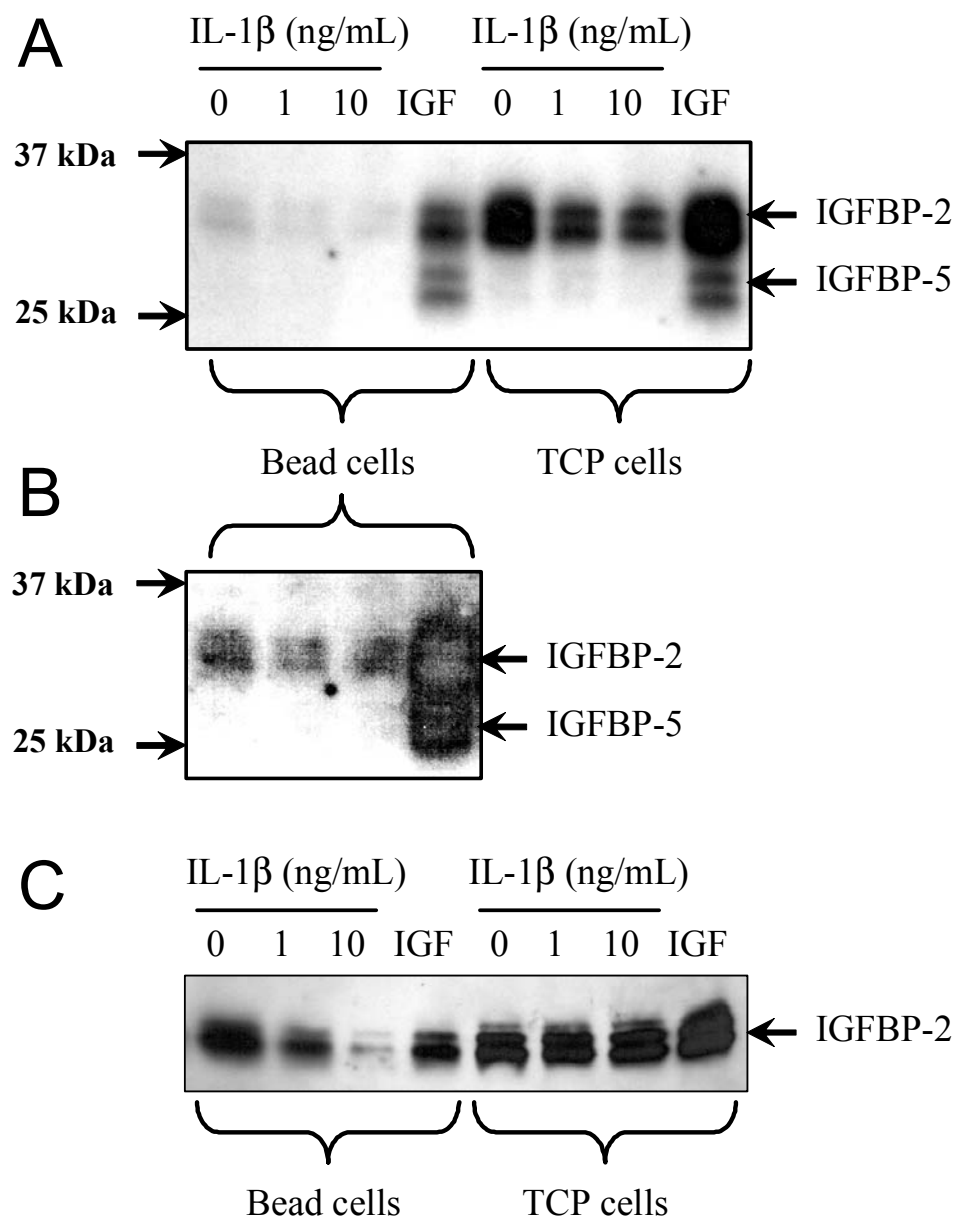
Figure 4.3. Ligand blot analysis of IGFBPs in cell-conditioned media. (**A**) Media samples were concentrated, resolved by SDS-PAGE, and probed for the binding proteins using [^{125}I]-IGF-I as described in Materials and Methods. (**B**) A darker exposure of the bead cell blot shown in **A**. "IGF" denotes cells treated with 50 ng/ml IGF-I. (**C**) Western blot analysis using IGFBP-2 antiserum confirmed the identity of the 32-34 kDa doublet. Blots are representative of three independent studies.
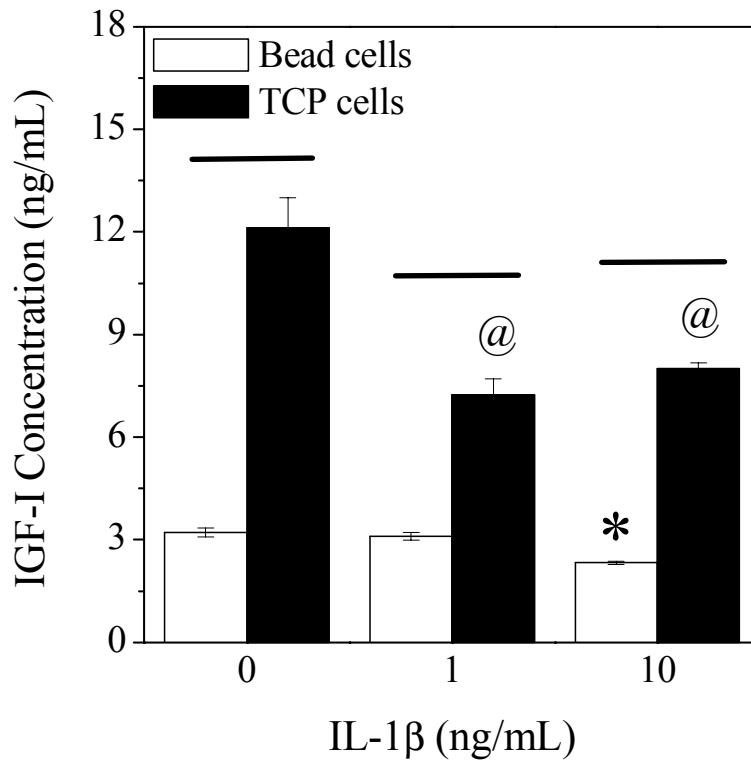
Figure 4.4. IGF-I concentrations in cell-conditioned media. Media samples were concentrated, binding proteins were extracted, and total IGF-I (free plus IGFBP-bound) was detected by radioimmunoassay as described in Materials and Methods. ∗ (beads) or @ (TCP) denotes a statistically significant difference compared to no-treatment control ($p<0.05$ by unpaired Students *t*-test), whereas horizontal bars represent significant differences between bead and TCP cell cultures at a particular treatment. Results are representative of three independent experiments.
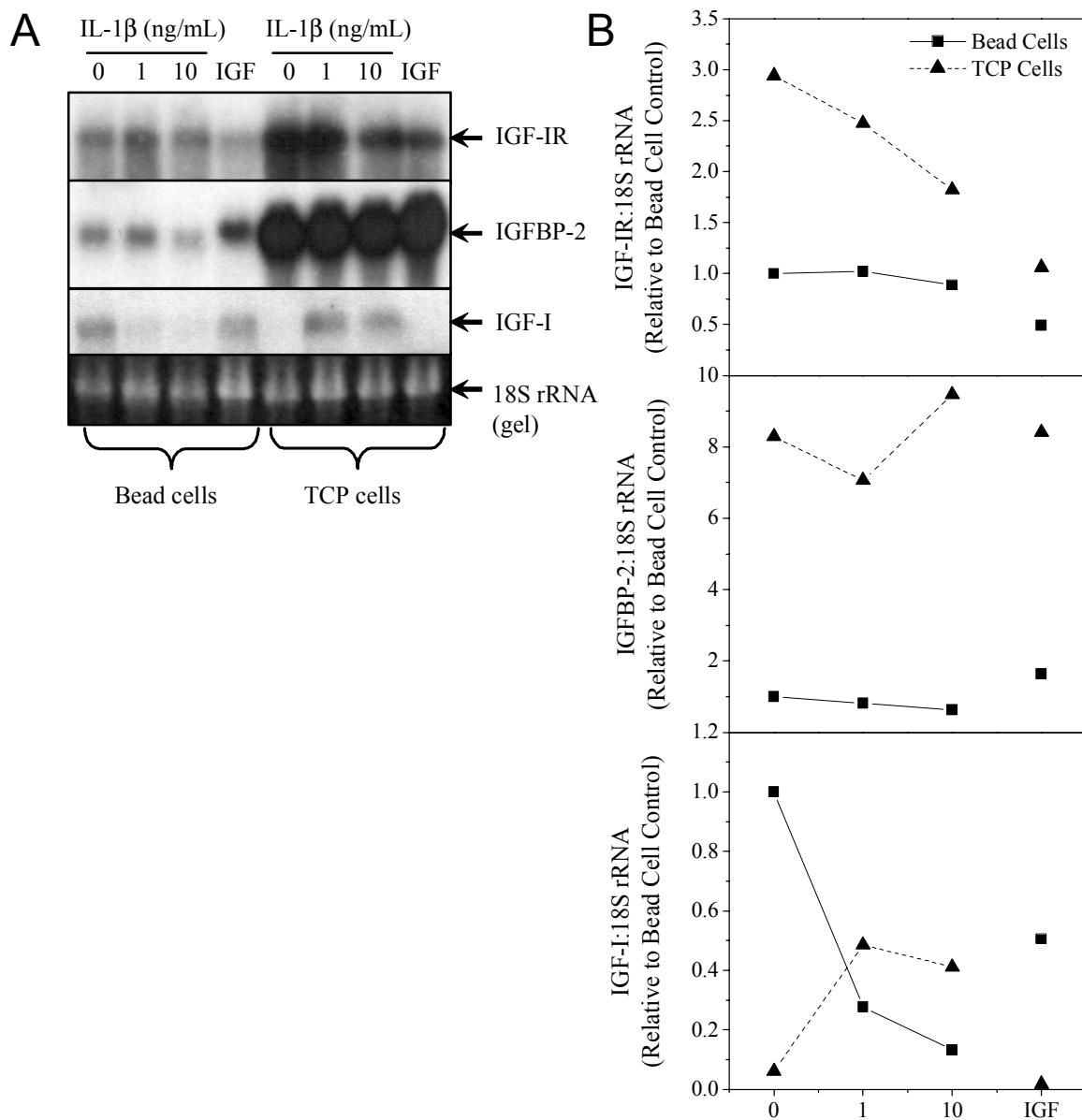
Figure 4.5. Northern blot analysis of IGF-I system transcripts. Total RNA isolates were resolved on a formaldehyde-agarose gel, transferred and crosslinked onto a membrane, and probed for various messenger RNAs of the IGF-I system using specific, radiolabeled cDNA probes. (**A**) Bands for IGF-IR, IGFBP-2, and IGF-I messages were detected by autoradiography and are presented alongside the gel image for 18S rRNA bands. (**B**) Band intensities were measured by densitometry and normalized to corresponding 18S rRNA intensities. Optical density ratios for bead (■) and TCP (▲) cells are presented relative to bead controls (0 ng/ml). "IGF" denotes cells treated with 50 ng/ml IGF-I. The blot is representative of three independent studies.
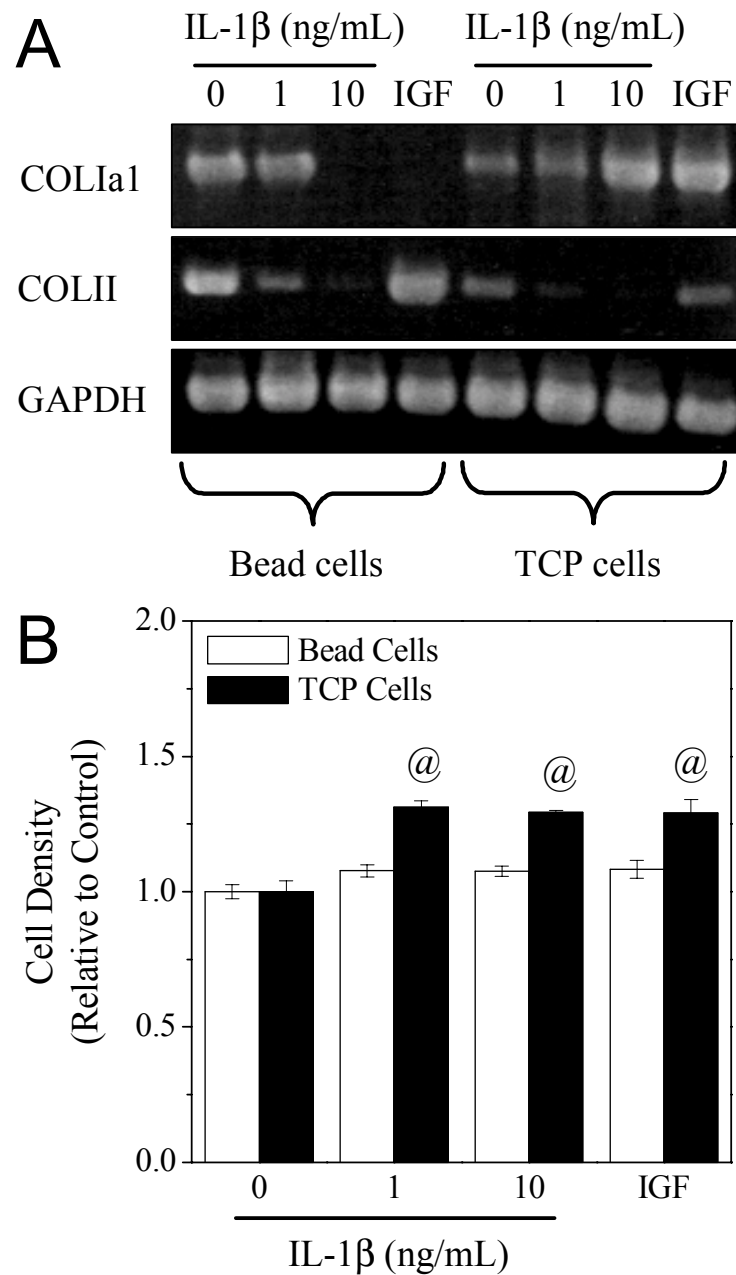
Figure 4.6. Phenotypic differences between bead and TCP cells. (**A**) RT-PCR analysis of collagen synthesis. Total RNA isolates collected after IL-1/IGF-I treatment were reverse transcribed and the resulting cDNA probed for collagen Ia1, collagen II, and GAPDH messengers by PCR using specific primer pairs (**Table 4.1**). "IGF" denotes cells treated with 50 ng/ml IGF-I. (**B**) Cell density as a function of IL-1β concentration. Chondrocytes from beads (open) or TCP (filled) were cultured in 24-well plates and treated with 0-10 ng/ml IL-1β or 50 ng/ml IGF-I for 48 hr. Cell numbers are presented relative to the respective culture system controls (0 ng/ml). Bars represent the mean ± SEM for 3 wells per treatment. @ denotes a statistically significant difference compared to no-treatment control ($p < 0.05$ by unpaired Students *t*-test). All results are representative of three independent experiments.

Chapter 5: Significance and Future Work

5.1   Relevance to Field of Research

The central goal of this work was to characterize the insulin-like growth factor-I and interleukin-1 signaling systems of articular chondrocytes in order to better understand how the anabolic (IGF-I) and catabolic (IL-1) chondrocyte stimuli are linked within articular cartilage. Studies demonstrated that IL-1β regulates IGF-I signaling mediators through both direct (i.e., transcription) and indirect (i.e., protease activity) mechanisms (Chapter 3). IL-1 effects on the levels and localization of binding proteins, particularly IGFBP-2 and IGFBP-3, may alter IGF-I signaling dynamics within cartilage and contribute to the development of chondrocyte hyporesponsiveness to IGF-I, a biochemical hallmark of osteoarthritis. These results have implications for molecular therapies directed at reversing cartilage deterioration associated with arthritis. Modalities currently under investigation include gene transfer of interleukin-1 receptor antagonist (IL-1ra) cDNA, blocking the inflammatory and catabolic activity of increased IL-1 levels in arthritic joints [262], and co-transfer of IL-1ra and IGF-I to simultaneously block degradation and enhance repair activity [243]. However, these first-generation strategies are more likely to be utilized in treating more advanced stages of the chronic disorder, where symptoms (e.g., inflammation, pain) are more easily recognized. Advanced-stage therapies may also need to address secondary regulators, such as MMPs and IGFBPs, in order to more effectively restore cartilage homeostasis. For example, augmented expression of the various tissue inhibitors of metalloproteinases (TIMPs) may counteract the effects of elevated MMP levels in cartilage. Ideally, therapies that target OA-inductive signaling systems would be introduced at earlier stages to prevent disease progression. Such preemptive measures first require improved understanding of the mechanisms associated with loss of metabolic homeostasis.

This research not only concerns cartilage function and dysfunction, but also applies to tissue engineering strategies for cartilage repair. As described in Chapter 4, we examined the influence of intermediate alginate suspension on the IGF-I system of equine ACs, observing that culture history impacted basal mediator levels and their regulation by IL-1. These effects coincided with altered phenotypic responses to exogenous IL-1 and IGF-I, suggesting scaffold selection and culture strategy can govern the capability of chondrocytes to form neocartilage *in*

vitro or mediate repair *in vivo* by altering the dynamics of hormonal signaling networks. Whether tissue engineering protocols involve mature, autologous chondrocytes or the differentiation of their mesenchymal progenitor cells, additional knowledge of growth factor and cytokine signaling dynamics is needed to effectively maintain cell phenotype *in vitro* and direct cell metabolism within artificial constructs. Specifically, alginate hydrogels have become attractive substrates for maintaining the phenotype of autologous cells prior to implantation. Therefore observations made here may prove valuable to those investigating alginate for its chondrogenic properties.

5.2 Directions for Future Research

Radiolabeled ligand binding studies indicated that the majority of IGF-I surface binding was associated with IGFBPs (**Figure A.1**). Interestingly, trends for IGFBP-associated surface binding did not correlate with secreted IGFBP levels detected by Western ligand blot. These findings suggest IGFBP surface sequestration – rather than simply a nonspecific function of extracellular concentration – could be directed though specific mechanisms for particular signaling purposes. For example, recent studies using cancer cell lines have reported a functional role for IGFBP-2 interaction with surface proteoglycans [253] and integrins [255]. IGFBP-2 has been reported to be highly cell-associated in bovine articular cartilage [99]. Our initial efforts to identify binding proteins on the chondrocyte surface focused on IGFBP-2, since this species was predominant in equine AC culture. As summarized in Appendix A, IGFBP-2 was detected on the chondrocyte surface by immunofluorescence (**Figures A.3** and **A.4**), but staining trends did not mirror ligand binding study results (**Figure A.5**). Further work is required to characterize the profile of cell surface IGFBPs, IGFBP membrane anchors, and the regulation of both by IL-1. To identify the anchor(s) for IGFBP-2, for example, radiolabeled IGFBP-2 could be employed in cell binding studies along with blocking agents (e.g., antibodies, RGD peptides) specific for various membrane receptors (e.g., integrins), as previously described [255].

These studies are the first, to the best of our knowledge, to establish a link between IGFBP and MMP levels within articular chondrocyte culture (**Figure 3.4**). The results may have important implications for the regulation of IGFBP – and thereby IGF-I – localization by IL-1 in osteoarthritic cartilage. However, more studies are needed to map out the interactions between

70

IGFBPs and MMPs. Specific MMP inhibitors could be combined with radiolabeled IGFBP-2 in chondrocyte-conditioned media (with or without IL-1 treatment) to identify the role of additional MMPs such as collagenase 1 (MMP-1). An initial attempt at measuring degradation of radiolabeled IGFBP-2 by concentrated conditioned media was unsuccessful, possibly due to incompatibility between the bovine recombinant protein and equine MMPs. Alternatively, iodination could have blocked the specific epitope for protease cleavage.

In addition to expanding the characterization of the chondrocyte IGF-I system, future studies are required to identify signaling pathways associated with IL-1 regulation. Among the potential candidates, the mitogen-activated protein kinase (MAPK) pathways are known to be activated by IL-1 in chondrocytes [147-149]. For example, the MAPK family has been shown to mediate chondocyte expression of MMPs [149, 151, 152]. Preliminary experiments were conducted to confirm IL-1 activation of MAPKs in equine chondrocyte culture, as highlighted in Appendix B. These studies demonstrated that IL-1 stimulated phosphorylation of extracellular signal-regulated kinases (ERK-1/2), p38 MAPK, and c-Jun NH_2-terminal kinases (JNKs) (**Figures B.2** and **B.3**), implicating these pathways in cytokine effects on the IGF-I system. Furthermore, elevated phosphorylation of ERK-1/2 following intermediate alginate suspension suggests this pathway could be involved in differential basal transcription of IGF-I mediators (**Figure 4.5**). In order to test these hypotheses, specific MAPK inhibitors can be employed to identify the contribution of individual pathways toward IL-1 and culture pathway effects. These inhibitors have proven effective for examining IL-1 activity in chondrocyte culture [149, 151-154, 218, 222, 263].

The majority of work in the field of cartilage biology, including that discussed here, has dealt with the study of individual signaling proteins or transduction pathways. In order to better understand disease pathogenesis at the molecular level, though, future studies must characterize the dynamics of whole signaling networks. With the arrival of DNA microarray technology, gene expression analysis has expanded in scope and complexity. Similar advancements are making high-throughput detection of protein levels (e.g., protein arrays) more cost-effective. However, real-time analysis of cell signaling remains impractical with current technologies. In the meantime, the coupling of single-factor experimentation with complex mathematical models (i.e., computational modeling) can provide a means to investigate the dynamics of signaling systems [264]. Computational models can be applied to describe mechanisms observed

experimentally as well as to predict potential mechanisms for future experimental testing. The utility of this tool has been most extensively proven with the epidermal growth factor (EGF) system [265]. Another network ripe for exploration by computational methods is that of IL-1, which includes endogenous ligand inhibitors and decoy receptors. A preliminary model of the IL-1 network is presented in Appendix C. Development of this model into a form that accurately describes extracellular IL-1 signaling as an integrated network could prove valuable for the formulation of therapeutic strategies against the progression of osteoarthritis. For example, the negative feedback mechanisms innate to this system may be exploited (e.g., using gene transfer techniques) to inhibit the catabolic actions of IL-1 (**Figures C.4** and **C.5**).

References

1.   van der Kraan, P.M. and W.B. van den Berg, *Anabolic and destructive mediators in osteoarthritis.* Curr Opin Clin Nutr Metab Care, 2000. **3**(3): p. 205-11.
2.   Takafuji, V.A., C.W. McIlwraith, and R.D. Howard, *Effects of equine recombinant interleukin-1alpha and interleukin-1beta on proteoglycan metabolism and prostaglandin E2 synthesis in equine articular cartilage explants.* Am J Vet Res, 2002. **63**(4): p. 551-8.
3.   Fortier, L.A., et al., *Insulin-like growth factor-I enhances cell-based repair of articular cartilage.* J Bone Joint Surg Br, 2002. **84**(2): p. 276-88.
4.   Dore, S., et al., *Human osteoarthritic chondrocytes possess an increased number of insulin-like growth factor 1 binding sites but are unresponsive to its stimulation. Possible role of IGF-1-binding proteins.* Arthritis Rheum, 1994. **37**(2): p. 253-63.
5.   Schalkwijk, J., et al., *Chondrocyte nonresponsiveness to insulin-like growth factor 1 in experimental arthritis.* Arthritis Rheum, 1989. **32**(7): p. 894-900.
6.   Verschure, P.J., et al., *IL-1 has no direct role in the IGF-1 non-responsive state during experimentally induced arthritis in mouse knee joints.* Ann Rheum Dis, 1995. **54**(12): p. 976-82.
7.   Tyler, J.A., *Insulin-like growth factor 1 can decrease degradation and promote synthesis of proteoglycan in cartilage exposed to cytokines.* Biochem J, 1989. **260**(2): p. 543-8.
8.   Lazarus, D.D., L.L. Moldawer, and S.F. Lowry, *Insulin-like growth factor-1 activity is inhibited by interleukin-1 alpha, tumor necrosis factor-alpha, and interleukin-6.* Lymphokine Cytokine Res, 1993. **12**(4): p. 219-23.
9.   Benya, P.D., S.R. Padilla, and M.E. Nimni, *Independent regulation of collagen types by chondrocytes during the loss of differentiated function in culture.* Cell, 1978. **15**(4): p. 1313-21.
10.   Benya, P.D. and J.D. Shaffer, *Dedifferentiated chondrocytes reexpress the differentiated collagen phenotype when cultured in agarose gels.* Cell, 1982. **30**(1): p. 215-24.
11.   von der Mark, K. and H. von der Mark, *Immunological and biochemical studies of collagen type transition during in vitro chrondrogenesis of chick limb mesodermal cells.* J Cell Biol, 1977. **73**(3): p. 736-47.
12.   Bonaventure, J., et al., *Reexpression of cartilage-specific genes by dedifferentiated human articular chondrocytes cultured in alginate beads.* Exp Cell Res, 1994. **212**(1): p. 97-104.
13.   Lee, D.A., T. Reisler, and D.L. Bader, *Expansion of chondrocytes for tissue engineering in alginate beads enhances chondrocytic phenotype compared to conventional monolayer techniques.* Acta Orthop Scand, 2003. **74**(1): p. 6-15.
14.   Lemare, F., et al., *Dedifferentiated chondrocytes cultured in alginate beads: restoration of the differentiated phenotype and of the metabolic responses to interleukin-1beta.* J Cell Physiol, 1998. **176**(2): p. 303-13.
15.   Grunder, T., et al., *Bone morphogenetic protein (BMP)-2 enhances the expression of type II collagen and aggrecan in chondrocytes embedded in alginate beads.* Osteoarthritis Cartilage, 2004. **12**(7): p. 559-67.
16.   Murphy, C.L. and J.M. Polak, *Control of human articular chondrocyte differentiation by reduced oxygen tension.* J Cell Physiol, 2004. **199**(3): p. 451-9.
17.   Johnston, S.A., *Osteoarthritis. Joint anatomy, physiology, and pathobiology.* Vet Clin North Am Small Anim Pract, 1997. **27**(4): p. 699-723.
18.   Mankin, H.J. and K.D. Brandt, *Biochemistry and Metabolism of Articular Cartilage in Osteoarthrtis*, in *Osteoarthritis: Diagnosis and Medical/Surgical Management*, R.M. Moskowitz, et al., Editors. 1992, W.B. Saunders Company: Philadelphia, PA. p. 109-154.
19.   Poole, A.R., et al., *Composition and structure of articular cartilage: a template for tissue repair.* Clin Orthop, 2001(391 Suppl): p. S26-33.
20.   Wu, J.J., P.E. Woods, and D.R. Eyre, *Identification of cross-linking sites in bovine cartilage type IX collagen reveals an antiparallel type II-type IX molecular relationship and type IX to type IX bonding.* J Biol Chem, 1992. **267**(32): p. 23007-14.
21.   McIlwraith, C.W., *General pathobiology of the joint and response to injury.*, in *Joint Diseases in the Horse.*, C.W. McIlwraith and G.W. Trotter, Editors. 1996, W.B. Saunders Company: Philadelphia, PA. p. 41-70.
22.   Mankin, H.J. and L. Lippiello, *The glycosaminoglycans of normal and arthritic cartilage.* J Clin Invest, 1971. **50**(8): p. 1712-9.
23.   Vignon, E., et al., *Hypertrophic repair of articular cartilage in experimental osteoarthrosis.* Ann Rheum Dis, 1983. **42**(1): p. 82-8.

24. Mankin, H.J., M.E. Johnson, and L. Lippiello, *Biochemical and metabolic abnormalities in articular cartilage from osteoarthritic human hips. III. Distribution and metabolism of amino sugar-containing macromolecules.* J Bone Joint Surg Am, 1981. **63**(1): p. 131-9.

25. Mankin, H.J., et al., *Biochemical and metabolic abnormalities in articular cartilage from osteo-arthritic human hips. II. Correlation of morphology with biochemical and metabolic data.* J Bone Joint Surg Am, 1971. **53**(3): p. 523-37.

26. Okada, Y., et al., *Simultaneous production of collagenase, matrix metalloproteinase 3 (stromelysin) and tissue inhibitor of metalloproteinases by rheumatoid synovial lining cells.* Matrix Suppl, 1992. **1**: p. 398-9.

27. Pelletier, J.P., et al., *Collagenase and collagenolytic activity in human osteoarthritic cartilage.* Arthritis Rheum, 1983. **26**(1): p. 63-8.

28. Shlopov, B.V., M.L. Gumanovskaya, and K.A. Hasty, *Autocrine regulation of collagenase 3 (matrix metalloproteinase 13) during osteoarthritis.* Arthritis Rheum, 2000. **43**(1): p. 195-205.

29. Nagase, H. and J.F. Woessner, Jr., *Matrix metalloproteinases.* J Biol Chem, 1999. **274**(31): p. 21491-4.

30. Billinghurst, R.C., et al., *Enhanced cleavage of type II collagen by collagenases in osteoarthritic articular cartilage.* J Clin Invest, 1997. **99**(7): p. 1534-45.

31. Gadher, S.J., et al., *Degradation of cartilage collagens type II, IX, X and XI by enzymes derived from human articular chondrocytes.* Matrix, 1990. **10**(3): p. 154-63.

32. Wu, J.J., et al., *Sites of stromelysin cleavage in collagen types II, IX, X, and XI of cartilage.* J Biol Chem, 1991. **266**(9): p. 5625-8.

33. Suzuki, K., et al., *Mechanisms of activation of tissue procollagenase by matrix metalloproteinase 3 (stromelysin).* Biochemistry, 1990. **29**(44): p. 10261-70.

34. Ogata, Y., et al., *Matrix metalloproteinase 9 (92-kDa gelatinase/type IV collagenase) is induced in rabbit articular chondrocytes by cotreatment with interleukin 1 beta and a protein kinase C activator.* Exp Cell Res, 1992. **201**(2): p. 245-9.

35. Clegg, P.D., et al., *Matrix metalloproteinases 2 and 9 in equine synovial fluids.* Equine Vet J, 1997. **29**(5): p. 343-8.

36. Clegg, P.D. and S.D. Carter, *Matrix metalloproteinase-2 and -9 are activated in joint diseases.* Equine Vet J, 1999. **31**(4): p. 324-30.

37. Kozaci, L.D., D.J. Buttle, and A.P. Hollander, *Degradation of type II collagen, but not proteoglycan, correlates with matrix metalloproteinase activity in cartilage explant cultures.* Arthritis Rheum, 1997. **40**(1): p. 164-74.

38. Gomez, D.E., et al., *Tissue inhibitors of metalloproteinases: structure, regulation and biological functions.* Eur J Cell Biol, 1997. **74**(2): p. 111-22.

39. Dean, D.D., et al., *Evidence for metalloproteinase and metalloproteinase inhibitor imbalance in human osteoarthritic cartilage.* J Clin Invest, 1989. **84**(2): p. 678-85.

40. Martel-Pelletier, J., et al., *Excess of metalloproteases over tissue inhibitor of metalloprotease may contribute to cartilage degradation in osteoarthritis and rheumatoid arthritis.* Lab Invest, 1994. **70**(6): p. 807-15.

41. Malfait, A.M., et al., *Inhibition of ADAM-TS4 and ADAM-TS5 prevents aggrecan degradation in osteoarthritic cartilage.* J Biol Chem, 2002. **277**(25): p. 22201-8.

42. Tortorella, M.D., et al., *The role of ADAM-TS4 (aggrecanase-1) and ADAM-TS5 (aggrecanase-2) in a model of cartilage degradation.* Osteoarthritis Cartilage, 2001. **9**(6): p. 539-52.

43. Caron, J.P., et al., *Chondroprotective effect of intraarticular injections of interleukin-1 receptor antagonist in experimental osteoarthritis. Suppression of collagenase-1 expression.* Arthritis Rheum, 1996. **39**(9): p. 1535-44.

44. van de Loo, F.A., et al., *Role of interleukin-1, tumor necrosis factor alpha, and interleukin-6 in cartilage proteoglycan metabolism and destruction. Effect of in situ blocking in murine antigen- and zymosan-induced arthritis.* Arthritis Rheum, 1995. **38**(2): p. 164-72.

45. Fernandes, J.C., J. Martel-Pelletier, and J.P. Pelletier, *The role of cytokines in osteoarthritis pathophysiology.* Biorheology, 2002. **39**(1-2): p. 237-46.

46. Joosten, L.A., et al., *IL-1 alpha beta blockade prevents cartilage and bone destruction in murine type II collagen-induced arthritis, whereas TNF-alpha blockade only ameliorates joint inflammation.* J Immunol, 1999. **163**(9): p. 5049-55.

47. Brennan, F.M., et al., *Inhibitory effect of TNF alpha antibodies on synovial cell interleukin-1 production in rheumatoid arthritis.* Lancet, 1989. **2**(8657): p. 244-7.

48. Daughaday, W.H., et al., *Somatomedin: proposed designation for sulphation factor.* Nature, 1972. **235**(5333): p. 107.

49. Le Roith, D., et al., *The somatomedin hypothesis: 2001.* Endocr Rev, 2001. **22**(1): p. 53-74.
50. Clemmons, D.R. and D.S. Shaw, *Purification and biologic properties of fibroblast somatomedin.* J Biol Chem, 1986. **261**(22): p. 10293-8.
51. Humbel, R.E., *Insulin-like growth factors I and II.* Eur J Biochem, 1990. **190**(3): p. 445-62.
52. Daughaday, W.H. and P. Rotwein, *Insulin-like growth factors I and II. Peptide, messenger ribonucleic acid and gene structures, serum, and tissue concentrations.* Endocr Rev, 1989. **10**(1): p. 68-91.
53. Adamo, M., C.T. Roberts, Jr., and D. LeRoith, *How distinct are the insulin and insulin-like growth factor I signalling systems?* Biofactors, 1992. **3**(3): p. 151-7.
54. Hall, K. and M. Tally, *The somatomedin-insulin-like growth factors.* J Intern Med, 1989. **225**(1): p. 47-54.
55. Daughaday, W.H., *The possible autocrine/paracrine and endocrine roles of insulin-like growth factors of human tumors.* Endocrinology, 1990. **127**(1): p. 1-4.
56. Isgaard, J., *Expression and regulation of IGF-I in cartilage and skeletal muscle.* Growth Regul, 1992. **2**(1): p. 16-22.
57. LeRoith, D. and C.T. Roberts, Jr., *Insulin-like growth factor I (IGF-I): a molecular basis for endocrine versus local action?* Mol Cell Endocrinol, 1991. **77**(1-3): p. C57-61.
58. Phillips, L.S., et al., *Regulation and action of insulin-like growth factors at the cellular level.* Proc Nutr Soc, 1990. **49**(3): p. 451-8.
59. Ullrich, A., et al., *Insulin-like growth factor I receptor primary structure: comparison with insulin receptor suggests structural determinants that define functional specificity.* Embo J, 1986. **5**(10): p. 2503-12.
60. Zhang, B. and R.A. Roth, *Binding properties of chimeric insulin receptors containing the cysteine-rich domain of either the insulin-like growth factor I receptor or the insulin receptor related receptor.* Biochemistry, 1991. **30**(21): p. 5113-7.
61. Sasaki, N., et al., *Characterization of insulin-like growth factor I-stimulated tyrosine kinase activity associated with the beta-subunit of type I insulin-like growth factor receptors of rat liver cells.* J Biol Chem, 1985. **260**(17): p. 9793-804.
62. Corps, A.N., *Signalling at the insulin and insulin-like growth factor receptors: transduction probed by transfection.* J Endocrinol, 1990. **124**(3): p. 349-51.
63. Craparo, A., T.J. O'Neill, and T.A. Gustafson, *Non-SH2 domains within insulin receptor substrate-1 and SHC mediate their phosphotyrosine-dependent interaction with the NPEY motif of the insulin-like growth factor I receptor.* J Biol Chem, 1995. **270**(26): p. 15639-43.
64. Backer, J.M., et al., *Phosphatidylinositol 3'-kinase is activated by association with IRS-1 during insulin stimulation.* Embo J, 1992. **11**(9): p. 3469-79.
65. Sasaoka, T., et al., *Evidence for a functional role of Shc proteins in mitogenic signaling induced by insulin, insulin-like growth factor-1, and epidermal growth factor.* J Biol Chem, 1994. **269**(18): p. 13689-94.
66. Czech, M.P., *Signal transmission by the insulin-like growth factors.* Cell, 1989. **59**(2): p. 235-8.
67. Dahms, N.M., et al., *46 kd mannose 6-phosphate receptor: cloning, expression, and homology to the 215 kd mannose 6-phosphate receptor.* Cell, 1987. **50**(2): p. 181-92.
68. Kiess, W., et al., *Biochemical evidence that the type II insulin-like growth factor receptor is identical to the cation-independent mannose 6-phosphate receptor.* J Biol Chem, 1988. **263**(19): p. 9339-44.
69. Oshima, A., et al., *The human cation-independent mannose 6-phosphate receptor. Cloning and sequence of the full-length cDNA and expression of functional receptor in COS cells.* J Biol Chem, 1988. **263**(5): p. 2553-62.
70. Haig, D. and C. Graham, *Genomic imprinting and the strange case of the insulin-like growth factor II receptor.* Cell, 1991. **64**(6): p. 1045-6.
71. Baker, J., et al., *Role of insulin-like growth factors in embryonic and postnatal growth.* Cell, 1993. **75**(1): p. 73-82.
72. Sessions, C.M., C.A. Emler, and D.S. Schalch, *Interaction of insulin-like growth factor II with rat chondrocytes: receptor binding, internalization, and degradation.* Endocrinology, 1987. **120**(5): p. 2108-16.
73. Watanabe, N., et al., *Characterization of a specific insulin-like growth factor-I/somatomedin-C receptor on high density, primary monolayer cultures of bovine articular chondrocytes: regulation of receptor concentration by somatomedin, insulin and growth hormone.* J Endocrinol, 1985. **107**(2): p. 275-83.
74. Jones, J.I. and D.R. Clemmons, *Insulin-like growth factors and their binding proteins: biological actions.* Endocr Rev, 1995. **16**(1): p. 3-34.
75. Baxter, R.C., *Insulin-like growth factor (IGF)-binding proteins: interactions with IGFs and intrinsic bioactivities.* Am J Physiol Endocrinol Metab, 2000. **278**(6): p. E967-76.

76. Baxter, R.C., *The binding protein's binding protein--clinical applications of acid-labile subunit (ALS) measurement.* J Clin Endocrinol Metab, 1997. **82**(12): p. 3941-3.

77. Clemmons, D.R., *IGF binding proteins: regulation of cellular actions.* Growth Regul, 1992. **2**(2): p. 80-7.

78. De Mellow, J.S. and R.C. Baxter, *Growth hormone-dependent insulin-like growth factor (IGF) binding protein both inhibits and potentiates IGF-I-stimulated DNA synthesis in human skin fibroblasts.* Biochem Biophys Res Commun, 1988. **156**(1): p. 199-204.

79. Forsten, K.E., R.M. Akers, and J.D. San Antonio, *Insulin-like growth factor (IGF) binding protein-3 regulation of IGF-I is altered in an acidic extracellular environment.* J Cell Physiol, 2001. **189**(3): p. 356-65.

80. Blum, W.F., et al., *Insulin-like growth factor I (IGF-I)-binding protein complex is a better mitogen than free IGF-I.* Endocrinology, 1989. **125**(2): p. 766-72.

81. Russo, V.C., et al., *Insulin-like growth factor binding protein-2 binds to cell surface proteoglycans in the rat brain olfactory bulb.* Endocrinology, 1997. **138**(11): p. 4858-67.

82. Shimasaki, S. and N. Ling, *Identification and molecular characterization of insulin-like growth factor binding proteins (IGFBP-1, -2, -3, -4, -5 and -6).* Prog Growth Factor Res, 1991. **3**(4): p. 243-66.

83. Ruoslahti, E. and M.D. Pierschbacher, *New perspectives in cell adhesion: RGD and integrins.* Science, 1987. **238**(4826): p. 491-7.

84. Nam, T.J., W.H. Busby, Jr., and D.R. Clemmons, *Human fibroblasts secrete a serine protease that cleaves insulin-like growth factor-binding protein-5.* Endocrinology, 1994. **135**(4): p. 1385-91.

85. Fowlkes, J.L., et al., *Matrix metalloproteinases degrade insulin-like growth factor-binding protein-3 in dermal fibroblast cultures.* J Biol Chem, 1994. **269**(41): p. 25742-6.

86. Rajah, R., et al., *Insulin-like growth factor binding protein (IGFBP) proteases: functional regulators of cell growth.* Prog Growth Factor Res, 1995. **6**(2-4): p. 273-84.

87. Salmon, W.D., Jr. and W.H. Daughaday, *A hormonally controlled serum factor which stimulates sulfate incorporation by cartilage in vitro.* J Lab Clin Med, 1957. **49**(6): p. 825-36.

88. Luyten, F.P., et al., *Insulin-like growth factors maintain steady-state metabolism of proteoglycans in bovine articular cartilage explants.* Arch Biochem Biophys, 1988. **267**(2): p. 416-25.

89. Willis, D.H., Jr. and J.P. Liberti, *Post-receptor actions of somatomedin on chondrocyte collagen biosynthesis.* Biochim Biophys Acta, 1985. **844**(1): p. 72-80.

90. Guenther, H.L., et al., *Effect of insulin-like growth factor on collagen and glycosaminoglycan synthesis by rabbit articular chondrocytes in culture.* Experientia, 1982. **38**(8): p. 979-81.

91. McQuillan, D.J., et al., *Stimulation of proteoglycan biosynthesis by serum and insulin-like growth factor-I in cultured bovine articular cartilage.* Biochem J, 1986. **240**(2): p. 423-30.

92. Tesch, G.H., et al., *Effects of free and bound insulin-like growth factors on proteoglycan metabolism in articular cartilage explants.* J Orthop Res, 1992. **10**(1): p. 14-22.

93. Bhaumick, B. and R.M. Bala, *Differential effects of insulin-like growth factors I and II on growth, differentiation and glucoregulation in differentiating chondrocyte cells in culture.* Acta Endocrinol (Copenh), 1991. **125**(2): p. 201-11.

94. Trippel, S.B., et al., *Characterization of a specific somatomedin-c receptor on isolated bovine growth plate chondrocytes.* Endocrinology, 1983. **112**(6): p. 2128-36.

95. Froger-Gaillard, B., et al., *Production of insulin-like growth factors and their binding proteins by rabbit articular chondrocytes: relationships with cell multiplication.* Endocrinology, 1989. **124**(5): p. 2365-72.

96. Morales, T.I., *The role and content of endogenous insulin-like growth factor-binding proteins in bovine articular cartilage.* Arch Biochem Biophys, 1997. **343**(2): p. 164-72.

97. Olney, R.C., et al., *Production and hormonal regulation of insulin-like growth factor binding proteins in bovine chondrocytes.* Endocrinology, 1993. **133**(2): p. 563-70.

98. Tardif, G., et al., *Normal expression of type 1 insulin-like growth factor receptor by human osteoarthritic chondrocytes with increased expression and synthesis of insulin-like growth factor binding proteins.* Arthritis Rheum, 1996. **39**(6): p. 968-78.

99. Morales, T.I. and E.B. Hunziker, *Localization of insulin-like growth factor binding protein-2 in chondrocytes of bovine articular cartilage.* J Orthop Res, 2003. **21**(2): p. 290-5.

100. Dore, S., et al., *Increased insulin-like growth factor 1 production by human osteoarthritic chondrocytes is not dependent on growth hormone action.* Arthritis Rheum, 1995. **38**(3): p. 413-9.

101. Olney, R.C., et al., *Chondrocytes from osteoarthritic cartilage have increased expression of insulin-like growth factor I (IGF-I) and IGF-binding protein-3 (IGFBP-3) and -5, but not IGF-II or IGFBP-4.* J Clin Endocrinol Metab, 1996. **81**(3): p. 1096-103.

102. Middleton, J.F. and J.A. Tyler, *Upregulation of insulin-like growth factor I gene expression in the lesions of osteoarthritic human articular cartilage.* Ann Rheum Dis, 1992. **51**(4): p. 440-7.

103. Middleton, J., A. Manthey, and J. Tyler, *Insulin-like growth factor (IGF) receptor, IGF-I, interleukin-1 beta (IL-1 beta), and IL-6 mRNA expression in osteoarthritic and normal human cartilage.* J Histochem Cytochem, 1996. **44**(2): p. 133-41.

104. Chevalier, X. and J.A. Tyler, *Production of binding proteins and role of the insulin-like growth factor I binding protein 3 in human articular cartilage explants.* Br J Rheumatol, 1996. **35**(6): p. 515-22.

105. Dinarello, C.A., *The many worlds of reducing interleukin-1.* Arthritis Rheum, 2005. **52**(7): p. 1960-7.

106. Kobayashi, Y., et al., *Identification of calcium-activated neutral protease as a processing enzyme of human interleukin 1 alpha.* Proc Natl Acad Sci U S A, 1990. **87**(14): p. 5548-52.

107. Kronheim, S.R., et al., *Purification of interleukin-1 beta converting enzyme, the protease that cleaves the interleukin-1 beta precursor.* Arch Biochem Biophys, 1992. **296**(2): p. 698-703.

108. Carter, D.B., et al., *Purification, cloning, expression and biological characterization of an interleukin-1 receptor antagonist protein.* Nature, 1990. **344**(6267): p. 633-8.

109. Eisenberg, S.P., et al., *Primary structure and functional expression from complementary DNA of a human interleukin-1 receptor antagonist.* Nature, 1990. **343**(6256): p. 341-6.

110. Sims, J.E., et al., *cDNA expression cloning of the IL-1 receptor, a member of the immunoglobulin superfamily.* Science, 1988. **241**(4865): p. 585-9.

111. McMahan, C.J., et al., *A novel IL-1 receptor, cloned from B cells by mammalian expression, is expressed in many cell types.* Embo J, 1991. **10**(10): p. 2821-32.

112. Greenfeder, S.A., et al., *Molecular cloning and characterization of a second subunit of the interleukin 1 receptor complex.* J Biol Chem, 1995. **270**(23): p. 13757-65.

113. Martin, M.U. and H. Wesche, *Summary and comparison of the signaling mechanisms of the Toll/interleukin-1 receptor family.* Biochim Biophys Acta, 2002. **1592**(3): p. 265-80.

114. Sims, J.E., et al., *Interleukin 1 signaling occurs exclusively via the type I receptor.* Proc Natl Acad Sci U S A, 1993. **90**(13): p. 6155-9.

115. Casadio, R., et al., *Model of interaction of the IL-1 receptor accessory protein IL-1RAcP with the IL-1beta/IL-1R(I) complex.* FEBS Lett, 2001. **499**(1-2): p. 65-8.

116. Cullinan, E.B., et al., *IL-1 receptor accessory protein is an essential component of the IL-1 receptor.* J Immunol, 1998. **161**(10): p. 5614-20.

117. Huang, J., et al., *Recruitment of IRAK to the interleukin 1 receptor complex requires interleukin 1 receptor accessory protein.* Proc Natl Acad Sci U S A, 1997. **94**(24): p. 12829-32.

118. Korherr, C., et al., *A critical role for interleukin-1 receptor accessory protein in interleukin-1 signaling.* Eur J Immunol, 1997. **27**(1): p. 262-7.

119. Wesche, H., et al., *The interleukin-1 receptor accessory protein (IL-1RAcP) is essential for IL-1-induced activation of interleukin-1 receptor-associated kinase (IRAK) and stress-activated protein kinases (SAP kinases).* J Biol Chem, 1997. **272**(12): p. 7727-31.

120. Wesche, H., K. Resch, and M.U. Martin, *Effects of IL-1 receptor accessory protein on IL-1 binding.* FEBS Lett, 1998. **429**(3): p. 303-6.

121. Lang, D., et al., *The type II IL-1 receptor interacts with the IL-1 receptor accessory protein: a novel mechanism of regulation of IL-1 responsiveness.* J Immunol, 1998. **161**(12): p. 6871-7.

122. Malinowsky, D., et al., *Interleukin-1 receptor accessory protein interacts with the type II interleukin-1 receptor.* FEBS Lett, 1998. **429**(3): p. 299-302.

123. Mantovani, A., et al., *Decoy receptors: a strategy to regulate inflammatory cytokines and chemokines.* Trends Immunol, 2001. **22**(6): p. 328-36.

124. Orlando, S., et al., *Role of metalloproteases in the release of the IL-1 type II decoy receptor.* J Biol Chem, 1997. **272**(50): p. 31764-9.

125. Jensen, L.E., et al., *IL-1 signaling cascade in liver cells and the involvement of a soluble form of the IL-1 receptor accessory protein.* J Immunol, 2000. **164**(10): p. 5277-86.

126. Liu, C., et al., *Cloning and characterization of an alternatively processed human type II interleukin-1 receptor mRNA.* J Biol Chem, 1996. **271**(34): p. 20965-72.

127. Burger, D., et al., *The inhibitory activity of human interleukin-1 receptor antagonist is enhanced by type II interleukin-1 soluble receptor and hindered by type I interleukin-1 soluble receptor.* J Clin Invest, 1995. **96**(1): p. 38-41.

128. Smeets, R.L., et al., *Effectiveness of the soluble form of the interleukin-1 receptor accessory protein as an inhibitor of interleukin-1 in collagen-induced arthritis.* Arthritis Rheum, 2003. **48**(10): p. 2949-58.

129. Smith, D.E., et al., *The soluble form of IL-1 receptor accessory protein enhances the ability of soluble type II IL-1 receptor to inhibit IL-1 action.* Immunity, 2003. **18**(1): p. 87-96.

130. Symons, J.A., P.R. Young, and G.W. Duff, *Soluble type II interleukin 1 (IL-1) receptor binds and blocks processing of IL-1 beta precursor and loses affinity for IL-1 receptor antagonist.* Proc Natl Acad Sci U S A, 1995. **92**(5): p. 1714-8.

131. Muzio, M., et al., *IRAK (Pelle) family member IRAK-2 and MyD88 as proximal mediators of IL-1 signaling.* Science, 1997. **278**(5343): p. 1612-5.

132. Burns, K., et al., *Tollip, a new component of the IL-1RI pathway, links IRAK to the IL-1 receptor.* Nat Cell Biol, 2000. **2**(6): p. 346-51.

133. Xu, Y., et al., *Structural basis for signal transduction by the Toll/interleukin-1 receptor domains.* Nature, 2000. **408**(6808): p. 111-5.

134. Burns, K., et al., *MyD88, an adapter protein involved in interleukin-1 signaling.* J Biol Chem, 1998. **273**(20): p. 12203-9.

135. Cao, Z., et al., *TRAF6 is a signal transducer for interleukin-1.* Nature, 1996. **383**(6599): p. 443-6.

136. Martin, M., et al., *Interleukin-1-induced activation of a protein kinase co-precipitating with the type I interleukin-1 receptor in T cells.* Eur J Immunol, 1994. **24**(7): p. 1566-71.

137. Kollewe, C., et al., *Sequential autophosphorylation steps in the interleukin-1 receptor-associated kinase-1 regulate its availability as an adapter in interleukin-1 signaling.* J Biol Chem, 2004. **279**(7): p. 5227-36.

138. Takaesu, G., et al., *TAB2, a novel adaptor protein, mediates activation of TAK1 MAPKKK by linking TAK1 to TRAF6 in the IL-1 signal transduction pathway.* Mol Cell, 2000. **5**(4): p. 649-58.

139. Takaesu, G., et al., *Interleukin-1 (IL-1) receptor-associated kinase leads to activation of TAK1 by inducing TAB2 translocation in the IL-1 signaling pathway.* Mol Cell Biol, 2001. **21**(7): p. 2475-84.

140. Deng, L., et al., *Activation of the IkappaB kinase complex by TRAF6 requires a dimeric ubiquitin-conjugating enzyme complex and a unique polyubiquitin chain.* Cell, 2000. **103**(2): p. 351-61.

141. Kishimoto, K., K. Matsumoto, and J. Ninomiya-Tsuji, *TAK1 mitogen-activated protein kinase kinase kinase is activated by autophosphorylation within its activation loop.* J Biol Chem, 2000. **275**(10): p. 7359-64.

142. Ninomiya-Tsuji, J., et al., *The kinase TAK1 can activate the NIK-I kappaB as well as the MAP kinase cascade in the IL-1 signalling pathway.* Nature, 1999. **398**(6724): p. 252-6.

143. Wang, C., et al., *TAK1 is a ubiquitin-dependent kinase of MKK and IKK.* Nature, 2001. **412**(6844): p. 346-51.

144. Bavelloni, A., et al., *Phosphatidylinositol 3-kinase translocation to the nucleus is induced by interleukin 1 and prevented by mutation of interleukin 1 receptor in human osteosarcoma Saos-2 cells.* J Cell Sci, 1999. **112 (Pt 5)**: p. 631-40.

145. Marmiroli, S., et al., *Phosphatidylinositol 3-kinase is recruited to a specific site in the activated IL-1 receptor I.* FEBS Lett, 1998. **438**(1-2): p. 49-54.

146. Reddy, S.A., J.H. Huang, and W.S. Liao, *Phosphatidylinositol 3-kinase in interleukin 1 signaling. Physical interaction with the interleukin 1 receptor and requirement in NFkappaB and AP-1 activation.* J Biol Chem, 1997. **272**(46): p. 29167-73.

147. Geng, Y., J. Valbracht, and M. Lotz, *Selective activation of the mitogen-activated protein kinase subgroups c-Jun NH2 terminal kinase and p38 by IL-1 and TNF in human articular chondrocytes.* J Clin Invest, 1996. **98**(10): p. 2425-30.

148. Scherle, P.A., et al., *The effects of IL-1 on mitogen-activated protein kinases in rabbit articular chondrocytes.* Biochem Biophys Res Commun, 1997. **230**(3): p. 573-7.

149. Mengshol, J.A., et al., *Interleukin-1 induction of collagenase 3 (matrix metalloproteinase 13) gene expression in chondrocytes requires p38, c-Jun N-terminal kinase, and nuclear factor kappaB: differential regulation of collagenase 1 and collagenase 3.* Arthritis Rheum, 2000. **43**(4): p. 801-11.

150. O'Neill, L.A. and C. Greene, *Signal transduction pathways activated by the IL-1 receptor family: ancient signaling machinery in mammals, insects, and plants.* J Leukoc Biol, 1998. **63**(6): p. 650-7.

151. Mengshol, J.A., M.P. Vincenti, and C.E. Brinckerhoff, *IL-1 induces collagenase-3 (MMP-13) promoter activity in stably transfected chondrocytic cells: requirement for Runx-2 and activation by p38 MAPK and JNK pathways.* Nucleic Acids Res, 2001. **29**(21): p. 4361-72.

152. Liacini, A., et al., *Inhibition of interleukin-1-stimulated MAP kinases, activating protein-1 (AP-1) and nuclear factor kappa B (NF-kappa B) transcription factors down-regulates matrix metalloproteinase gene expression in articular chondrocytes.* Matrix Biol, 2002. **21**(3): p. 251-62.

153. Mendes, A.F., et al., *Role of mitogen-activated protein kinases and tyrosine kinases on IL-1-Induced NF-kappaB activation and iNOS expression in bovine articular chondrocytes.* Nitric Oxide, 2002. **6**(1): p. 35-44.

154. Studer, R.K., et al., *Chondrocyte response to growth factors is modulated by p38 mitogen-activated protein kinase inhibition.* Arthritis Res Ther, 2004. **6**(1): p. R56-R64.

155. Sylvester, J., et al., *Interleukin-17 signal transduction pathways implicated in inducing matrix metalloproteinase-3, -13 and aggrecanase-1 genes in articular chondrocytes.* Cell Signal, 2004. **16**(4): p. 469-76.

156. Cuenda, A., et al., *SB 203580 is a specific inhibitor of a MAP kinase homologue which is stimulated by cellular stresses and interleukin-1.* FEBS Lett, 1995. **364**(2): p. 229-33.

157. Han, Z., et al., *Jun N-terminal kinase in rheumatoid arthritis.* J Pharmacol Exp Ther, 1999. **291**(1): p. 124-30.

158. Dudley, D.T., et al., *A synthetic inhibitor of the mitogen-activated protein kinase cascade.* Proc Natl Acad Sci U S A, 1995. **92**(17): p. 7686-9.

159. Favata, M.F., et al., *Identification of a novel inhibitor of mitogen-activated protein kinase kinase.* J Biol Chem, 1998. **273**(29): p. 18623-32.

160. Pelletier, J.P. and J. Martel-Pelletier, *Evidence for the involvement of interleukin 1 in human osteoarthritic cartilage degradation: protective effect of NSAID.* J Rheumatol Suppl, 1989. **18**: p. 19-27.

161. Tiku, K., et al., *Articular chondrocytes secrete IL-1, express membrane IL-1, and have IL-1 inhibitory activity.* Cell Immunol, 1992. **140**(1): p. 1-20.

162. Towle, C.A., et al., *Regulation of cartilage remodeling by IL-1: evidence for autocrine synthesis of IL-1 by chondrocytes.* J Rheumatol, 1987. **14 Spec No**: p. 11-3.

163. Nietfeld, J.J., et al., *The effect of human interleukin 1 on proteoglycan metabolism in human and porcine cartilage explants.* J Rheumatol, 1990. **17**(6): p. 818-26.

164. Saha, N., et al., *Interleukin-1beta-converting enzyme/caspase-1 in human osteoarthritic tissues: localization and role in the maturation of interleukin-1beta and interleukin-18.* Arthritis Rheum, 1999. **42**(8): p. 1577-87.

165. Neidel, J. and U. Zeidler, *Independent effects of interleukin 1 on proteoglycan synthesis and proteoglycan breakdown of bovine articular cartilage in vitro.* Agents Actions, 1993. **39**(1-2): p. 82-90.

166. Tyler, J.A., *Articular cartilage cultured with catabolin (pig interleukin 1) synthesizes a decreased number of normal proteoglycan molecules.* Biochem J, 1985. **227**(3): p. 869-78.

167. Xu, C., et al., *Effects of growth factors and interleukin-1 alpha on proteoglycan and type II collagen turnover in bovine nasal and articular chondrocyte pellet cultures.* Endocrinology, 1996. **137**(8): p. 3557-65.

168. Benton, H.P. and J.A. Tyler, *Inhibition of cartilage proteoglycan synthesis by interleukin I.* Biochem Biophys Res Commun, 1988. **154**(1): p. 421-8.

169. Goldring, M.B., et al., *Interleukin 1 suppresses expression of cartilage-specific types II and IX collagens and increases types I and III collagens in human chondrocytes.* J Clin Invest, 1988. **82**(6): p. 2026-37.

170. Lefebvre, V., C. Peeters-Joris, and G. Vaes, *Production of collagens, collagenase and collagenase inhibitor during the dedifferentiation of articular chondrocytes by serial subcultures.* Biochim Biophys Acta, 1990. **1051**(3): p. 266-75.

171. Frisch, S.M. and H.E. Ruley, *Transcription from the stromelysin promoter is induced by interleukin-1 and repressed by dexamethasone.* J Biol Chem, 1987. **262**(34): p. 16300-4.

172. Gowen, M., et al., *Stimulation by human interleukin 1 of cartilage breakdown and production of collagenase and proteoglycanase by human chondrocytes but not by human osteoblasts in vitro.* Biochim Biophys Acta, 1984. **797**(2): p. 186-93.

173. McCachren, S.S., P.K. Greer, and J.E. Niedel, *Regulation of human synovial fibroblast collagenase messenger RNA by interleukin-1.* Arthritis Rheum, 1989. **32**(12): p. 1539-45.

174. Mort, J.S., et al., *Direct evidence for active metalloproteinases mediating matrix degradation in interleukin 1-stimulated human articular cartilage.* Matrix, 1993. **13**(2): p. 95-102.

175. Chang, J., S.C. Gilman, and A.J. Lewis, *Interleukin 1 activates phospholipase A2 in rabbit chondrocytes: a possible signal for IL 1 action.* J Immunol, 1986. **136**(4): p. 1283-7.

176. Campbell, I.K., D.S. Piccoli, and J.A. Hamilton, *Stimulation of human chondrocyte prostaglandin E2 production by recombinant human interleukin-1 and tumour necrosis factor.* Biochim Biophys Acta, 1990. **1051**(3): p. 310-8.

177. Palmer, R.M., et al., *Induction of nitric oxide synthase in human chondrocytes.* Biochem Biophys Res Commun, 1993. **193**(1): p. 398-405.

178. Stadler, J., et al., *Articular chondrocytes synthesize nitric oxide in response to cytokines and lipopolysaccharide.* J Immunol, 1991. **147**(11): p. 3915-20.

179. Henderson, B., et al., *Inhibition of interleukin-1-induced synovitis and articular cartilage proteoglycan loss in the rabbit knee by recombinant human interleukin-1 receptor antagonist.* Cytokine, 1991. **3**(3): p. 246-9.

180. Verschure, P.J. and C.J. Van Noorden, *The effects of interleukin-1 on articular cartilage destruction as observed in arthritic diseases, and its therapeutic control.* Clin Exp Rheumatol, 1990. **8**(3): p. 303-13.

181. Chambers, M.G., M.T. Bayliss, and R.M. Mason, *Chondrocyte cytokine and growth factor expression in murine osteoarthritis.* Osteoarthritis Cartilage, 1997. **5**(5): p. 301-8.

182. Moos, V., et al., *Immunohistological analysis of cytokine expression in human osteoarthritic and healthy cartilage.* J Rheumatol, 1999. **26**(4): p. 870-9.

183. Tetlow, L.C., D.J. Adlam, and D.E. Woolley, *Matrix metalloproteinase and proinflammatory cytokine production by chondrocytes of human osteoarthritic cartilage: associations with degenerative changes.* Arthritis Rheum, 2001. **44**(3): p. 585-94.

184. Smith, J.B., et al., *Occurrence of interleukin-1 in human synovial fluid: detection by RIA, bioassay and presence of bioassay-inhibiting factors.* Rheumatol Int, 1989. **9**(2): p. 53-8.

185. Westacott, C.I., et al., *Synovial fluid concentration of five different cytokines in rheumatic diseases.* Ann Rheum Dis, 1990. **49**(9): p. 676-81.

186. Martel-Pelletier, J., et al., *The interleukin-1 receptor in normal and osteoarthritic human articular chondrocytes. Identification as the type I receptor and analysis of binding kinetics and biologic function.* Arthritis Rheum, 1992. **35**(5): p. 530-40.

187. Sadouk, M.B., et al., *Human synovial fibroblasts coexpress IL-1 receptor type I and type II mRNA. The increased level of the IL-1 receptor in osteoarthritic cells is related to an increased level of the type I receptor.* Lab Invest, 1995. **73**(3): p. 347-55.

188. Homandberg, G.A., C. Wen, and F. Hui, *Agents that block fibronectin fragment-mediated cartilage damage also promote repair.* Inflamm Res, 1997. **46**(11): p. 467-71.

189. Pelletier, J.P., et al., *In vivo suppression of early experimental osteoarthritis by interleukin-1 receptor antagonist using gene therapy.* Arthritis Rheum, 1997. **40**(6): p. 1012-9.

190. Fernandes, J., et al., *In vivo transfer of interleukin-1 receptor antagonist gene in osteoarthritic rabbit knee joints: prevention of osteoarthritis progression.* Am J Pathol, 1999. **154**(4): p. 1159-69.

191. Neidel, J., M. Schulze, and L. Sova, *Insulin-like growth factor I accelerates recovery of articular cartilage proteoglycan synthesis in culture after inhibition by interleukin 1.* Arch Orthop Trauma Surg, 1994. **114**(1): p. 43-8.

192. Fosang, A.J., J.A. Tyler, and T.E. Hardingham, *Effect of interleukin-1 and insulin like growth factor-1 on the release of proteoglycan components and hyaluronan from pig articular cartilage in explant culture.* Matrix, 1991. **11**(1): p. 17-24.

193. Hui, W., A.D. Rowan, and T. Cawston, *Insulin-like growth factor 1 blocks collagen release and down regulates matrix metalloproteinase-1, -3, -8, and -13 mRNA expression in bovine nasal cartilage stimulated with oncostatin M in combination with interleukin 1alpha.* Ann Rheum Dis, 2001. **60**(3): p. 254-61.

194. Matsumoto, T., et al., *Effects of interleukin-1 beta on insulin-like growth factor-I autocrine/paracrine axis in cultured rat articular chondrocytes.* Ann Rheum Dis, 1994. **53**(2): p. 128-33.

195. Olney, R.C., et al., *Interleukin-1 and tumor necrosis factor-alpha increase insulin-like growth factor-binding protein-3 (IGFBP-3) production and IGFBP-3 protease activity in human articular chondrocytes.* J Endocrinol, 1995. **146**(2): p. 279-86.

196. Sunic, D., et al., *Regulation of insulin-like growth factor-binding protein-5 by insulin-like growth factor I and interleukin-1alpha in ovine articular chondrocytes.* Endocrinology, 1998. **139**(5): p. 2356-62.

197. Studer, R.K., et al., *Nitric oxide inhibits chondrocyte response to IGF-I: inhibition of IGF-IRbeta tyrosine phosphorylation.* Am J Physiol Cell Physiol, 2000. **279**(4): p. C961-9.

198. Homicz, M.R., et al., *Human septal chondrocyte redifferentiation in alginate, polyglycolic acid scaffold, and monolayer culture.* Laryngoscope, 2003. **113**(1): p. 25-32.

199. Mandl, E.W., et al., *Multiplication of human chondrocytes with low seeding densities accelerates cell yield without losing redifferentiation capacity.* Tissue Eng, 2004. **10**(1-2): p. 109-18.

200. Brittberg, M., et al., *Treatment of deep cartilage defects in the knee with autologous chondrocyte transplantation.* N Engl J Med, 1994. **331**(14): p. 889-95.

201. Peterson, L., et al., *Two- to 9-year outcome after autologous chondrocyte transplantation of the knee.* Clin Orthop, 2000(374): p. 212-34.

202. Litzke, L.E., et al., *Repair of extensive articular cartilage defects in horses by autologous chondrocyte transplantation.* Ann Biomed Eng, 2004. **32**(1): p. 57-69.

203. Homicz, M.R., et al., *Effects of serial expansion of septal chondrocytes on tissue-engineered neocartilage composition.* Otolaryngol Head Neck Surg, 2002. **127**(5): p. 398-408.

204. van Osch, G.J., S.W. van der Veen, and H.L. Verwoerd-Verhoef, *In vitro redifferentiation of culture-expanded rabbit and human auricular chondrocytes for cartilage reconstruction.* Plast Reconstr Surg, 2001. **107**(2): p. 433-40.

205. Veilleux, N.H., I.V. Yannas, and M. Spector, *Effect of passage number and collagen type on the proliferative, biosynthetic, and contractile activity of adult canine articular chondrocytes in type I and II collagen-glycosaminoglycan matrices in vitro.* Tissue Eng, 2004. **10**(1-2): p. 119-27.

206. Malemud, C.J. and R.S. Papay, *The in vitro cell culture age and cell density of articular chondrocytes alter sulfated-proteoglycan biosynthesis.* J Cell Physiol, 1984. **121**(3): p. 558-68.

207. Mallein-Gerin, F., R. Garrone, and M. van der Rest, *Proteoglycan and collagen synthesis are correlated with actin organization in dedifferentiating chondrocytes.* Eur J Cell Biol, 1991. **56**(2): p. 364-73.

208. Watt, F.M., *Effect of seeding density on stability of the differentiated phenotype of pig articular chondrocytes in culture.* J Cell Sci, 1988. **89 (Pt 3)**: p. 373-8.

209. Guerne, P.A., A. Sublet, and M. Lotz, *Growth factor responsiveness of human articular chondrocytes: distinct profiles in primary chondrocytes, subcultured chondrocytes, and fibroblasts.* J Cell Physiol, 1994. **158**(3): p. 476-84.

210. Guo, J.F., G.W. Jourdian, and D.K. MacCallum, *Culture and growth characteristics of chondrocytes encapsulated in alginate beads.* Connect Tissue Res, 1989. **19**(2-4): p. 277-97.

211. Hauselmann, H.J., et al., *Synthesis and turnover of proteoglycans by human and bovine adult articular chondrocytes cultured in alginate beads.* Matrix, 1992. **12**(2): p. 116-29.

212. Hauselmann, H.J., et al., *Phenotypic stability of bovine articular chondrocytes after long-term culture in alginate beads.* J Cell Sci, 1994. **107 (Pt 1)**: p. 17-27.

213. Martinsen, A., G. Skjakbraek, and O. Smidsrod, *Alginate as Immobilization Material .1. Correlation between Chemical and Physical-Properties of Alginate Gel Beads.* Biotechnology and Bioengineering, 1989. **33**(1): p. 79-89.

214. Mok, S.S., et al., *Aggrecan synthesized by mature bovine chondrocytes suspended in alginate. Identification of two distinct metabolic matrix pools.* J Biol Chem, 1994. **269**(52): p. 33021-7.

215. Petit, B., et al., *Characterization of crosslinked collagens synthesized by mature articular chondrocytes cultured in alginate beads: comparison of two distinct matrix compartments.* Exp Cell Res, 1996. **225**(1): p. 151-61.

216. Beekman, B., et al., *Matrix degradation by chondrocytes cultured in alginate: IL-1 beta induces proteoglycan degradation and proMMP synthesis but does not result in collagen degradation.* Osteoarthritis Cartilage, 1998. **6**(5): p. 330-40.

217. D'Souza, A.L., et al., *Differential effects of interleukin-1 on hyaluronan and proteoglycan metabolism in two compartments of the matrix formed by articular chondrocytes maintained in alginate.* Arch Biochem Biophys, 2000. **374**(1): p. 59-65.

218. Thomas, B., et al., *Differentiation regulates interleukin-1beta-induced cyclo-oxygenase-2 in human articular chondrocytes: role of p38 mitogen-activated protein kinase.* Biochem J, 2002. **362**(Pt 2): p. 367-73.

219. van Osch, G.J., et al., *Differential effects of IGF-1 and TGF beta-2 on the assembly of proteoglycans in pericellular and territorial matrix by cultured bovine articular chondrocytes.* Osteoarthritis Cartilage, 1998. **6**(3): p. 187-95.

220. Wang, J., et al., *Homeostasis of the extracellular matrix of normal and osteoarthritic human articular cartilage chondrocytes in vitro.* Osteoarthritis Cartilage, 2003. **11**(11): p. 801-9.

221. Phillips, T., et al., *Differential regulation of the GLUT1 and GLUT3 glucose transporters by growth factors and pro-inflammatory cytokines in equine articular chondrocytes.* Vet J, 2005. **169**(2): p. 216-22.

222. Robbins, J.R., et al., *Immortalized human adult articular chondrocytes maintain cartilage-specific phenotype and responses to interleukin-1beta.* Arthritis Rheum, 2000. **43**(10): p. 2189-201.

223. Morris, E.A. and B.V. Treadwell, *Effect of interleukin 1 on articular cartilage from young and aged horses and comparison with metabolism of osteoarthritic cartilage.* Am J Vet Res, 1994. **55**(1): p. 138-46.

224. Alwan, W.H., et al., *Glycosaminoglycans in horses with osteoarthritis.* Equine Vet J, 1991. **23**(1): p. 44-7.

225. Frean, S.P., et al., *Influence of interleukin-1beta and hyaluronan on proteoglycan release from equine navicular hyaline cartilage and fibrocartilage.* J Vet Pharmacol Ther, 2000. **23**(2): p. 67-72.

226. Frisbie, D.D. and A.J. Nixon, *Insulin-like growth factor 1 and corticosteroid modulation of chondrocyte metabolic and mitogenic activities in interleukin 1-conditioned equine cartilage.* Am J Vet Res, 1997. **58**(5): p. 524-30.

227. MacDonald, M.H., et al., *Regulation of matrix metabolism in equine cartilage explant cultures by interleukin 1.* Am J Vet Res, 1992. **53**(12): p. 2278-85.

228. Platt, D. and M.T. Bayliss, *An investigation of the proteoglycan metabolism of mature equine articular cartilage and its regulation by interleukin-1.* Equine Vet J, 1994. **26**(4): p. 297-303.

229. Lederer, J.A. and C.J. Czuprynski, *Species preference of bovine thymocytes and fibroblasts for bovine interleukin 1.* Vet Immunol Immunopathol, 1989. **23**(3-4): p. 213-22.

230. May, S.A., R.E. Hooke, and P. Lees, *Interleukin-1 stimulation of equine articular cells.* Res Vet Sci, 1992. **52**(3): p. 342-8.

231. Howard, R.D., et al., *CLoning of equine interleukin 1 alpha and equine interleukin 1 beta and determination of their full-length cDNA sequences.* Am J Vet Res, 1998. **59**(6): p. 704-11.

232. Kato, H., et al., *Molecular cloning of equine interleukin-1 alpha and -beta cDNAs.* Vet Immunol Immunopathol, 1995. **48**(3-4): p. 221-31.

233. Tung, J.T., et al., *Evaluation of the influence of prostaglandin E2 on recombinant equine interleukin-1beta-stimulated matrix metalloproteinases 1, 3, and 13 and tissue inhibitor of matrix metalloproteinase 1 expression in equine chondrocyte cultures.* Am J Vet Res, 2002. **63**(7): p. 987-93.

234. Nixon, A.J., G. Lust, and M. Vernier-Singer, *Isolation, propagation, and cryopreservation of equine articular chondrocytes.* Am J Vet Res, 1992. **53**(12): p. 2364-70.

235. Richardson, D.W. and G.R. Dodge, *Effects of interleukin-1beta and tumor necrosis factor-alpha on expression of matrix-related genes by cultured equine articular chondrocytes.* Am J Vet Res, 2000. **61**(6): p. 624-30.

236. Platt, D., T. Wells, and M.T. Bayliss, *Proteoglycan metabolism of equine articular chondrocytes cultured in alginate beads.* Res Vet Sci, 1997. **62**(1): p. 39-47.

237. Thompson, C.C., P.D. Clegg, and S.D. Carter, *Differential regulation of gelatinases by transforming growth factor beta-1 in normal equine chondrocytes.* Osteoarthritis Cartilage, 2001. **9**(4): p. 325-31.

238. Goldring, S.R. and M.B. Goldring, *The role of cytokines in cartilage matrix degeneration in osteoarthritis.* Clin Orthop Relat Res, 2004(427 Suppl): p. S27-36.

239. Dingle, J.T., *The role of catabolin in the control of cartilage matrix integrity.* J Rheumatol Suppl, 1983. **11**: p. 38-44.

240. Dingle, J.T., et al., *A cartilage catabolic factor from synovium.* Biochem J, 1979. **184**(1): p. 177-80.

241. Morris, E.A., et al., *Identification of interleukin-1 in equine osteoarthritic joint effusions.* Am J Vet Res, 1990. **51**(1): p. 59-64.

242. Morales, T.I., *The insulin-like growth factor binding proteins in uncultured human cartilage: increases in insulin-like growth factor binding protein 3 during osteoarthritis.* Arthritis Rheum, 2002. **46**(9): p. 2358-67.

243. Nixon, A.J., et al., *Gene-mediated restoration of cartilage matrix by combination insulin-like growth factor-I/interleukin-1 receptor antagonist therapy.* Gene Ther, 2005. **12**(2): p. 177-86.

244. Frisbie, D.D., et al., *Treatment of experimental equine osteoarthritis by in vivo delivery of the equine interleukin-1 receptor antagonist gene.* Gene Ther, 2002. **9**(1): p. 12-20.

245. Akers, R.M., et al., *Radioimmunoassay for measurement of bovine alpha-lactalbumin in serum, milk and tissue culture media.* J Dairy Res, 1986. **53**(3): p. 419-29.

246. Hossenlopp, P., et al., *Analysis of serum insulin-like growth factor binding proteins using western blotting: use of the method for titration of the binding proteins and competitive binding studies.* Anal Biochem, 1986. **154**(1): p. 138-43.

247. Berry, S.D., et al., *A local increase in the mammary IGF-1: IGFBP-3 ratio mediates the mammogenic effects of estrogen and growth hormone.* Domest Anim Endocrinol, 2001. **21**(1): p. 39-53.

248. Bayne, M.L., et al., *The roles of tyrosines 24, 31, and 60 in the high affinity binding of insulin-like growth factor-I to the type 1 insulin-like growth factor receptor.* J Biol Chem, 1990. **265**(26): p. 15648-52.

249. Schalch, D.S., et al., *Interaction of insulin-like growth factor I/somatomedin-C with cultured rat chondrocytes: receptor binding and internalization.* Endocrinology, 1986. **118**(4): p. 1590-7.

250. Loeser, R.F. and G. Shanker, *Autocrine stimulation by insulin-like growth factor 1 and insulin-like growth factor 2 mediates chondrocyte survival in vitro.* Arthritis Rheum, 2000. **43**(7): p. 1552-9.

251. Rajah, R., et al., *Leukotriene D4 induces MMP-1, which functions as an IGFBP protease in human airway smooth muscle cells.* Am J Physiol, 1996. **271**(6 Pt 1): p. L1014-22.

252. Rajah, R., et al., *Elevated levels of the IGF-binding protein protease MMP-1 in asthmatic airway smooth muscle.* Am J Respir Cell Mol Biol, 1999. **20**(2): p. 199-208.

253. Russo, V.C., et al., *Insulin-like growth factor binding protein-2 binding to extracellular matrix plays a critical role in neuroblastoma cell proliferation, migration, and invasion.* Endocrinology, 2005. **146**(10): p. 4445-55.

254. Loeser, R.F., C.S. Carlson, and M.P. McGee, *Expression of beta 1 integrins by cultured articular chondrocytes and in osteoarthritic cartilage.* Exp Cell Res, 1995. **217**(2): p. 248-57.

255. Schutt, B.S., et al., *Integrin-mediated action of insulin-like growth factor binding protein-2 in tumor cells.* J Mol Endocrinol, 2004. **32**(3): p. 859-68.

256. Madry, H., et al., *Enhanced repair of articular cartilage defects in vivo by transplanted chondrocytes overexpressing insulin-like growth factor I (IGF-I).* Gene Ther, 2005. **12**(15): p. 1171-9.

257. Martel-Pelletier, J., et al., *IGF/IGFBP axis in cartilage and bone in osteoarthritis pathogenesis.* Inflamm Res, 1998. **47**(3): p. 90-100.

258. Guicheux, J., et al., *Primary human articular chondrocytes, dedifferentiated chondrocytes, and synoviocytes exhibit differential responsiveness to interleukin-4: correlation with the expression pattern of the common receptor gamma chain.* J Cell Physiol, 2002. **192**(1): p. 93-101.

259. Trippel, S.B., *Growth factor inhibition: potential role in the etiopathogenesis of osteoarthritis.* Clin Orthop Relat Res, 2004(427 Suppl): p. S47-52.

260. Darling, E.M. and K.A. Athanasiou, *Rapid phenotypic changes in passaged articular chondrocyte subpopulations.* J Orthop Res, 2005. **23**(2): p. 425-32.

261. Dell'Accio, F., C. De Bari, and F.P. Luyten, *Molecular markers predictive of the capacity of expanded human articular chondrocytes to form stable cartilage in vivo.* Arthritis Rheum, 2001. **44**(7): p. 1608-19.

262. Evans, C.H., et al., *Gene therapy for the treatment of musculoskeletal diseases.* J Am Acad Orthop Surg, 2005. **13**(4): p. 230-42.

263. Hwang, S.G., et al., *c-Jun/activator protein-1 mediates interleukin-1beta-induced dedifferentiation but not cyclooxygenase-2 expression in articular chondrocytes.* J Biol Chem, 2005. **280**(33): p. 29780-7.

264. Forsten-Williams, K., C.C. Chua, and M.A. Nugent, *The kinetics of FGF-2 binding to heparan sulfate proteoglycans and MAP kinase signaling.* J Theor Biol, 2005. **233**(4): p. 483-99.

265. Wiley, H.S., S.Y. Shvartsman, and D.A. Lauffenburger, *Computational modeling of the EGF-receptor system: a paradigm for systems biology.* Trends Cell Biol, 2003. **13**(1): p. 43-50.

266. Frost, R.A., G.J. Nystrom, and C.H. Lang, *Stimulation of insulin-like growth factor binding protein-1 synthesis by interleukin-1beta: requirement of the mitogen-activated protein kinase pathway.* Endocrinology, 2000. **141**(9): p. 3156-64.

267. Smeets, R.L., et al., *Soluble interleukin-1 receptor accessory protein ameliorates collagen-induced arthritis by a different mode of action from that of interleukin-1 receptor antagonist.* Arthritis Rheum, 2005. **52**(7): p. 2202-11.

268. Hendriks, B.S., et al., *Quantitative analysis of HER2-mediated effects on HER2 and epidermal growth factor receptor endocytosis: distribution of homo- and heterodimers depends on relative HER2 levels.* J Biol Chem, 2003. **278**(26): p. 23343-51.

269. Chin, J.E. and R. Horuk, *Interleukin 1 receptors on rabbit articular chondrocytes: relationship between biological activity and receptor binding kinetics.* Faseb J, 1990. **4**(5): p. 1481-7.

270. Qwarnstrom, E.E., et al., *Binding, internalization, and intracellular localization of interleukin-1 beta in human diploid fibroblasts.* J Biol Chem, 1988. **263**(17): p. 8261-9.

271. Slack, J., et al., *Independent binding of interleukin-1 alpha and interleukin-1 beta to type I and type II interleukin-1 receptors.* J Biol Chem, 1993. **268**(4): p. 2513-24.

272. Valles, S., et al., *Recruitment of a heparan sulfate subunit to the interleukin-1 receptor complex. Regulation by fibronectin attachment.* J Biol Chem, 1999. **274**(29): p. 20103-9.

273. Dower, S.K., et al., *Detection and characterization of high affinity plasma membrane receptors for human interleukin 1.* J Exp Med, 1985. **162**(2): p. 501-15.

Appendix A: IGFBP Surface Binding

A.1 Introduction

Radiolabeled ligand binding studies revealed approximately equivalent binding of IGF-I to the surface of both bead and TCP cells under basal conditions (**Figure A.1.A**). IL-1 treatment reduced IGF-I binding on TCP cells, but this was not evident in bead cell culture. Approximately 85 (bead cells) and 70% (TCP cells) of IGF-I binding sites on chondrocyte surfaces were blocked by the additional of unlabeled Y60L-IGF-I (**Figure A.1.B**), an IGF-I analog with substantially reduced affinity for IGF-IR but similar affinity for IGFBPs [248], suggesting IGFBPs constitute the majority of these sites. Cell monolayers were incubated with radioiodinated Y60L-IGF-I to assess the effects of culture strategy and IL-1β treatment on IGFBP surface levels. Bead cells demonstrated slightly higher [^{125}I]-Y60L-IGF-I binding than TCP cells at basal conditions (**Figure A.1.C**), despite the fact that TCP cells secreted nearly an order-of-magnitude more IGFBPs into the culture medium (**Figure 4.3**). Moreover, Y60L-IGF-I binding did not change significantly on bead cells following IL-1β treatment but decreased on the surface of TCP cells (**Figure A.1.C**), as seen with total IGF-I binding (**Figure A.1.A**). The similarity between [^{125}I]-IGF-I and [^{125}I]-Y60L-IGF-I binding trends indicates a prominent role for surface-sequestered IGFBPs in IGF-I localization and signaling. Based on these results, we attempted to identify the source of Y60L-specific binding on the chondrocyte surface, postulating that IGFBP-2, the predominant species in conditioned media (**Figures 4.3**), constituted the majority of binding sites. IGFBP-2 was detected in cell lysate by Western blot and on fixed cell layers by immunofluorescent staining.

A.2 Materials and Methods

A.2.1 *Materials*

Lab-Tek chamber slides were purchased from Nalge Nunc (Naperville, IL). Rabbit anti-bovine IGFBP-2 antibody and generic rabbit IgG were obtained from Upstate Biotechnology (Charlottesville, VA). Horseradish peroxidase (HRP)- and Cy3-conjugated secondary antibodies were acquired from Zymed (San Francisco, CA), and SYTOX™ Blue nuclear stain was supplied

by Molecular Probes (Eugene, OR). Additional materials for cell culture and Western blotting were obtained as described in Chapter 4, section 4.2.1.

A.2.2 *Cell culture*

Equine ACs were isolated, expanded in monolayer culture, and either suspended in alginate beads or maintained on TCP as described in Chapter 4, section 4.2.2. For Western blot analysis of cell lysate, bead and TCP cells were seeded onto 12-well plates at $\sim 1.3 \times 10^5$ cells/cm^2. For immunofluorescence, $\sim 1.5 \times 10^5$ viable cells/chamber were seeded into Lab-Tek chamber slides. Forty-eight-to-72 hr post-plating, cells were rinsed with PBS and treated with 0, 1, or 10 ng/ml IL-1β or 50 ng/ml IGF-I in 'low-serum' media (RPMI-1640 with 0.2% FBS and 1% P/S). Plates were cultured for an additional 48 hr and assayed as described below.

A.2.3 *Radiolabeled ligand binding*

Binding studies were performed as described in Chapter 4, section 4.2.3, except that additional wells were also incubated with 1 ng of either [^{125}I]-IGF-I or [^{125}I]-Y60L-IGF-I without pre-addition of unlabeled Y60L analog.

A.2.4 *Western blot*

Cell layers were rinsed with PBS and lysed in 1X Laemmli buffer (Bio-Rad, Hercules, CA). Protein concentrations were determined using a RC/DC assay kit (Bio-Rad). Sample protein (30 µg/lane) was resolved by SDS-PAGE (10% gels; 150 V for ~ 1 hr) and transferred to PVDF membranes (100 V for 90 min). Non-specific binding was blocked by pre-incubating membranes with 5% nonfat milk in TBS-T for 30 min, followed by incubation with rabbit anti-bovine IGFBP-2 in blocking buffer (1:10,000 dilution) overnight at 4°C. The membranes were then rinsed three times with TBS-T and incubated with a goat anti-rabbit IgG conjugated to HRP (1:15,000 dilution in blocking buffer) for 1 hr at room temperature. After rinsing thrice with TBS-T, bound antibodies were detected on BioMax film using SuperSignal chemiluminescent substrate (Pierce, Rockford, IL).

A.2.5 *Immunofluorescence*

Cell monolayers were rinsed twice with PBS, fixed in 4% formaldehyde solution for 10 min, rinsed twice more in PBS, and incubated in 50 mM NH_4Cl_2 (Sigma) solution for an additional 5 min to quench free aldehydes. Cells were then pre-incubated with 5% BSA in PBS for 30 min to block non-specific binding of antibodies. Fixed cells were incubated with the primary antibody (1:200 in blocking buffer) or rabbit control serum (0.5 µM in blocking buffer) for one hour at room temperature. Cell layers were rinsed with PBS and co-stained with goat anti-rabbit secondary antibody conjugated to Cy3 fluorophore (1:150 dilution) and SYTOX™ Blue nucleic acid stain (0.1 µM), both in blocking buffer. The slides were covered in aluminum foil for 45 minutes to prevent quenching of Cy3 during staining. After rinsing twice more in PBS, chamber dividers were removed and cover slips mounted onto the slides. Representative images of fixed cell layers (four per chamber) were captured under wide blue (200-ms exposure) and wide green (400-ms exposure) excitation lights along with their corresponding phase contrast images. To determine optical densities from wide green images (specific for Cy3 staining), image histograms were collected and integrated over either the entire intensity range (0-4095 for 12-bit images) or a range beyond the threshold for non-specific binding of rabbit control serum (1200-4095). Optical densities were normalized by nuclei counts from wide blue images (specific for SYTOX™ Blue staining) to calculate IGFBP-2 staining per cell.

A.2.6 *Statistics*

For immunofluorescence analysis, four images per slide were collected from two replicate chambers per treatment. Figure bars represent the mean optical density per cell ± the standard error of the mean (SEM) for all eight images per treatment from a single experiment. Differences between treatment means were identified by two-tailed Student's *t*-test, with p-values less than 0.05 considered significant.

A.3   Results and Discussion

A.3.1 *IGFBP-2 Western does not support binding study trends*

Assuming surface-bound protein constituted the majority of IGFBP-2 associated with chondrocyte layers, a Western blot of cell lysate should demonstrate differences in surface IGFBP-2 among treatments. As seen in **Figure A.2**, IGFBP-2 levels in cell lysate did not match

Y60L-IGF-I binding study results. Instead, trends more closely mirrored IGFBP-2 expression results (**Figure 4.5**), as protein levels were approximately nearly 5-fold higher in TCP cells than bead cells. Neither IL-1β nor IGF-I treatment substantially affected protein levels. Based on these results, either the Western of whole cell lysate detected intracellular IGFBP-2 (i.e., within the protein secretory pathway) in addition to surface IGFBP-2 or surface bound IGF-I was mediated primarily by another IGFBP. Future immunoblots should first isolate membrane proteins prior to Western analysis.

A.3.2 *Significant cell-surface levels of IGFBP-2 detected by immunofluorescence*

To specifically detect IGFBP-2 on the chondrocyte surface, fixed cell monolayers were probed for the binding protein by immunofluorescence. To estimate the contribution of non-specific binding, parallel layers were incubated with a generic IgG (i.e., control serum). As represented in **Figure A.3.A**, substantially higher fluorescence was detected with the anti-IGFBP-2 IgG than the control serum, demonstrating the presence of IGFBP-2 on chondrocyte surfaces. When normalizing image optical densities by corresponding cell counts, mean staining per cell was not significantly different between bead and TCP cells (**Figure A.3.B**). However, analysis of serum-control images indicated that non-specific staining contributed significantly to overall optical density for test images. Therefore the histogram integration was refined to include only intensities above 1200 (of 4095 maximum intensity for 12-bit images) (**Figure A.4.A**), since the majority of pixels from control images fell below this threshold. **Figure A.5** presents the resulting staining intensities per cell. No differences in intensity could be detected between bead and TCP cells at basal conditions, though staining trends in response to IL-1 treatment diverged between the two cell populations, such that TCP cells displayed higher levels than bead cells at both concentrations ($p<0.05$) (**Figure A.5.B**). These results differ from both ligand binding (**Figure A.1**) and Western blot analyses (**Figure A.2**), suggesting further optimization of staining and image analysis procedures may be needed to more accurately compare IGFBP-2 levels among test groups. Intensity contour plots of representative images demonstrated a qualitative difference between staining on bead and TCP cell surfaces (**Figure A.6.A**), with the former population displaying more areas of high-intensity staining, but this difference was not captured by quantification using the 1200 threshold. However, when pixels with intensities below 2500 were excluded from optical density calculations, the ratio of bead-to-

TCP cell staining increased significantly ($p < 0.05$), as shown in **Figure A.6.B**. Future studies should more thoroughly characterize the localization of specific and non-specific staining on cell surfaces in order to determine appropriate quantification of IGFBP-2 fluorescence. Assuming this binding protein is the primary species on chondrocyte surfaces, differences in IGFBP-2 immunofluorescence and ligand binding studies could also indicate that surface sequestration blocks the ability of IGFBP-2 to bind IGF-I, as discussed in Chapter 3, section 3.4.

A.4   Acknowledgements
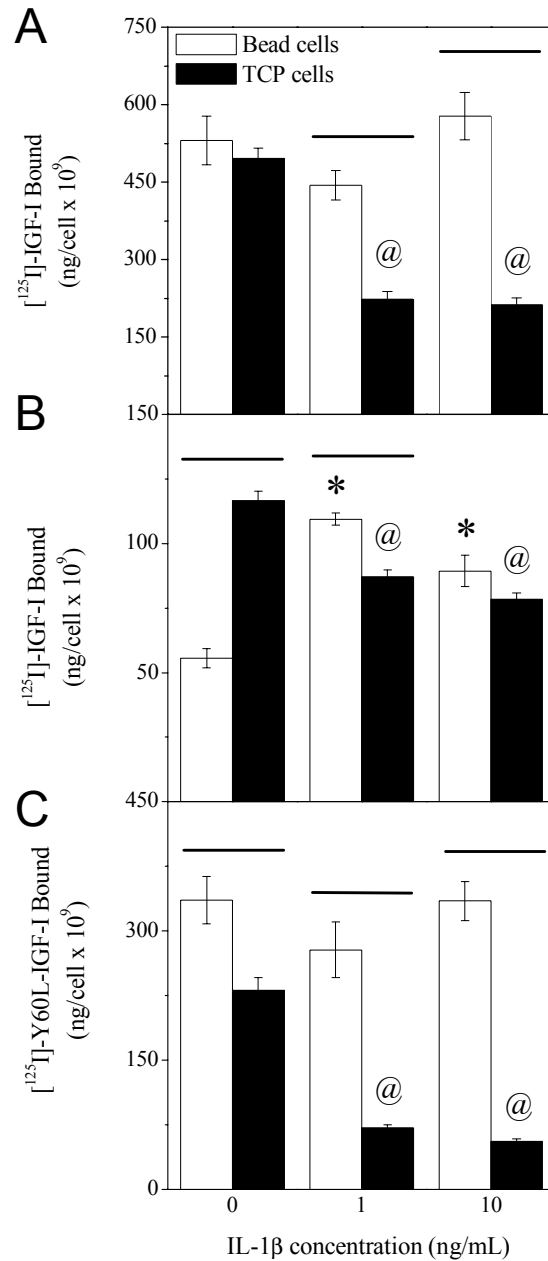
Figure A.1. Differences in IGF-I surface binding between bead and TCP cells. The binding of [^{125}I]-IGF-I – in the absence (**A**) or presence (**B**) of 1 ug blocking Y60L-IGF-I – or [^{125}I]-Y60L-IGF-I (**C**) to bead (open) or TCP (filled) cell monolayers was measured as described in Materials and Methods. Binding levels were normalized by cell densities. Bars represent the mean ± SEM for 3 wells per treatment. ∗ (beads) or @ (TCP) denotes statistically significant differences compared to no-treatment control ($p < 0.05$ by unpaired Students t-test), and horizontal bars represent significant differences between bead and TCP cell cultures at a particular treatment. Results are representative of 3 independent experiments.

IL-1β (ng/mL)   IL-1β (ng/mL)

0   1   10   IGF   0   1   10   IGF

IGFBP-2 →

Bead cells   TCP cells
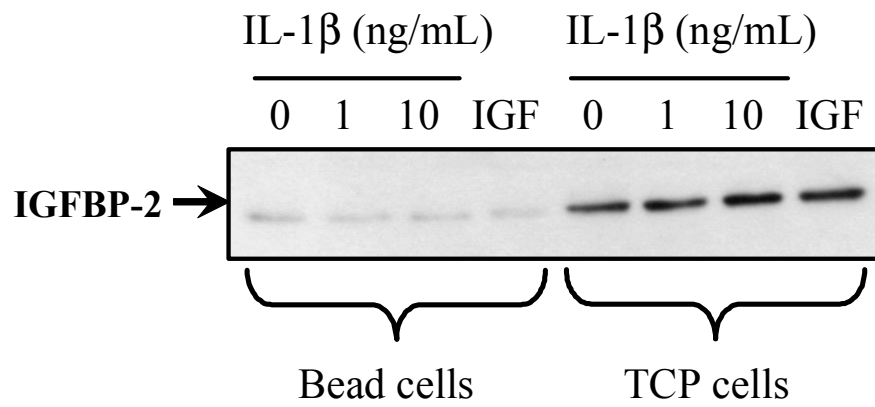
Figure A.2. IGFBP-2 levels in cell lysate mirror transcript expression. Cell lysate samples (30 μg) from bead and TCP cell cultures were resolved by SDS-PAGE and probed for IGFBP-2 (~32 kDa). Numbers indicate concentration of IL-1β treatment, while "IGF" denotes cells treated with 50 ng/ml IGF-I. The blot is representative of three independent experiments.
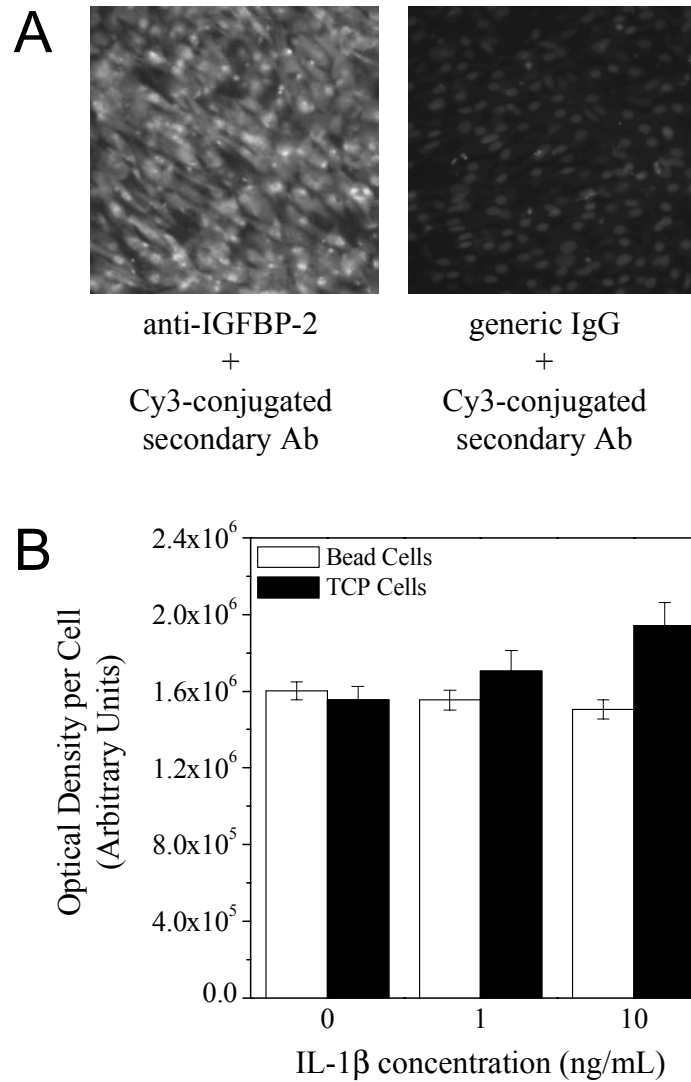
Figure A.3. Significant specific staining for IGFBP-2. Fixed cell layers were incubated with either a rabbit anti-bovine IGFBP-2 (left) or generic rabbit IgG (right) prior to staining with goat anti-rabbit IgG conjugated to the Cy3 fluorophore, as described in Materials and Methods. Cy3 staining was detected under wide green excitation light. Monolayers were co-incubated with SYTOX™ Blue nuclear stain for determining cell counts. Although the SYTOX™ stain primarily emits under wide blue light, some fluorescence could be detected using the wide green filter, as seen in serum-controls (right). (**B**) Optical density values for bead (open) and TCP (filled) cell images were normalized by cell counts from SYTOX™ Blue staining and are presented as a function of IL-1 concentration. Bars represent the mean ± SEM for 8 images per treatment (from duplicate chambers). Results are representative of one experiment.
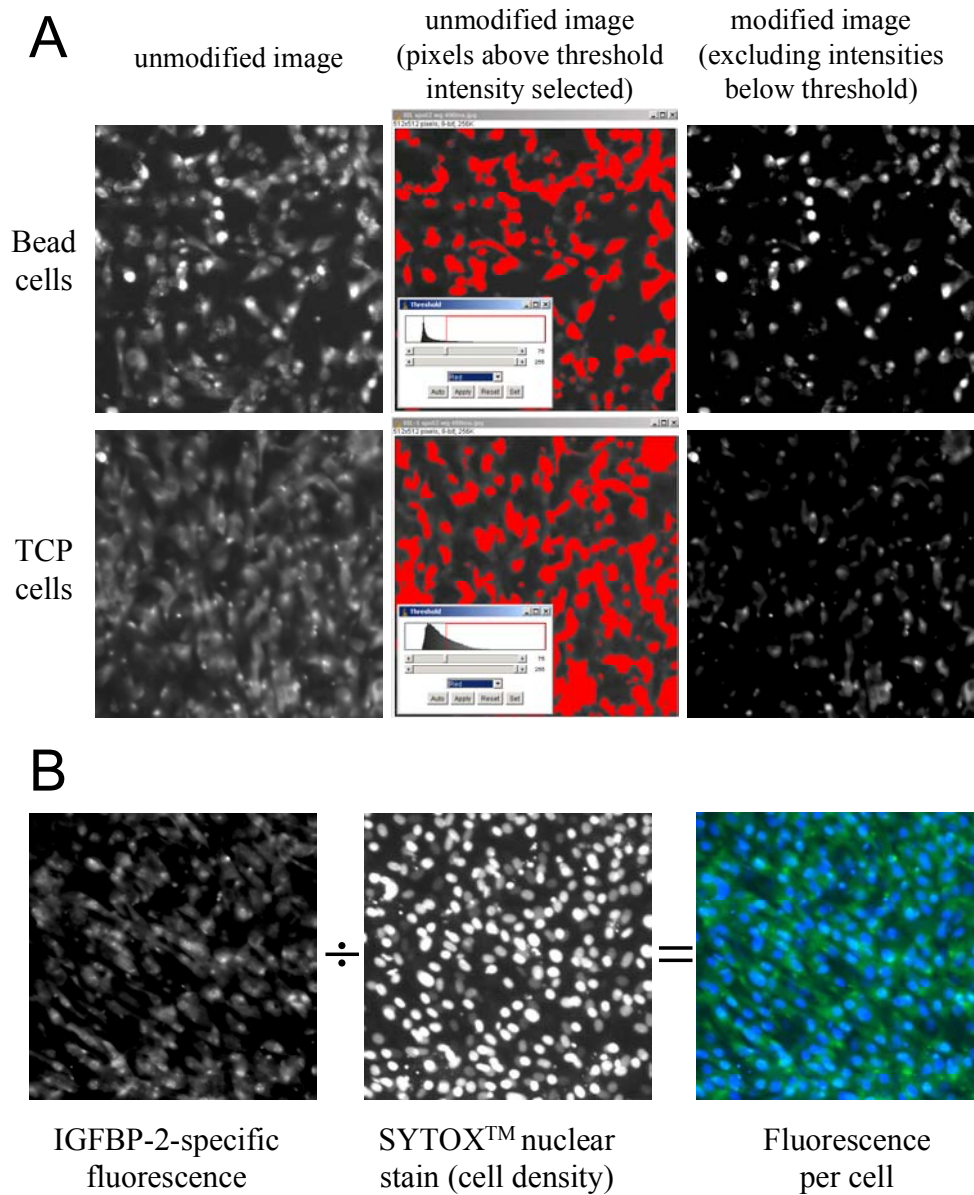
Figure A.4. Calculation of IGFBP-2-specific staining intensity per cell. (**A**) Fixed cell layers were incubated with rabbit anti-bovine IGFBP-2 and stained with Cy3-conjugated goat anti-rabbit IgG. Cy3 staining was detected under wide green excitation light (left). As described in **Figure A.3**, non-specific fluorescence was identified using generic IgG controls. Based on the histograms from control images, intensities below 1200 (for a 12-bit image) were deemed to constitute non-specific binding. Therefore, integration of image histograms was refined to include only pixels above the threshold intensity (center), which are represented in red. The right-most images represent the portion of fluorescence included for optical density calculations. (**B**) To normalize IGFBP-2 staining by cell density, monolayers were co-stained with SYTOX™ Blue nuclear stain (center) and imaged under wide blue light. Individual nuclei were counted within ImagePro, and optical density values from wide green images were normalized by cell counts from corresponding wide blue images.
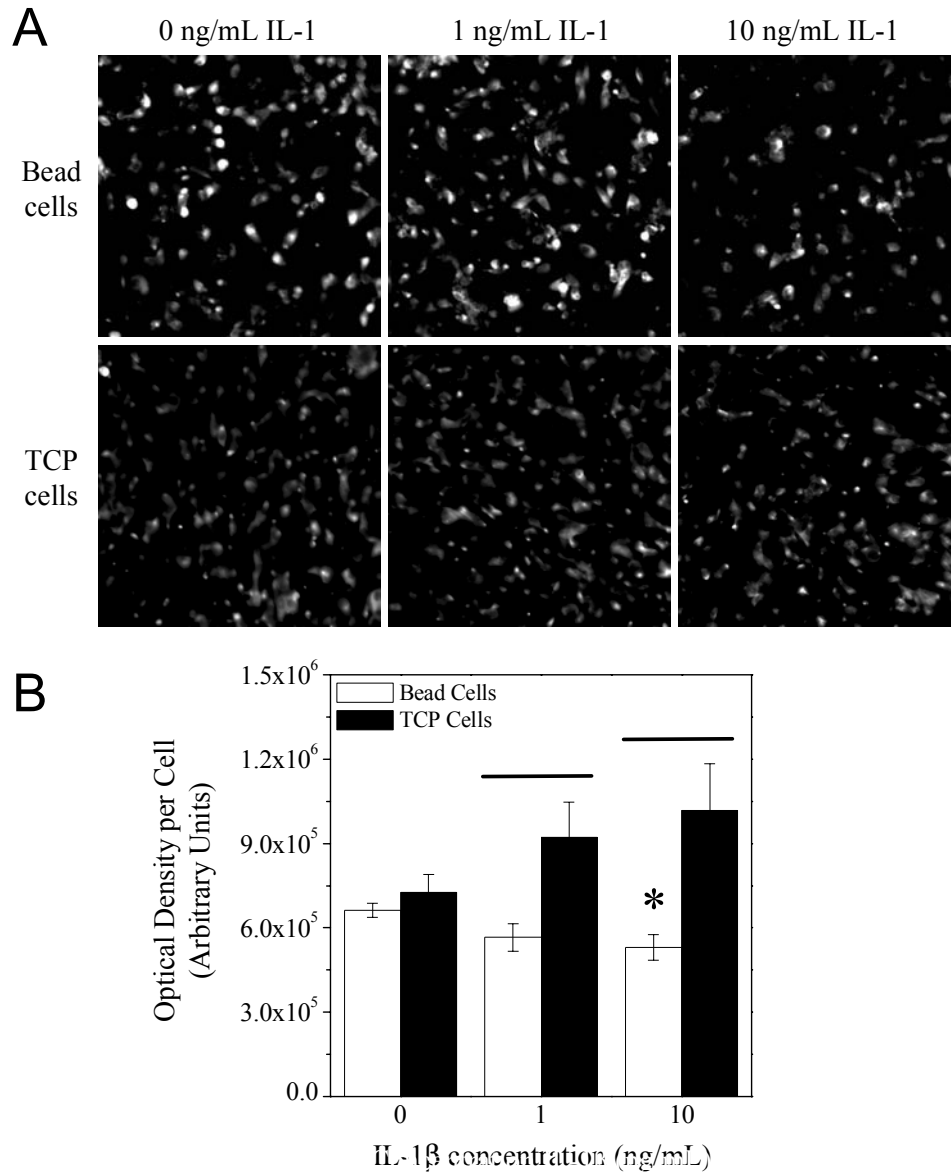
Figure A.5. Quantification of IGFBP-2 immunofluorescence does not reflect binding study trends. (**A**) Bead and TCP cell layers treated and stained as described in Materials and Methods, and fluorescent images captured under wide green excitation light. Only pixels with intensities greater than 1200 (for a 12-bit image) were included in optical density calculations, as represented by the modified images. (**B**) Optical density values for bead (open) and TCP (filled) cell images were normalized by cell counts from SYTOX™ Blue staining and are presented as a function of IL-1 concentration. Bars represent the mean ± SEM for 8 images per treatment (from duplicate chambers). ∗ denotes statistically significant differences compared to no-treatment control ($p<0.05$ by unpaired Students *t*-test), and horizontal bars represent significant differences between bead and TCP cell cultures at a particular treatment. Results are representative of one experiment.
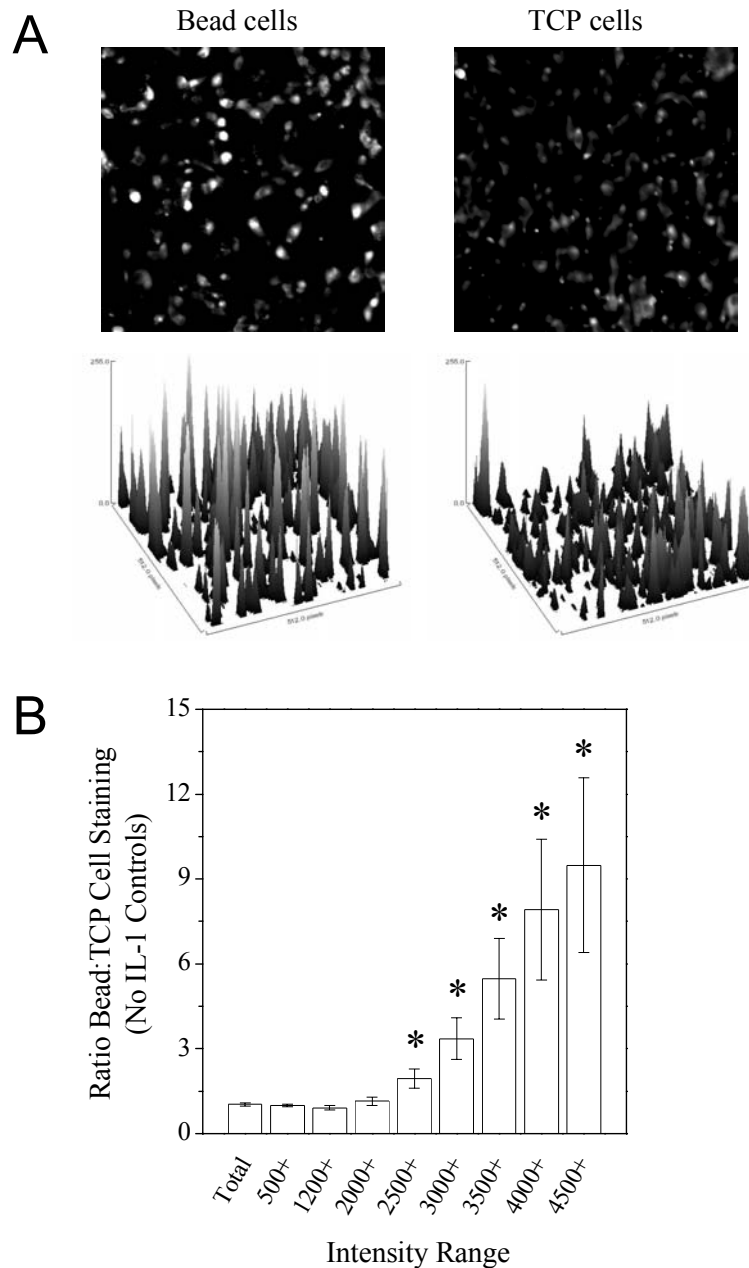
Figure A.6. Intensity-dependent differences in IGFBP-2 staining between bead and TCP cells. (**A**) Two representative images from bead and TCP cell monolayers (untreated) were modified to remove intensities below the 1200 cutoff, as described in **Figure A.4**. Intensity contour plots are shown for the modified images, indicating that bead cell layers have more areas with high-intensity staining. (**B**) The ratio of IGFBP-2 staining (optical density per cell) between bead and TCP cells was calculated for various ranges of pixel intensity ("Total" range = 0-4095 for 12-bit image). Bars represent the mean ± SEM for 8 images per treatment (from duplicate chambers). ∗ denotes statistically significant differences compared to the total intensity range ($p < 0.05$ by unpaired Students t-test). Results are representative of one study.

Appendix B: MAPK Activity

B.1   Introduction

The mitogen-activated protein kinase (MAPK) family includes the extracellular signal-regulated kinases (ERK-1 and-2), p38 MAPK, and c-Jun NH_2-terminal kinases (JNKs; also known as stress-activated protein kinases, SAPKs) [150]. These three subclasses regulate cell growth/apoptosis, differentiation, and metabolic activity by transducing signal from various extracellular stimuli, including that of interleukin-1 (IL-1) and insulin-like growth factor-I (IGF-I). IL-1 has been reported to activate various MAPKs in articular chondrocytes from multiple species [147-149], and recent studies have utilized specific MAPK inhibitors to demonstrate the role of these kinases in IL-1 regulation of chondrocyte gene expression [149, 151-154, 218, 222, 263] (**Figure B.1**). These studies are detailed in Chapter 2 (section 2.4.3). However, few studies have examined the role of MAPKs in the regulation of IGF-I signaling by either IL-1 or chondrocyte culture strategy. One study using a human hepatoma cell line (HepG2) reported that up-regulation of IGFBP-1 mRNA by IL-1β involved a MAPK signaling pathway [266]. Similar results have not yet been demonstrated in chondrocytes. We hypothesized that the transcriptional effects of 10-day alginate subculture and IL-1 treatment on the IGF-I signaling system, as described in Chapters 3 and 4, were mediated by one or more of the three MAPK subclasses. As a first step towards testing this hypothesis, we examined phosphorylation (i.e., activation) of MAPKs in response to exogenous IL-1 for chondrocytes either subcultured in alginate beads or maintained on tissue culture plastic (TCP). The effects of various MAPK inhibitors on chondrocyte viability were also assessed as a prelude to future inhibition studies.

B.2   Materials and Methods

B.2.1 *Materials*

Phosphorylation-specific and -nonspecific rabbit polyclonal antibodies against human ERK-1/2 (p44/p42), p38, and JNK-1/2 (p54/p46) were acquired from Cell Signaling Technologies (Beverly, MA). Goat anti-rabbit secondary conjugated to horseradish peroxidase (HRP) was purchased from Zymed (San Francisco, CA). The MAPK inhibitors PD98059 (ERK-1/2), SB203580 (p38), and SP600125 (JNK-1/2) and the negative control SB202474 were all

95

obtained from Calbiochem (La Jolla, CA). Additional materials for cell culture and Western blotting were obtained as described in Chapter 4, section 4.2.1.

B.2.2 *Cell culture*

Equine ACs were isolated, expanded in monolayer culture, and either suspended in alginate beads or maintained on TCP as described in Chapter 4, section 4.2.2. Isolated bead and TCP cells were seeded onto 12-well plates at $\sim 1.3 \times 10^5$ cells/cm^2. Forty-eight-to-72 hr post-plating, cells were rinsed with PBS and assayed as described below.

B.2.3 *Western blot*

For initial detection of MAPK activation, bead and TCP cell monolayers were given 10 ng/ml IL-1β at one of the following timepoints: 0 min, 30 min, or 50 min. One set of wells was left untreated to serve as a control. At the 60-min mark, cell layers were quickly collected in ice-cold 1X Laemmli buffer and the lysates from triplicate wells were pooled and stored at -70°C. Upon analysis, samples were sonicated and their protein concentrations quantified by RC/DC assay (Bio-Rad). Sample protein (50 μg/lane) was resolved by SDS-PAGE (10% gels; 150 V for ~ 1 hr) and transferred to PVDF membranes (100 V for 90 min). Non-specific binding was blocked by pre-incubating membranes with 5% nonfat milk in TBS-T (10 mM Tris-HCl, 150 mM NaCl, pH 7.4 with 0.1% Tween-20) for 30 min, followed by incubation with phospho-ERK-1/2, phospho-p38, or phospho-JNK (1:1,000 dilution with 5% bovine serum albumin in TBS-T) overnight at 4°C. The next day, blots were rinsed thrice with TBS-T and incubated with HRP-conjugated goat anti-rabbit secondary (1:15,000 dilution in blocking buffer) for 1 hr at room temperature. After rinsing thrice more with TBS-T, bound antibodies were detected using SuperSignal chemiluminescent substrate (Pierce). Blots were then stripped at 50°C for 30 min in TBS-T with 10% SDS and β-mercaptoethanol, rinsed five times with TBS-T, and probed with total (i.e., phosphorylation non-specific) MAPK antibodies (1:1,000 dilution) as described above.

To better resolve the timecourse of MAPK activation, TCP cells were given 10 ng/ml IL-1β at one of the following timepoints: 0, 60, 90, 100, 105, 110, or 115 min. Again, one set of wells was left untreated to serve as a control. At the 120-min mark, cell layers were collected and analyzed as described above, with two exceptions: membranes were first probed for total MAPKs before stripping and re-probing for phoshorylated kinases, and all primary antibody

dilutions were reduced to 1:2,000. For all blots, band intensities were analyzed by scanning densitometry of unsaturated films.

B.2.4 *MTS assay*

For MAPK inhibition studies, TCP cells were pre-incubated in low-serum media (RMPI-1640 with 0.2% FBS and 1% penicillin/streptomycin) with various MMP inhibitors (all at 40 µM) or DMSO (vehicle control). After 30 min, a portion of the wells were given IL-1β (1 ng/ml). After 24-hr stimulation, cell monolayers were analyzed for relative cell viability using a CellTiter 96® Aqueous Non-Radioactive Cell Proliferation Assay kit, following kit instructions. Briefly, wells were rinsed with PBS and given 1.2 ml low-serum media supplemented with MTS/PMS solution (200 µL MTS/PMS solution: 1 ml media), and the cells incubated at 37°C for four hours. Conditioned media aliquots (100 µL/well) were transferred in triplicate to individual wells of a 96-well plate. Fresh media + MTS/PMS solution was also added in triplicate to provide background signal. Sample absorbances were measured at 490 nm, and test sample values were corrected for background.

B.2.5 *Statistics*

Figure bars represent the mean ± the standard error of the mean (SEM) for three wells per treatment from a single experiment. Differences between treatment means were identified by two-tailed Student's *t*-test, with p-values less than 0.05 considered significant.

B.3   Results and Discussion

B.3.1 *IL-1 regulation through MAPK pathways*

In order to identify which MAPKs could be involved in culture substrate and IL-1 effects on the IGF-I signaling system, kinase phosphorylation in response to IL-1 stimulation was examined for both bead and TCP cells. As shown in **Figure B.2**, measurable levels of all three MAPK subclasses, including their phosphorylated forms, were detected in both bead and TCP cell populations. Total MAPK blots displayed inconsistent chemiluminescence, particularly that of p44/p42 (ERK-1/2), suggesting an adverse effect of stripping. However, phosphorylated kinase blots demonstrated differences in MAPK activation between bead and TCP cell

populations. In the absence of IL-1 stimulation, bead cells presented nearly an order-of-magnitude more phospho-p44/p42 than TCP cells. Phospho-p38 levels were also higher in bead cell lysate at basal conditions, but to a lesser extent (approximately 4-fold). Significant phosphorylation levels could not be detected for either p54 (JNK-2) or p46 (JNK-1) without IL-1 stimulation. When cells were introduced to the cytokine, phosphorylation levels initially increased for all three MAPK subclasses. Although phospho-p44/p42 was strongly up-regulated in TCP cell culture, peak levels remained substantially lower than corresponding bead cell levels, which increased by approximately 40% over the entire stimulation period. Phospho-p38 was enhanced by approximately 5- and 8-fold for bead and TCP cells, respectively, at 30 min post-stimulation. Phosphorylation of both p54 and p46 JNKs could be detected following introduction of IL-1, although the degree of stimulation was more pronounced in bead cell culture. Interestingly, although kinase phosphorylation either steadily increased or leveled off during the 60-min stimulation period for bead cells, phospho-p44/p42 and phospho-p54/p46 levels declined between 30 and 60 min for TCP cells. Therefore a second study was conducted on TCP cells to better resolve the time dependence of MAPK activation.

To determine whether blot stripping was responsible for poor detection of total MAPKs during the previous study, membranes were first probed for total kinase. As expected, total MAPK band resolution was improved, though detection of phospho-MAPK bands became less consistent, particularly for ERK-1/2 (**Figure B.3**). As shown in the first study, exogenous IL-1 enhanced phosphorylation of all MAPK subclasses. Phospho-p54 and -p46 levels peaked after nearly 30 min treatment then declined by the 120-min mark, in partial agreement with the initial Western analysis. Taken together, these phosphorylation studies support the hypothesis that MAPKs could mediate IL-1 effects on IGF-I, IGFBP-3, and IGF-IR transcription (**Figure 3.3, Figure 4.5**). Moreover, the marked difference in ERK-1/2 phosphorylation between bead and TCP cell cultures may account for the shift in basal expression of IGFBP-2 attributed to intermediate alginate suspension (**Figure 4.5**). The results warrant further investigation of the MAPK signaling pathways.


B.3.2 *p38 and JNKs involved in IL-1-induced proliferation*

The inhibitors SB203580 (specific for p38), PD98059 (specific for ERK-1/2), and SP600125 (specific for JNKs) have been established as useful tools for identifying how

individual MAPK family members regulate chondrocyte expression [149, 151, 152, 154, 155, 218, 222]. A preliminary study was conducted to assess the feasibility of using these inhibitors in chondrocyte culture for periods sufficient to detect transcription effects. TCP cell cultures were incubated with various inhibitors for 24 hr – with or without stimulation with 1 ng/ml IL-1β, after which cultures were assayed for relative cell viability by conversion of MTS in the culture media to formazan. As shown in **Figure B.4.A**, IL-1β treatment significantly increased formazan absorbance in conditioned media ($p<0.05$), in agreement with cell number measurements following 48-hr treatment (**Figure 4.6.B**). Introduction of inhibitors at 40 µM did not adversely affect cell viability at basal conditions. However, incubation with SB203580 and SP600125 partially blocked the increase in MTS conversion by IL-1β treatment, such that the absorbance ratio between IL-1β-stimulated and control samples was significantly reduced (**Figure B.4.B**). These results suggest that p38 and the JNKs may mediate the proliferation response of dedifferentiated chondrocytes to IL-1. Assuming Western analysis of MAPK phosphorylation indicates sufficient blocking at the applied concentrations, these inhibitors can be used to determine the role of specific MAPKs in mediating IL-1 effects on IGF-I mediator expression.

B.4   Acknowledgements
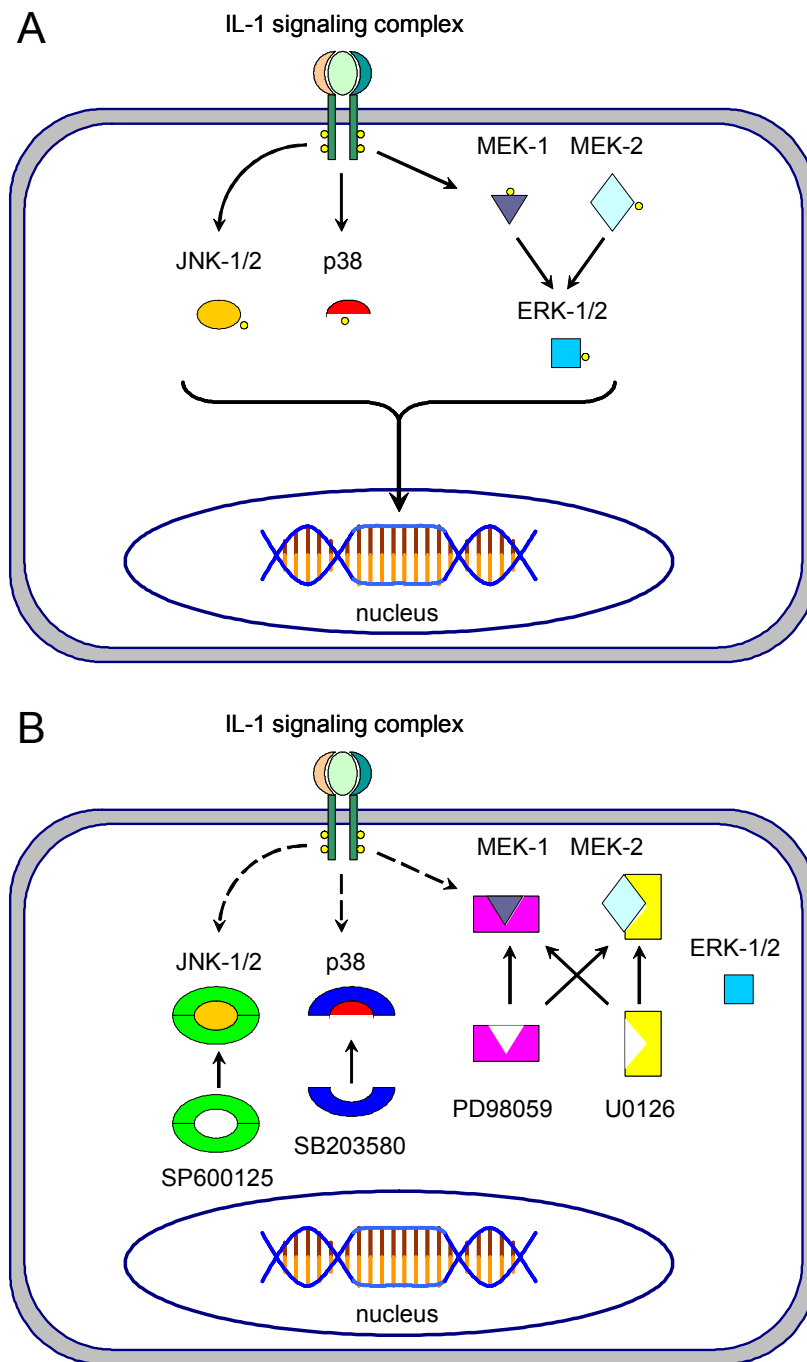
Figure B.1. The role of MAP kinases in IL-1 signal transduction. (**A**) Downstream effectors of the activated IL-1 signaling complex include MAPK family members p38, c-jun NH_2-terminal kinases (JNK-1/2), and extracellular signal-related kinases (ERK-1 and -2). MAPK/ERK kinases 1 and 2 (MEK-1 and -2) activate ERK-1 and -2. Phosphorylated MAPKs regulate the actions of multiple transcription factors. (**B**) Specific MAPK inhibitors have been shown to block IL-1 signaling. SB203580 and SP600125 block p38 and the JNKs, respectively, and both PD98059 and U0126 inhibit ERK-1/2 activation by blocking MEK-1/2 activity. These inhibitory agents can be used in concert to indentify the role of MAPKs in IL-1 regulation of IGF-I axis.
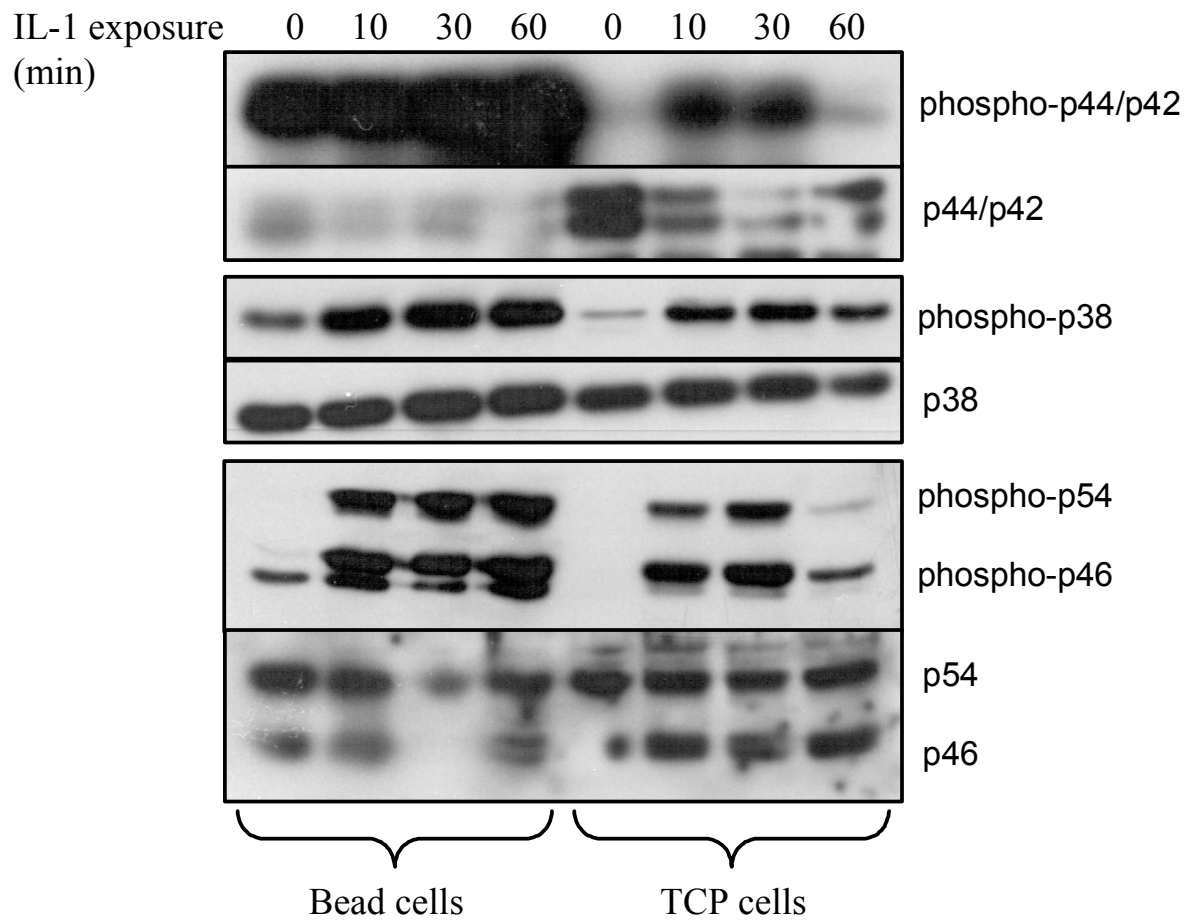
Figure B.2. Differences in basal levels of phosphorylated ERK-1/2 attributed to culture pathway. Bead and TCP cell monolayers were stimulated with 10 ng/ml IL-1β for 0, 10, 30 or 60 min prior to collection of cell lysate. Protein samples (50 µg) were resolved by SDS-PAGE, transferred to membranes, and probed for the following phosphorylated MAPKs: p44/p42 (ERK-1/2), p38, and p46/p54 (JNK-1/2). Blots were then stripped and re-probed for total MAPK levels.
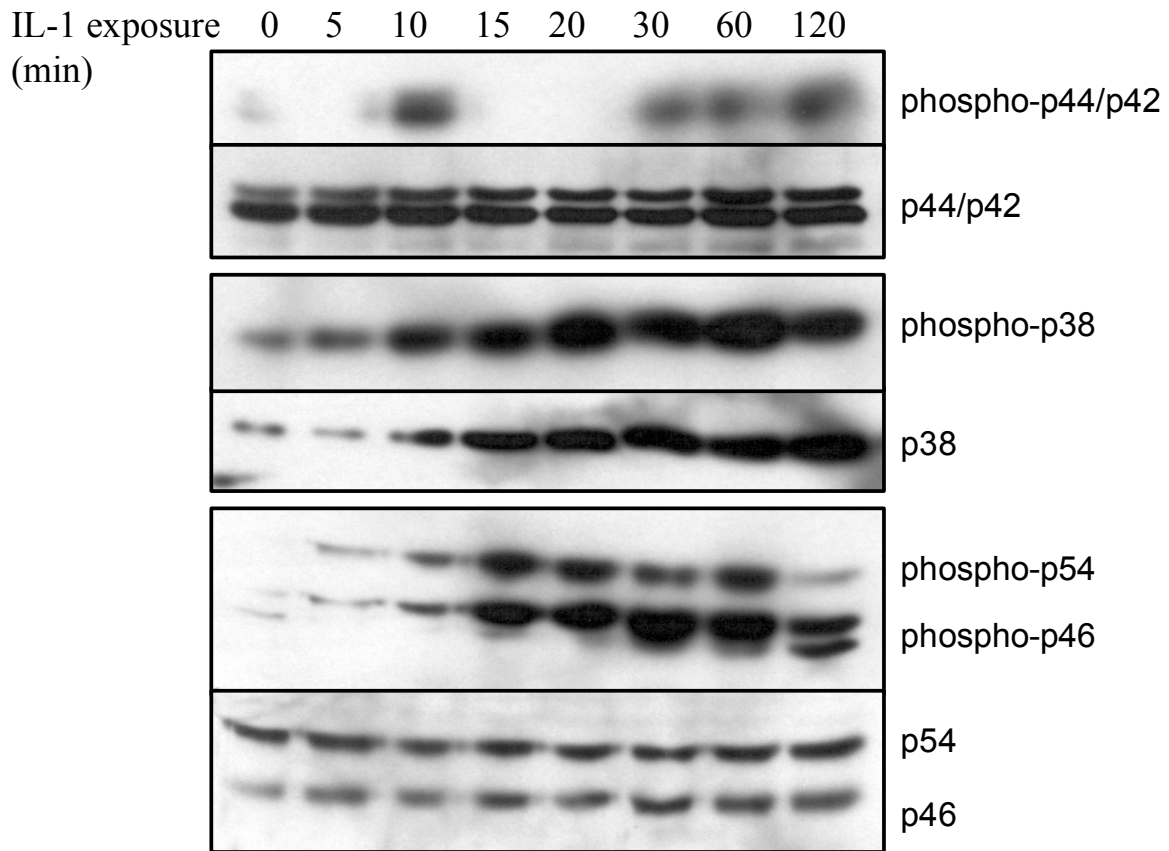
Figure B.3. Time-dependent activation of MAPKs by IL-1. TCP cell monolayers were stimulated with 10 ng/ml IL-1β for 0, 5, 10, 15, 20, 30, 60, or 120 min prior to collection of cell lysate. Protein samples (50 μg) were resolved by SDS-PAGE, transferred to membranes, and probed for total levels of the following MAPKs: p44/p42 (ERK-1/2), p38, and p46/p54 (JNK-1/2). Blots were stripped and re-probed for the corresponding levels of phosphorylated MAPKs.
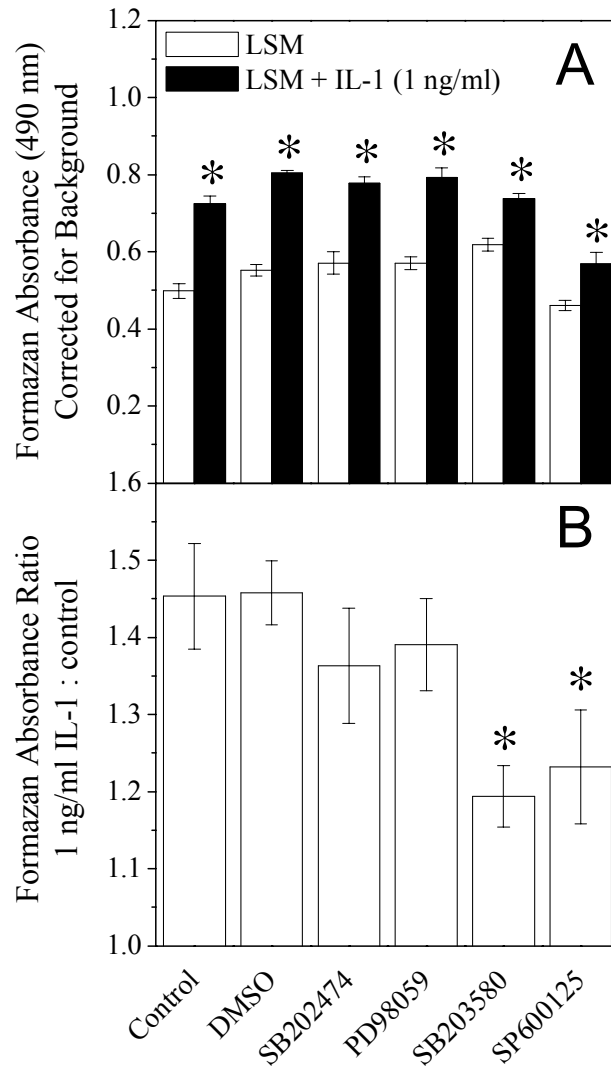
Figure B.4. Inhibitors of p38 MAPK and JNKs block cell growth by IL-1. (**A**) TCP cell cultures were incubated with the following inhibitors with or without 1 ng/ml IL-1β: DMSO (vehicle control), SB202474 (negative control), PD98059 (ERK inhibitor), SB203580 (p38 inhibitor), SP600125 (JNK inhibitor). After 24 hr, cultures were assayed for relative cell viability by conversion of MTS in the culture media to formazan, which was detected by absorbance at 490 nm. Bars represent the mean ± SEM for triplicate wells per treatment, and an ∗ denotes a significant increase in absorbance compared to no-IL-1 control (p<0.05 by unpaired Student's *t*-test). (**B**) Absorbance ratios between IL-1β-stimulated and control wells were calculated for each inhibitor set. Bars represent the mean ± SEM for triplicate wells per inhibitor set, and an ∗ denotes a significant decrease in absorbance ratio compared to no-inhibitor control (p<0.05 by unpaired Student's *t*-test).

Appendix C: Computational Model of Extracellular IL-1 Signaling

C.1   Introduction

The interleukin-1 (IL-1) signaling system consists of a complex network of extracellular ligands and ligand inhibitors, transmembrane receptors, and intracellular adapter proteins and signaling kinases. The extracellular portion of this network resembles that of the IGF-I system, involving the interaction of multiple ligands, multiple membrane-bound ligand receptors, and soluble proteins with ligand binding capability (**Figure C.1**). Individual component functions and multi-component dynamics are still under investigation; however, the general compliment of extracellular components has been well characterized. These components are described in detail in Chapter 2 (section 2.4.1) and are reviewed elsewhere [105, 113]. The extracellular domains of the three membrane receptors (IL-1RI, IL-1RII, and IL-1RAcP) can be found in soluble form (sIL-1RI, sIL-1RII, and sIL-1RAcP) within the extracellular environment. These soluble receptors are believed to offer addition inhibitory mechanisms to the signaling system, sequestering free IL-1 and preventing the formation of the signaling receptor complex [125, 127-130, 267]. Though only sIL-1RI and sIL-1RII are believed to initiate binding with IL-1 – like their membrane counterparts, sIL-1RAcP may also inhibit IL-1 activity by stabilizing these soluble complexes [129]. The complexity of this system limits the understanding of IL-1 regulatory activity as well as the development of therapeutic strategies to counteract its destructive actions.

The merging of experimental cell biology with mathematical modeling (i.e., computational modeling) has evolved over the past 15 years into a useful tool for the investigation of signaling dynamics. Many of the innovations over this period have been applied to the epidermal growth factor (EGF) system [265]. Computational models have been utilized to better describe EGF receptor (EGFR)-mediated processes that had been observed experimentally as well as to predict potential mechanisms for experimental testing. These models have allowed for in-depth characterizations of EGFR binding and trafficking, EGF signal transduction, and autocrine control loops. However, other signaling systems, including the IL-1 network, have not been explored by computational means. Here we introduce a preliminary mathematical model that begins to describe extracellular IL-1 signaling as an integrated network. The application of

such a model could help elucidate complex regulatory pathways, such as those governing the metabolic activity of chondrocytes.

C.2   Preliminary Model of Ligand-receptor Interactions

The following mathematical model describes the binding kinetics among IL-1β, IL-1ra, and the complete family of known transmembrane and soluble IL-1 receptors. For simplicity, the model assumes no synthesis, degradation, or internalization of either ligands or receptors, an environment similar to that used for radiolabeled ligand binding studies (e.g., 4-8°C). Furthermore, it assumes a uniform distribution of ligands and receptors both in solution and on the cell surface, as well as uniform receptor densities among cells. The entire compliment of model components, including ligand-receptor and ligand-receptor-coreceptor complexes, is listed in **Table C.1**. Not all possible interactions are considered, but only those that are thought to be physiologically relevant (see Chapter 2, section 2.4.1).   For example, while IL-1/receptor complexes interact with the accessory protein to form heterodimers, IL-1ra/receptor complexes do not, in accordance with published results [112]. Non-specific dimerization of receptors (e.g., between two IL-1RI chains), though recently added to some models of the EGFR system [268], is also neglected. Altogether 20 different components are included in the model, and their interactions are described in both **Figure C.2** and **Table C.2**.   These interactions can be described by a set of 20 ordinary differential equations, which are provided in **Table C.3**.

Each equation in **Table C.3** describes the rate of change for one component and assumes that component-component interactions can be described by mass action kinetics. For example, the first ODE listed, d[mRI]/dt, describes the change of type I receptor (membrane-bound) with respect to time following the introduction of IL-1 (L) to the system. The equation has four terms that describe both the "depletion" of receptor levels by formation of complex with IL-1 ($k_{f,mRI \cdot L} \times [mRI] \times [L]$) and IL-1ra ($k_{f,mRI \cdot Lra} \times [mRI] \times [Lra]$) and the "accumulation" of receptor by dissociation of these complexes ($k_{r,mRI \cdot L} \times [mRI \cdot L]$ and $k_{r,mRI \cdot Lra} \times [mRI \cdot Lra]$).   Receptors on the membrane surface are described in terms of cell density (#/cell), while ligands and soluble receptors are described by molarity (M). Due to the change in units from cell surface to solution, the ligand ODEs include a conversion factor, ρ/N_{AV}, where ρ is the cell density (cells/volume). Because this model assumes no synthesis or degradation of solution or membrane receptors, two algebraic equations describe the balance of system receptors (**Table C.3**, equations 21 and 22).

These constraints were used to eliminate two components from the model (mRI·L and sRI·L), reducing the system to 18 ODEs.

To solve this system of ODEs for various initial conditions, the kinetic association and dissociation rate constants for component-component interactions must be determined. Since these values have yet to be measured for equine chondrocytes, appropriate approximations were taken from the scientific literature. These parameters are provided in **Table C.4**. Typical surface levels for IL-1RI and IL-1RII on chondrocytes were determined from studies of human and rabbit chondrocytes [186, 269]. An excess of membrane IL-1RAcP was assumed (10-fold over mIL-1RI) in order to make IL-1 the limiting signaling receptor. However, this assumption agrees with ratio of soluble receptors measured in serum (5 nM for sIL-1RAcP compared to 0.12 nM for sIL-1RII) [129]. Order-of-magnitude estimations of the association and dissociation rate constants were estimated based on a combination of K_D values measured for chondrocytes [186, 269] and more-detailed parameter calculations from other cell types [129, 270-272]. Absolute receptor and ligand levels in the model space were based on a well with 2×10^5 cells in 1 ml of solution. Binding of ligand to cell surface proteins was considered to be reaction-limited, so rate constants were not adjusted to account for diffusivity near the surface (i.e., due to pericellular matrix). The kinetic rates for dimerization of ligand-bound receptors with IL-1RAcP were estimated from diffusion-limited values used for the EGFR system [268].

C.3   Model Results

The system of 18 differential equations was solved in MATLAB (version 6 release 12, The Mathworks) using the stiff ODE solver, ode15s. All default options for this subroutine were kept except for the relative tolerance, which was lowered to 10^{-6}. Representative MATLAB code is provided in section C.5. Initial values were set as described in **Table C.4**, with all other receptor levels set to zero. These initial values resemble experimental conditions at the onset for radiolabeled ligand association.

As shown in **Figure C.3**, formation of both IL-1/IL-1RI/IL-1RAcP and IL-1/IL-1RII/IL-1RAcP complexes increased after introduction of ligand. Most of the type I and II membrane receptors were occupied at steady state, which was expected when considering the excess concentration of ligand for this simulation. The ratio of "signaling" (mCI) to "decoy" (mCII)

heterodimers reflected the ratio of surface receptors, since IL-1 affinities for IL-1RI and IL-1RII were set as equal in this model.

Perturbations to this base model were made in order to characterize the actions of IL-1 inhibitors, namely IL-1RII and IL-1ra. **Figure C.4** demonstrates the effects of increasing IL-1RII concentration on steady state levels of signaling and non-signaling heterodimers. As IL-1RII concentration approached that of IL-1RAcP (10^4/cell), the formation of signaling complexes was inhibited in favor of non-signaling complexes, with the latter approaching saturation levels (i.e., IL-1RAcP levels). This simulation result supports the role of IL-1RII as an IL-1 inhibitor and suggests that over-expression of IL-1RII would suppress IL-1 signaling by IL-1RII sequestration of both free ligand and surface IL-1RAcP. Similarly, increased levels of IL-1ra have an inhibitory effect on signaling complex formation, as shown in **Figure C.5**. As IL-1ra concentration became much greater than that of IL-1, steady state levels of signaling complexes were substantially reduced. However, IL-1ra concentration did not have a significant effect on levels of non-signaling complexes due to the relatively low affinity of IL-1ra for IL-1RII. The patterns demonstrated by **Figures C.4** and **C.5** support experimental studies that have suggested the inhibitory actions of IL-1ra and IL-1RII are additive, since they act at different levels within the IL-1 system [127, 130].

This preliminary model demonstrates the utility of computational techniques for predicting signaling system dynamics at an integrated level. However, to more accurately describe IL-1 signaling within our culture system, future models must account for additional cellular processes such as receptor synthesis, receptor-ligand internalization/recycling/degradation, and proteolytic conversion of membrane receptors to soluble forms. Furthermore, kinetic parameters must be determined for the specific cell type and differentiation state. Diffusion-limited ligand-receptor association/dissociation may also need to be considered at the cell surface. A more accurate model of the chondrocyte IL-1 system may be applied to the analysis of disease pathogenesis and the identification of potential targets for therapeutic intervention.

C.4   Directions for Model Improvement

To accurately characterize the IL-1 signaling dynamics for equine chondrocytes, the parameters that describe ligand-receptor and receptor-receptor interactions must be measured

specifically for this culture system. Association (k_f) and dissociation (k_r) rate constants for the various ligand-receptor interactions in this system can be determined with binding assays using radiolabeled ligands (e.g., [^{125}I]-IL-1β, [^{125}I]-IL-1ra) [270]. For example, incubation of cell monolayers with a range of radiolabeled ligand concentrations – collecting bound ligand by cell lysis at multiple timepoints – can provide kinetic association rates. However, these experiments must be conducted under conditions that inhibit cellular receptor synthesis and processing during the study. Cell incubation at 4-8°C is commonly used for this purpose, although inhibitors may also be used in order to measure rate constants at 37°C. Kinetic dissociation rates may also be determined by pre-incubating cells with saturating levels of ligand until equilibrium binding is attained, removing ligand from solution, and measuring binding levels at multiple timepoints after removal. Alternatively, dissociation rates can be calculated indirectly from equilibrium binding data. If steady-state binding levels are determined for a range of initial ligand concentrations, the data can be fit to the following equation by least squares analysis:

$$\frac{C}{L} = \left(-\frac{1}{K_D}\right)C + \left(\frac{R_T}{K_D}\right)$$

where C represents the steady-state concentration of bound receptor, L stands for the concentration of unbound ligand, R_T represents the total number of receptor sites, and K_D stands for equilibrium dissociation constant, which is the ratio of kinetic dissociation and association constants ($K_D = k_r/k_f$). The slope of the line gives the negative inverse of K_D, while the y-intercept provides the ratio R_T/K_D. This technique is known as the Scatchard analysis and assumes a single binding site and sufficiently large ligand concentrations (so that $R_T/N_{AV} \gg L/n$, where N_{AV} is Avagadro's number and n is the cell density). For all of these techniques, radiolabeled binding measurements must be corrected for non-specific binding (i.e., background). This can be accomplished by pre-incubation with high concentrations of a binding competitor such as the unlabeled ligand itself, a natural receptor antagonist with comparable affinity, or a receptor antibody that neutralizes the binding site.

In the event that multiple ligand binding sites are present on the cell surface – the IL-1 system has such complexity – the methods described above will not provide rate constants for each ligand-receptor combination, but rather composite values that represent the mean binding

properties on the cell surface. To circumvent this problem, binding competitors may be employed to effectively block one of the receptor sites, assuming they are specific for only the target site. With one site blocked, the remaining site may be analyzed using the methods described above. This technique was used in analyzing the IGF-I system, as described in Chapter 3, section 3.2.3.

The techniques described above could be used to determine binding kinetics of recombinant equine IL-1β (rEqIL-1β) and rEqIL-1ra with the receptors expressed by equine articular chondrocytes. rEqIL-1β and rEqIL-1ra could be radiolabeled using a previously described protocol [270, 273]. Individual ligand-receptor interactions may be characterized with the aid of neutralizing antibodies for one of the receptor types (e.g., the anti-human monoclonal antibody M4, which has the capability to neutralize IL-1RI) [272]. Alternatively, since IL-1ra is thought to have significantly reduced affinity for IL-1RII, the antagonist may be used to specifically block IL-1RI receptors for the quantification of $[^{125}\text{I}]$-IL-1β/IL-1RII interactions. A third option is to use more advanced mathematical techniques that consider multi-site binding and allow for non-linear fitting of parameters. For the latter option, the two sites must have distinct ligand binding affinities (i.e., different K_D values).

C.5 MATLAB Code for Computational Model

The system of 18 differential equations was solved in MATLAB (version 6 release 12, The Mathworks) using the stiff ODE solver, ode15s. The code for the main program (section C.5.1) and ODE subroutine (section C.5.2) are provided below.

C.5.1 *Main Program*

```
% Ryan M. Porter
% computational model of IL-1 signaling system
% competitive ligand binding at 4 degrees Celcius
%

clear all

format short e

global kon koff mRt sRt density N

% rate contants for membrane receptor complexes

kon(2)=5e7;    % < M-1 min-1 >
```

```matlab
koff(2)=5e-2;    % < min-1 >
kon(3)=1e-3;     % < (#/cell)-1 min-1 >
koff(3)=0.1;     % < min-1 >
kon(4)=5e7;      % < M-1 min-1 >
koff(4)=5e-2;    % < min-1 >
kon(6)=5e7;      % < M-1 min-1 >
koff(6)=5e-2;    % < min-1 >
kon(7)=1e-3;     % < (#/cell)-1 min-1 >
koff(7)=0.1;     % < min-1 >
kon(8)=5e5;      % < M-1 min-1 >
koff(8)=5e-2;    % < min-1 >

% rate constants for soluble receptor complexes

kon(11)=5e7;    % < M-1 min-1 >
koff(11)=5e-2;  % < min-1 >
kon(12)=1e5;    % < M-1 min-1 >
koff(12)=1e-2;  % < min-1 >
kon(13)=5e7;    % < M-1 min-1 >
koff(13)=5e-2;  % < min-1 >
kon(15)=5e7;    % < M-1 min-1 >
koff(15)=5e-2;  % < min-1 >
kon(16)=1e5;    % < M-1 min-1 >
koff(16)=1e-2;  % < min-1 >
kon(17)=5e4;    % < M-1 min-1 >
koff(17)=5e-2;  % < min-1>

% additional constants

% radius=5E-4;                  % <cm cell-1 >
% diff=2.1E-6;                  % < cm2 s-1 >
% sD=radius*diff*60/1000;       % < L min-1 >           radius*diff
N=6.02e23;                      % < # cell-1 >      avogadro's number
% kplus=4*pi*sD*N;
cell=200000;                    % < # >                 cells per well
vol=0.001;                      % < L >                 volume per well
density=cell/vol;       % < # L-1 >          cell density

% initial conditions
mRI=2e3;        % < # cell-1 >
mRII=1e3;       % < # cell-1 >
mRAcP=1e4;      % < # cell-1 >
sRI=1.33e-13;       % < M >
sRII=6.64e-14;      % < M >
sRAcP=6.64e-13;     % < M >
L=1.14e-10;         % < M >
Lra=1.14e-10;       % < M >

% Constraint equations
mRt=mRI+mRII+mRAcP;
sRt=sRI+sRII+sRAcP;

% list of parameters
parameters=[cell; vol; density; kon(2); koff(2); kon(3); koff(3); kon(4);
koff(4);  kon(6);  koff(6);  kon(7);  koff(7);  kon(8);  koff(8);  kon(11);
koff(11); kon(12); koff(12); kon(13); koff(13); kon(15); koff(15); kon(16);
koff(16); kon(17); koff(17); mRI; mRII; mRAcP; sRI; sRII; sRAcP; L; Lra];
```

110

```
% initial condition matrix
y0=[mRI, 0, 0, mRII, 0, 0, 0, mRAcP, sRI, 0, 0, sRII, 0, 0, 0, sRAcP, L, Lra]

% y=(mRI mCI mRI-Lra mRII mRII-L mCII mRII-Lra mRAcP
%    sRI sCI sRI-Lra sRII sRII-L sCII sRII-Lra sRAcP
%    L Lra)

% preparing the ODE solver
time=1440;   % < min >
options=odeset('RelTol',1e-6)
[t,y]=ode15s('diffeqs',[0 time],y0,options);

% combining the data
totalmatrix=[t y];
final=totalmatrix(end,:)

% saving the results to text files
save results totalmatrix /ascii;
save results_parameters parameters /ascii;
```

C.5.2 *Differential Equation Subroutine*

```
function yp=diffeqs(t,y)

global kon koff mRt sRt density N

%mRI
yp(1)=-kon(2)*y(1)*y(17)...
    -kon(4)*y(1)*y(18)...
    +koff(2)*(mRt-y(1)-2*y(2)-y(3)-y(4)-y(5)-2*y(6)-y(7)-y(8))...
    +koff(4)*y(3);

%mCI
yp(2)=kon(3)*(mRt-y(1)-2*y(2)-y(3)-y(4)-y(5)-2*y(6)-y(7)-y(8))*y(8)...
    -koff(3)*y(2);

%mRI-Lra
yp(3)=kon(4)*y(1)*y(18)...
    -koff(4)*y(3);

%mRII
yp(4)=-kon(6)*y(4)*y(17)...
    -kon(8)*y(4)*y(18)...
    +koff(6)*y(5)...
    +koff(8)*y(7);

%mRII-L
yp(5)=kon(6)*y(4)*y(17)...
    +koff(7)*y(6)...
    -koff(6)*y(5)...
    -kon(7)*y(5)*y(8);

%mCII
yp(6)=kon(7)*y(5)*y(8)...
```

```
    -koff(7)*y(6);

%mRII-Lra
yp(7)=kon(8)*y(4)*y(18)...
    -koff(8)*y(7);

%mRAcP
yp(8)=-kon(3)*(mRt-y(1)-2*y(2)-y(3)-y(4)-y(5)-2*y(6)-y(7)-y(8))*y(8)...
    -kon(7)*y(5)*y(8)...
    +koff(3)*y(2)...
    +koff(7)*y(6);

%sRI
yp(9)=-kon(11)*y(9)*y(17)...
    -kon(13)*y(9)*y(18)...
    +koff(11)*(sRt-y(9)-2*y(10)-y(11)-y(12)-y(13)-2*y(14)-y(15)-y(16))...
    +koff(13)*y(11);

%sCI
yp(10)=kon(12)*(sRt-y(9)-2*y(10)-y(11)-y(12)-y(13)-2*y(14)-y(15)-
y(16))*y(16)...
    -koff(12)*y(10);

%sRI-Lra
yp(11)=kon(13)*y(9)*y(18)...
    -koff(13)*y(11);

%sRII
yp(12)=-kon(15)*y(12)*y(17)...
    -kon(17)*y(12)*y(18)...
    +koff(15)*y(13)...
    +koff(17)*y(15);

%sRII-L
yp(13)=kon(15)*y(12)*y(17)...
    +koff(16)*y(14)...
    -koff(15)*y(13)...
    -kon(16)*y(13)*y(16);

%sCII
yp(14)=kon(16)*y(13)*y(16)...
    -koff(16)*y(14);

%sRII-Lra
yp(15)=kon(17)*y(12)*y(18)...
    -koff(17)*y(15);

%sRAcP
yp(16)=-kon(12)*(sRt-y(9)-2*y(10)-y(11)-y(12)-y(13)-2*y(14)-y(15)-
y(16))*y(16)...
    -kon(16)*y(13)*y(16)...
    +koff(12)*y(10)...
    +koff(16)*y(14);

%L
yp(17)=(-kon(2)*y(1)*y(17)...
    -kon(6)*y(4)*y(17)...
```

```
    +koff(2)*(mRt-y(1)-2*y(2)-y(3)-y(4)-y(5)-2*y(6)-y(7)-y(8))...
    +koff(6)*y(5))*(density/N)...
    -kon(11)*y(9)*y(17)...
    -kon(15)*y(12)*y(17)...
    +koff(11)*(sRt-y(9)-2*y(10)-y(11)-y(12)-y(13)-2*y(14)-y(15)-y(16))...
    +koff(15)*y(13);

%Lra
yp(18)=(-kon(4)*y(1)*y(18)...
    -kon(8)*y(4)*y(18)...
    +koff(4)*y(3)...
    +koff(8)*y(7))*(density/N)...
    -kon(13)*y(9)*y(18)...
    -kon(17)*y(12)*y(18)...
    +koff(13)*y(11)...
    +koff(17)*y(15);

yp=yp';
t;
```

Table C.1. Ligand, receptor, and receptor complex species for model.

#	Symbol	Location	Description
1	mRI	membrane	Type I receptor (IL-1RI)
2	mRI·L	membrane	IL-1/IL-1RI complex
3	mCI	membrane	IL-1/IL-1RI/IL-1RAcP complex
4	mRI·Lra	membrane	IL-1ra/IL-1RI complex
5	mRII	membrane	Type II receptor (IL-1RII)
6	mRII·L	membrane	IL-1/IL-1RII complex
7	mCII	membrane	IL-1/IL-1RII/IL-1RAcP complex
8	mRII·Lra	membrane	IL-1ra/IL-1RII complex
9	mRAcP	membrane	Receptor accessory protein (IL-1RAcP)
10	sRI	solution	Type I receptor (IL-1RI)
11	sRI·L	solution	IL-1/IL-1RI complex
12	sCI	solution	IL-1/IL-1RI/IL-1RAcP complex
13	sRI·Lra	solution	IL-1ra/IL-1RI complex
14	sRII	solution	Type II receptor (IL-1RII)
15	sRII·L	solution	IL-1/IL-1RII complex
16	sCII	solution	IL-1/IL-1RII/IL-1RAcP complex
17	sRII·Lra	solution	IL-1ra/IL-1RII complex
18	sRAcP	solution	Receptor accessory protein (IL-1RAcP)
19	L	solution	Interluekin-1β (IL-1β)
20	Lra	solution	IL-1 receptor antagonist (IL-1ra)
--	mR[tot]	membrane	Total membrane-bound receptors
--	sR[tot]	solution	Total soluble receptors

Table C.2. Ligand-receptor interactions.

#	Location	Reaction	Description
1	membrane	$L + mRI \Leftrightarrow mRI \cdot L$	IL-1/IL-1RI formation
2	membrane	$mRI \cdot L + mRAcP \Leftrightarrow mCI$	IL-1/IL-1RI/IL-1RAcP formation
3	membrane	$Lra + mRI \Leftrightarrow mRI \cdot Lra$	IL-1ra/IL-1RI formation
4	membrane	$L + mRII \Leftrightarrow mRII \cdot L$	IL-1/IL-1RII formation
5	membrane	$mRII \cdot L + mRAcP \Leftrightarrow mCII$	IL-1/IL-1RII/IL-1RAcP formation
6	membrane	$Lra + mRII \Leftrightarrow mRII \cdot Lra$	IL-1ra/IL-1RII formation
7	solution	$L + sRI \Leftrightarrow sRI \cdot L$	IL-1/sIL-1RI formation
8	solution	$sRI \cdot L + sRAcP \Leftrightarrow sCI$	IL-1/sIL-1RI/sIL-1RAcP formation
9	solution	$Lra + sRI \Leftrightarrow sRI \cdot Lra$	IL-1ra/sIL-1RI formation
10	solution	$L + sRII \Leftrightarrow sRII \cdot L$	IL-1/sIL-1RII formation
11	solution	$sRII \cdot L + sRAcP \Leftrightarrow sCII$	IL-1/sIL-1RII/sIL-1RAcP formation
12	solution	$Lra + sRII \Leftrightarrow sRII \cdot Lra$	IL-1ra/sIL-1RII formation

Table C.3. Kinetic and constraint equations.

| #	Equation
1	$\dfrac{d[mRI]}{dt} = -\,k_{f,mRI\cdot L}[mRI][L] + k_{r,mRI\cdot L}[mRI\cdot L] - k_{f,mRI\cdot Lra}[mRI][Lra]$ $\qquad + k_{r,mRI\cdot Lra}[mRI\cdot Lra]$
2	$\dfrac{d[mRI\cdot L]}{dt} = k_{f,mRI\cdot L}[mRI][L] - k_{r,mRI\cdot L}[mRI\cdot L] - k_{f,mCI}[mRI\cdot L][mRAcP]$ $\qquad + k_{r,mCI}[mCI]$
3	$\dfrac{d[mCI]}{dt} = k_{f,mCI}[mRI\cdot L][mRAcP] - k_{r,mCI}[mCI]$
4	$\dfrac{d[mRI\cdot Lra]}{dt} = k_{f,mRI\cdot Lra}[mRI][Lra] - k_{r,mRI\cdot Lra}[mRI\cdot Lra]$
5	$\dfrac{d[mRII]}{dt} = -\,k_{f,mRII\cdot L}[mRII][L] + k_{r,mRII\cdot L}[mRII\cdot L] - k_{f,mRII\cdot Lra}[mRII][Lra]$ $\qquad + k_{r,mRII\cdot Lra}[mRII\cdot Lra]$
6	$\dfrac{d[mRII\cdot L]}{dt} = k_{f,mRII\cdot L}[mRII][L] - k_{r,mRII\cdot L}[mRII\cdot L] - k_{f,mCII}[mRII\cdot L][mRAcP]$ $\qquad + k_{r,mCII}[mCII]$
7	$\dfrac{d[mCII]}{dt} = k_{f,mCII}[mRII\cdot L][mRAcP] - k_{r,mCII}[mCII]$
8	$\dfrac{d[mRII\cdot Lra]}{dt} = k_{f,mRII\cdot Lra}[mRII][Lra] - k_{r,mRII\cdot Lra}[mRII\cdot Lra]$
9	$\dfrac{d[mRAcP]}{dt} = -\,k_{f,mCI}[mRI\cdot L][mRAcP] + k_{r,mCI}[mCI] - k_{f,mCII}[mRII\cdot L][mRAcP]$ $\qquad + k_{r,mCII}[mCII]$
10	$\dfrac{d[sRI]}{dt} = -\,k_{f,sRI\cdot L}[sRI][L] + k_{r,sRI\cdot L}[sRI\cdot L] - k_{f,sRI\cdot Lra}[sRI][Lra] + k_{r,sRI\cdot Lra}[sRI\cdot Lra]$
11	$\dfrac{d[sRI\cdot L]}{dt} = k_{f,sRI\cdot L}[sRI][L] - k_{r,sRI\cdot L}[sRI\cdot L] - k_{f,sCI}[sRI\cdot L][sRAcP]$ $\qquad + k_{r,sCI}[sCI]$
12	$\dfrac{d[sCI]}{dt} = k_{f,sCI}[sRI][sRAcP] - k_{r,sCI}[sCI]$
13	$\dfrac{d[sRI\cdot Lra]}{dt} = k_{f,sRI\cdot Lra}[sRI][Lra] - k_{r,sRI\cdot Lra}[sRI\cdot Lra]$
14	$\dfrac{d[sRII]}{dt} = -\,k_{f,sRII\cdot L}[sRII][L] + k_{r,sRII\cdot L}[sRII\cdot L] - k_{f,sRII\cdot Lra}[sRII][Lra]$ $\qquad + k_{r,sRII\cdot Lra}[sRII\cdot Lra]$

Table C.3 continued

15 $$\frac{d[sRII \cdot L]}{dt} = k_{f,sRII\cdot L}[sRII][L] - k_{r,sRII\cdot L}[sRII \cdot L] - k_{f,sCII}[sRII \cdot L][sRAcP]$$
$$+ k_{r,sCII}[sCII]$$

16 $$\frac{d[sCII]}{dt} = k_{f,sCII}[sRII \cdot L][sRAcP] - k_{r,sCII}[sCII]$$

17 $$\frac{d[mRII \cdot Lra]}{dt} = k_{f,mRII\cdot Lra}[mRII][Lra] - k_{r,mRII\cdot Lra}[mRII \cdot Lra]$$

18 $$\frac{d[sRAcP]}{dt} = -k_{f,sCI}[sRI \cdot L][sRAcP] + k_{r,sCI}[sCI] - k_{f,sCII}[sRII \cdot L][sRAcP] + k_{r,sCII}[sCII]$$

19 $$\frac{d[L]}{dt} = \left(\frac{\rho}{Nav}\right)\{-k_{f,mRI\cdot L}[mRI][L] + k_{r,mRI\cdot L}[mRI \cdot L] - k_{f,mRII\cdot L}[mRII][L]$$
$$- k_{r,mRII\cdot L}[mRII \cdot L]\} - k_{f,sRI\cdot L}[sRI][L] + k_{r,sRI\cdot L}[sRI \cdot L]$$
$$- k_{f,sRII\cdot L}[sRII][L] + k_{r,sRII\cdot L}[sRII \cdot L]$$

20 $$\frac{d[Lra]}{dt} = \left(\frac{\rho}{Nav}\right)\{-k_{f,mRI\cdot L}[mRI][Lra] + k_{r,mRI\cdot L}[mRI \cdot Lra] - k_{f,mRII\cdot L}[mRII][Lra]$$
$$- k_{r,mRII\cdot L}[mRII \cdot Lra]\} - k_{f,sRI\cdot L}[sRI][Lra] + k_{r,sRI\cdot L}[sRI \cdot Lra]$$
$$- k_{f,sRII\cdot L}[sRII][Lra] + k_{r,sRII\cdot L}[sRII \cdot Lra]$$

21 $$[mR\{tot\}] = [mRI] + [mRI \cdot L] + 2\times[mCI] + [mRI \cdot Lra] + [mRII] + [mRII \cdot L]$$
$$+ 2\times[mCII] + [mRII \cdot Lra] + [mRAcP]$$

22 $$[sR\{tot\}] = [sRI] + [sRI \cdot L] + 2\times[sCI] + [sRI \cdot Lra] + [sRII] + [sRII \cdot L] + 2\times[sCII]$$
$$+ [sRII \cdot Lra] + [sRAcP]$$

**Table C.4. Model parameters and estimated values from the literature.**

Symbol	Description	Value	Units	Ref.
$k_{f,mRI \cdot L}$	association rate, IL-1/IL-1RI	1×10^7	$M^{-1}\ min^{-1}$	†
$k_{r,mRI \cdot L}$	dissociation rate, IL-1/IL-1RI	1×10^{-2}	min^{-1}	†
$k_{f,mCI}$	association rate, IL-1/IL-1RI/IL-1RAcP	1×10^{-3}	$(\#/cell)^{-1}\ min^{-1}$	[268]
$k_{r,mCI}$	dissociation rate, IL-1/IL-1RI/IL-1RAcP	1×10^{-1}	min^{-1}	[268]
$k_{f,mRI \cdot Lra}$	association rate, IL-1ra/IL-1RI	1×10^7	$M^{-1}\ min^{-1}$	†
$k_{r,mRI \cdot Lra}$	dissociation rate, IL-1ra/IL-1RI	1×10^{-2}	min^{-1}	†
$k_{f,mRII \cdot L}$	association rate, IL-1/IL-1RII	1×10^7	$M^{-1}\ min^{-1}$	†
$k_{r,mRII \cdot L}$	dissociation rate, IL-1/IL-1RII	1×10^{-2}	min^{-1}	†
$k_{f,mCII}$	association rate, IL-1/IL-1RII/IL-1RAcP	1×10^{-3}	$(\#/cell)^{-1}\ min^{-1}$	[268]
$k_{r,mCII}$	dissociation rate, IL-1/IL-1RII/IL-1RAcP	1×10^{-1}	min^{-1}	[268]
$k_{f,mRII \cdot Lra}$	association rate, IL-1ra/IL-1RII	1×10^5	$M^{-1}\ min^{-1}$	†
$k_{r,mRII \cdot Lra}$	dissociation rate, IL-1ra/IL-1RII	1×10^{-2}	min^{-1}	†
$k_{f,sRI \cdot L}$	association rate, IL-1/sIL-1RI	1×10^7	$M^{-1}\ min^{-1}$	†
$k_{r,sRI \cdot L}$	dissociation rate, IL-1/sIL-1RI	1×10^{-2}	min^{-1}	†
$k_{f,sCI}$	association rate, IL-1/sIL-1RI/sIL-1RAcP	1×10^5	$M^{-1}\ min^{-1}$	†
$k_{r,sCI}$	dissociation rate, IL-1/sIL-1RI/sIL-1RAcP	1×10^{-2}	min^{-1}	†
$k_{f,sRI \cdot Lra}$	association rate, IL-1ra/sIL-1RI	1×10^7	$M^{-1}\ min^{-1}$	†
$k_{r,sRI \cdot Lra}$	dissociation rate, IL-1ra/sIL-1RI	1×10^{-2}	min^{-1}	†
$k_{f,sRII \cdot L}$	association rate, IL-1/sIL-1RII	1×10^7	$M^{-1}\ min^{-1}$	†
$k_{r,sRII \cdot L}$	dissociation rate, IL-1/sIL-1RII	1×10^{-2}	min^{-1}	†
$k_{f,sCII}$	association rate, IL-1/sIL-1RII/sIL-1RAcP	1×10^5	$M^{-1}\ min^{-1}$	†
$k_{r,sCII}$	dissociation rate, IL-1/sIL-1RII/sIL-1RAcP	1×10^{-2}	min^{-1}	†
$k_{f,sRII \cdot Lra}$	association rate, IL-1ra/sIL-1RII	1×10^4	$M^{-1}\ min^{-1}$	†
$k_{r,sRII \cdot Lra}$	dissociation rate, IL-1ra/sIL-1RII	1×10^{-2}	min^{-1}	†
mRI{0}	Initial conc. of membrane-bound IL-1RI	2×10^3	# cell^{-1}	‡
mRII{0}	Initial conc. of membrane-bound IL-1RII	1×10^3	# cell^{-1}	‡
mRAcP{0}	Initial conc. of membrane-bound IL-1RAcP	1×10^4	# cell^{-1}	--
sRI{0}	Initial concentration of solution IL-1RI	1.3×10^{-13}	M	[129]
sRII{0}	Initial concentration of solution IL-1RII	6.6×10^{-14}	M	[129]
sRAcP{0}	Initial concentration of solution IL-1RAcP	6.6×10^{-13}	M	[129]
L{0}	Initial concentration of IL-1β	1.1×10^{-10}	M	--
Lra{0}	Initial concentration of IL-1ra	1.1×10^{-10}	M	--
mR{tot}	Total membrane-bound receptors (constant)	1.3×10^4	# cell^{-1}	--
sR{tot}	Total solution receptors (constant)	8.5×10^{-13}	M	--
Cells	Cells per well	2.0×10^5	# well^{-1}	--
Volume	Volume per well	1.0×10^{-3}	L well^{-1}	--
ρ	Cell density = Cells ÷ Volume	2.0×10^8	# L^{-1}	--
Nav	Avagadro's Number	6.02×10^{23}	# mol^{-1}	--

Order-of-magnitude estimates from multiple papers: † [129, 186, 269-272], ‡ [186, 269]
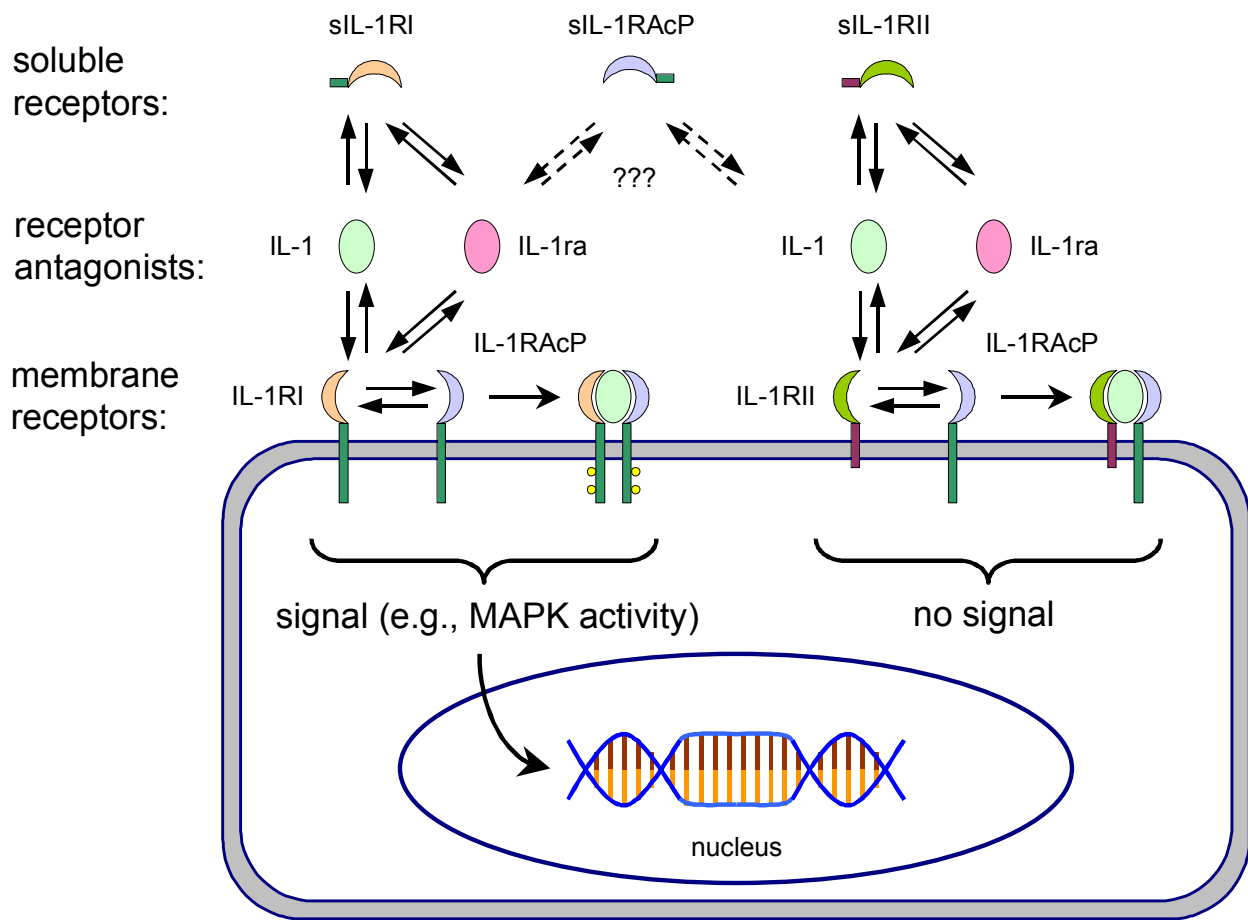
**Figure C.1.** Ligand-receptor interactions of the IL-1 signaling system. IL-1β competes with a receptor antagonist (IL-1ra) for binding to both type I (IL-1RI) and type II (IL-1RII) transmembrane receptors. After binding with ligand, both receptor types are thought to interact with a transmembrane accessory protein (IL-1RAcP). While the heterodimeric complex formed by IL-1RI/IL-1β and IL-1RAcP leads to receptor phosphorylation and signal transduction, interaction of IL-1RII/IL-1β with IL-1RAcP does not transduce signal. In addition to cell-bound receptors, the extracellular domains of IL-1RI, IL-1RII, and IL-1RAcP are released by chondocytes into the extracellular environment. These soluble receptors (sIL-1RI, sIL-1RII, and sIL-1RAcP) may affect IL-1β signaling by sequestering the ligand. Transient levels of these network components can be described by a set of ordinary differential equations.
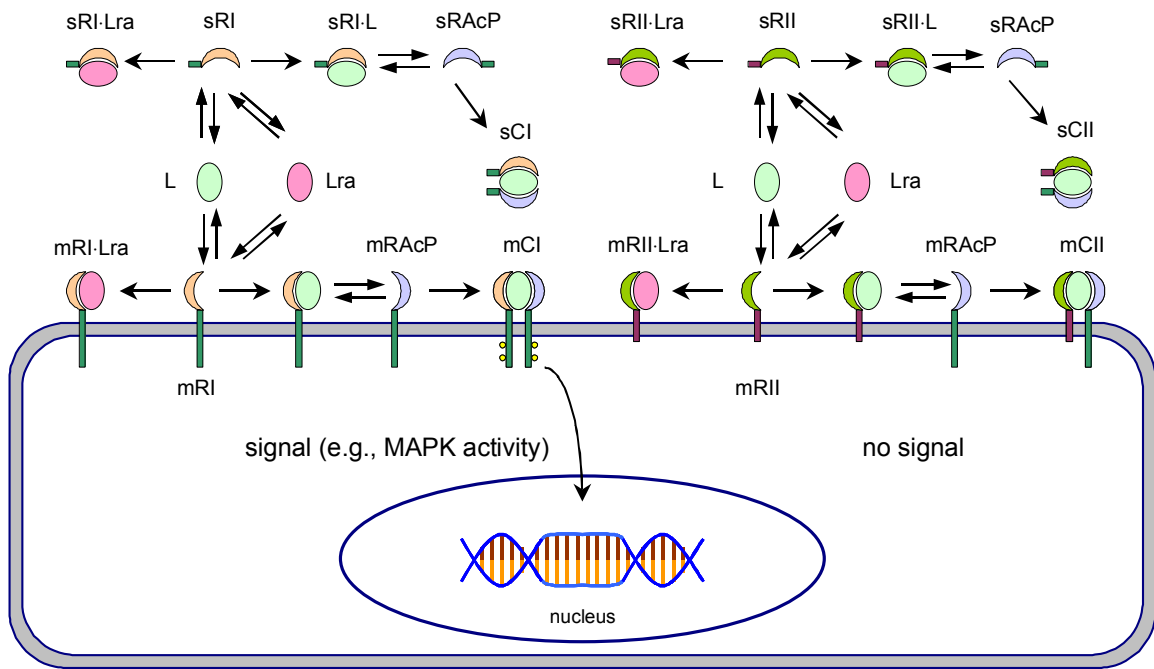
Figure C.2. Development of computational model for IL-1 system. Two ligands (IL-1 and IL-1ra) and six different receptor forms (IL-1RI, IL-1RII, and IL-1RAcP; both solution (s) and membrane-bound (m)) are addressed in this model. Both IL-1 and IL-1ra bind with solution and surface IL-1RI and IL-1RII. However, only IL-1/receptor complexes subsequently associate with accessory protein (IL-1RAcP). Of all the ligand-receptor complexes formed, only the IL-1/IL-1RI/IL-1RAcP (mCI) complex initiates signal transduction.
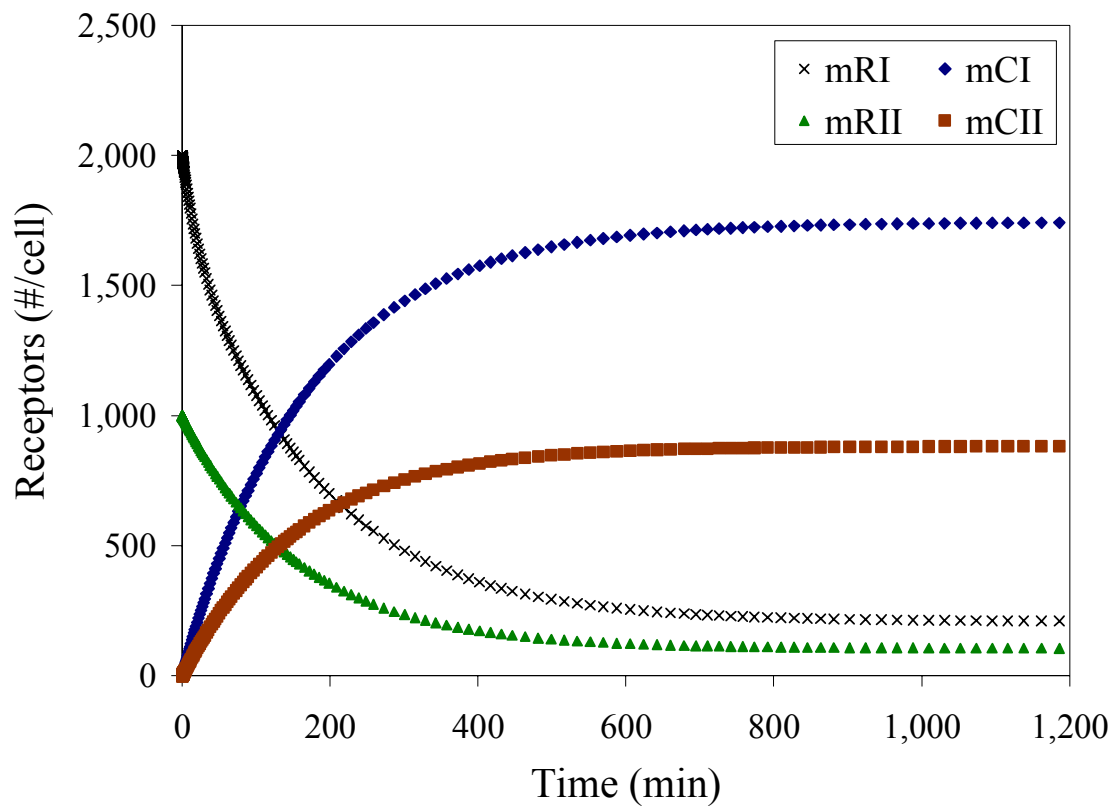
Figure C.3. Kinetics of receptor species for "base" model. The system of 18 ODEs was solved for the parameters and initial conditions given in **Table C.4**. Initial values for all ligand-receptor complexes were set to 0, simulating an association experiment. The numbers of IL-1/IL-1RI/IL-1RAcP and IL-1/IL-1RII/IL-1RAcP complexes increased with ligand binding until steady state values were reached after about 12 hr. Most type I and type II receptors were occupied at steady state. The ratio of "signaling" complexes (mCI) to "decoy" complexes (mCII) reflects their respective initial values.
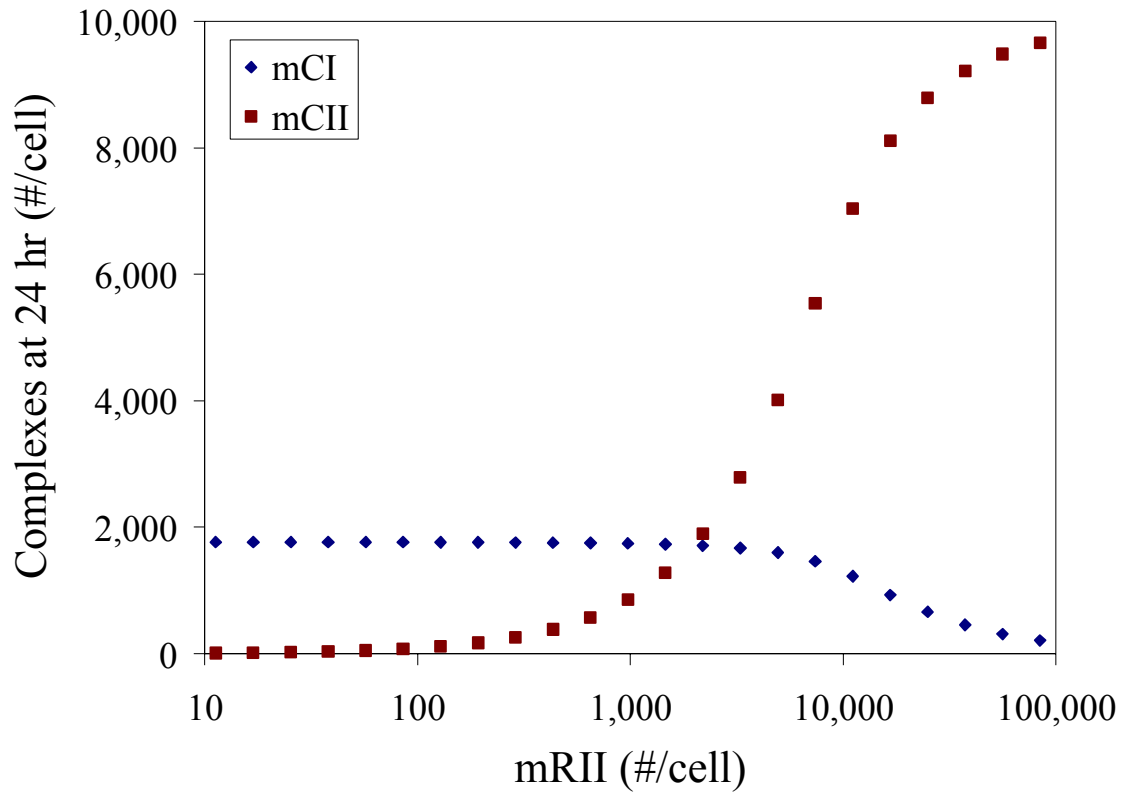
Figure C.4. Effect of membrane type II receptor levels on formation of signaling complexes. The concentration of IL-1RII on the cell surface (mRII) was varied by several orders of magnitude, and the steady state levels of IL-1/IL-1RI/IL-1RAcP and IL-1/IL-1RII/IL-1RAcP complexes were determined for each case. The model indicates that as IL-1RII levels on the surface approach those of IL-1RAcP, the formation of "signaling" complexes (mCI) is inhibited, whereas the number of "decoy" complexes (mCII) reaches saturation levels.
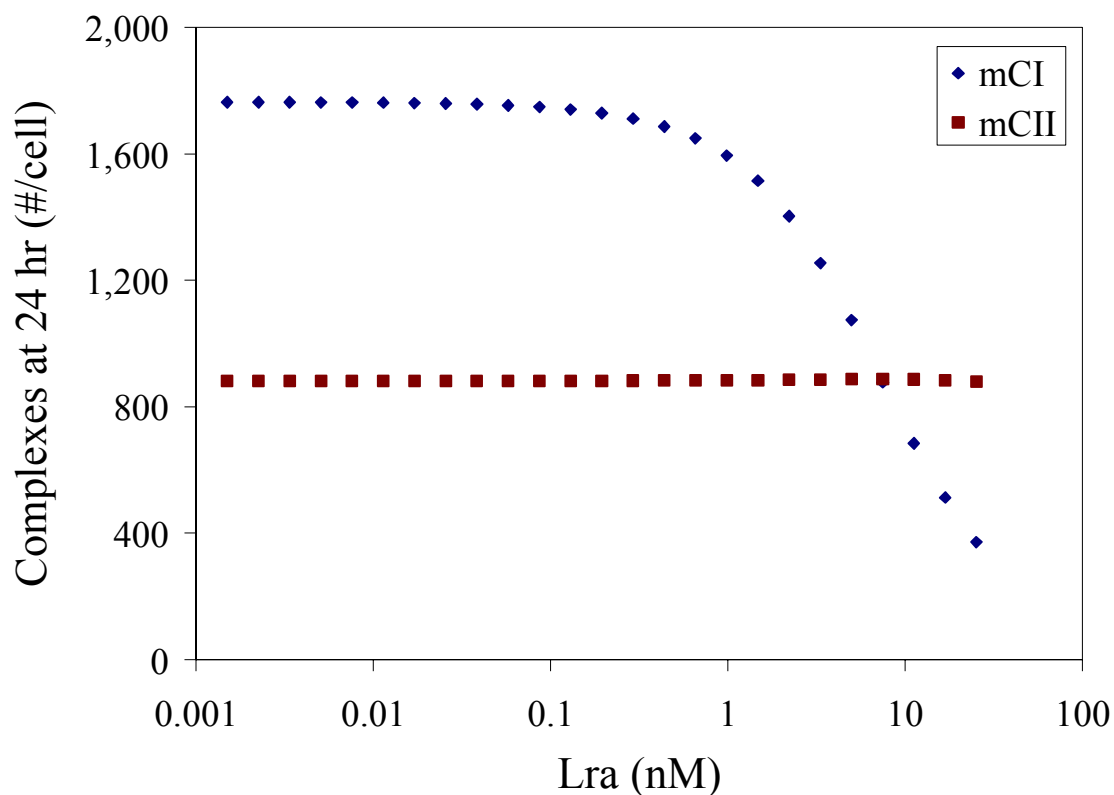
Figure C.5. Effect of receptor antagonist levels on formation of signaling complexes. The concentration of IL-1ra (Lra) in solution was varied by several orders of magnitude, and the steady state levels of IL-1/IL-1RI/IL-1RAcP and IL-1/IL-1RII/IL-1RAcP complexes were determined for each case. The model indicates that as IL-1ra levels in solution exceed that of IL-1, the formation of "signaling" complexes (mCI) is inhibited, whereas the number of "decoy"complexes (mCII) is not affected. This plot demonstrates that the inhibitory actions of IL-1ra and IL-1RII are additive, since the two factors act at different levels within the IL-1 system.

Vita – Ryan Michael Porter

DATE OF BIRTH   August 27, 1977

EDUCATION

M.S. in Chemical Engineering – October 2002
Virginia Polytechnic Institute & State University (Blacksburg)
Thesis: "Examination of Glucocorticoid Treatment on Bone Marrow Stroma: Implications for Bone Disease and Applied Bone Regeneration."
Advisor: Professor Aaron S. Goldstein

B.S. *summa cum laude* in Chemical Engineering – May 2000
University of Kentucky (Lexington)

EXPERIENCE

2002-present   **Research Assistant – Dept. of Chemical Engineering, Virginia Tech**
Advisor: Professor Kimberly Forsten Williams

2001-2002   **Research Assistant – Dept. of Chemical Engineering, Virginia Tech**
Advisor: Professor Aaron S. Goldstein

2000-2002   **Teaching Assistant – Dept. of Chemical Engineering, Virginia Tech**
- Unit Operations Laboratory
- Chemical Engineering Simulations (i.e., computational methods)

1997-1999   **Process Engineering Intern**
Protein Technologies International (Louisville, KY)

AWARDS & ACTIVITIES

- Outstanding Presentation, PhD student competition – *The Virginia Tech – Wake Forest University School of Biomedical Engineering and Sciences 4th Student Research Symposium*, Meadows of Dan, VA (May 12, 2005)
- Relay for Life (American Cancer Society) – Graduate Student Assembly Team Captain (2005)
- Among four Tech students selected to attend *A Gathering of Nobel Laureates: Science for the 21st Century*, University of North Carolina at Charlotte (February 28 - March 1, 2005)
- Travel Fund Program Chair – Graduate Student Assembly (2004-2005)
- NSF Fellow – *3rd International Summer School on Biocomplexity: from System to Gene*, Dartmouth College, Hanover, NH (July 19-25, 2003)

- Outstanding Presentation, MS student competition – *The Virginia Tech Center for Biomedical Engineering and the Wake Forest University School of Medicine 1st Student Research Symposium*, Blacksburg, VA (May 2, 2002)
- Virginia Tech Center for Biomedical Engineering Pratt Fellowship (2000-2001)
- University of Kentucky General Vending Scholarship (1995-1998)

PUBLICATIONS

- Porter, R.M., R.M. Akers, R.D. Howard, and K. Forsten-Williams. "Transcriptional and Proteolytic Regulation of the Insulin-like Growth Factor-I System of Equine Articular Chondrocytes by Recombinant Equine Interleukin-1β." (in preparation).
- Porter, R.M., R.M. Akers, R.D. Howard, and K. Forsten-Williams. "Culture Strategy Impacts the Insulin-like Growth Factor-I System of Equine Articular Chondrocytes and Cell Response to Interleukin-1β." (in preparation).
- Porter, R.M., W.R. Huckle, and A.S. Goldstein. "Effect of dexamethasone withdrawal on osteoblastic differentiation of bone marrow stromal cells." *J. Cellular Biochem.*, 90: 13-22 (2003).

PRESENTATIONS

- "Culture Strategy Mediates the Insulin-like Growth Factor-I Axis for Chondrocytes Challenged with Interleukin-1." (Platform) *The Virginia Tech – Wake Forest University School of Biomedical Engineering and Sciences 4th Student Research Symposium*; Meadows of Dan, VA (May 12, 2005).
- "Interleukin-1 and Alginate Bead Culture Regulate IGF-I Signaling for Equine Articular Chondrocytes." (Platform) *American Institute of Chemical Engineers 2004 Annual Meeting*; Austin, TX (November 7-12, 2004).
- "Interleukin-1 and Alginate Bead Culture Regulate IGF-I Signaling for Equine Articular Chondrocytes." (Platform) *Biomedical Engineering Society 2004 Annual Fall Meeting*; Philadelphia, PA (October 13-16, 2004).
- "Exogenous IL-1 and alginate bead culture regulate the IGF-I signaling system of equine articular chondrocytes." (Poster) *2004 Biotechnology Symposium*; Charlottesville, VA (May 6, 2004).
- "Exogenous interleukin-1 regulates the IGF-axis of equine chondrocytes cultured in alginate beads." (Platform) *22nd Southern Biomedical Engineering Conference*; Charlotte, NC (September 27, 2003).
- "Effects of dexamethasone treatment duration on the osteogenic potential of rat bone marrow stromal cells cultured *in vitro*." (Platform) *The Virginia Tech Center for Biomedical Engineering and the Wake Forest School of Medicine 1st Student Research Symposium*; Blacksburg, VA (May 2, 2002).